



National Library
of Canada

Bibliothèque nationale
du Canada

Canadian Theses Service

Service des thèses canadiennes

Ottawa, Canada
K1A 0N4

NOTICE

The quality of this microform is heavily dependent upon the quality of the original thesis submitted for microfilming. Every effort has been made to ensure the highest quality of reproduction possible.

If pages are missing, contact the university which granted the degree.

Some pages may have indistinct print especially if the original pages were typed with a poor typewriter ribbon or if the university sent us an inferior photocopy.

Reproduction in full or in part of this microform is governed by the Canadian Copyright Act, R.S.C. 1970, c. C-30, and subsequent amendments.

AVIS

La qualité de cette microforme dépend grandement de la qualité de la thèse soumise au microfilmage. Nous avons tout fait pour assurer une qualité supérieure de reproduction.

S'il manque des pages, veuillez communiquer avec l'université qui a conféré le grade.

La qualité d'impression de certaines pages peut laisser à désirer, surtout si les pages originales ont été dactylographiées à l'aide d'un ruban usé ou si l'université nous a fait parvenir une photocopie de qualité inférieure.

La reproduction, même partielle, de cette microforme est soumise à la Loi canadienne sur le droit d'auteur, SRC 1970, c. C-30, et ses amendements subséquents.

UNIVERSITY OF ALBERTA
PROPERTIES OF CALCIUM CURRENTS IN HERMISSEDA NEURONS

by
EBENEZER NKETIA YAMOAH



A THESIS
SUBMITTED TO THE FACULTY OF GRADUATE STUDIES AND RESEARCH IN
PARTIAL FULFILMENT OF THE REQUIREMENTS FOR THE DEGREE OF
DOCTOR OF PHILOSOPHY

DEPARTMENT OF SURGERY

EDMONTON, ALBERTA

FALL 1991



National Library
of Canada

Bibliothèque nationale
du Canada

Canadian Theses Service Service des thèses canadiennes

Ottawa, Canada
K1A 0N4

The author has granted an irrevocable non-exclusive licence allowing the National Library of Canada to reproduce, loan, distribute or sell copies of his/her thesis by any means and in any form or format, making this thesis available to interested persons.

The author retains ownership of the copyright in his/her thesis. Neither the thesis nor substantial extracts from it may be printed or otherwise reproduced without his/her permission.

L'auteur a accordé une licence irrévocable et non exclusive permettant à la Bibliothèque nationale du Canada de reproduire, prêter, distribuer ou vendre des copies de sa thèse de quelque manière et sous quelque forme que ce soit pour mettre des exemplaires de cette thèse à la disposition des personnes intéressées.

L'auteur conserve la propriété du droit d'auteur qui protège sa thèse. Ni la thèse ni des extraits substantiels de celle-ci ne doivent être imprimés ou autrement reproduits sans son autorisation.

ISBN 0-315-70300-8

Canada

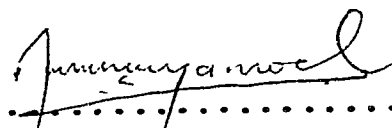
UNIVERSITY OF ALBERTA

RELEASE FORM

NAME OF AUTHOR EBENEZER NKETIA YAMOA
TITLE OF THESIS PROPERTIES OF CALCIUM CURRENTS IN
HERMISSENDA NEURONS
DEGREE FOR WHICH THESIS WAS PRESENTED DOCTOR OF PHILOSOPHY
YEAR THIS DEGREE GRANTED FALL, 1991.

Permission is hereby granted to THE UNIVERSITY OF ALBERTA LIBRARY to reproduce single copies of this thesis and lend or sell such copies for private, scholarly or scientific research purposes only.

The author reserves other publication rights, and neither the thesis nor extensive extracts from it may be printed or otherwise reproduced without the author's written permission.

(SIGNED) 

PERMANENT ADDRESS:

11732 - 83 Avenue
Edmonton, Alberta
Canada T6G 0V3

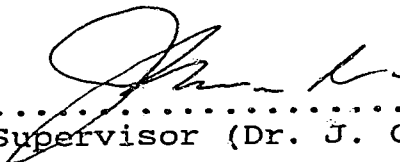
DATED... 11/10/91


Short title for spine.

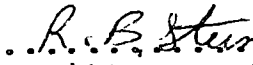
CALCIUM CURRENTS IN HERMISSENDA NEURONS

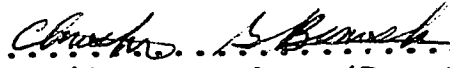
UNIVERSITY OF ALBERTA
FACULTY OF GRADUATE STUDIES AND RESEARCH


The undersigned certify that they have read, and recommend to the Faculty of Graduate Studies and Research, for acceptance, a thesis entitled PROPERTIES OF CALCIUM CURRENTS IN HERMISSENDA NEURONS submitted by EBENEZER NKETIA YAMOA in partial fulfilment of the requirements for the degree of DOCTOR OF PHILOSOPHY.


.....
Supervisor (Dr. J. C. Russell)


.....
External examiner (Dr. Elis Stanley)


.....
Committee member (Dr. R. B. Stein)


.....
Committee member (Dr. C. Benishin)


.....
Committee member (Dr. E. Karpinski)

Date Oct 11 / 91.....

Abstract

The properties of calcium channels were studied and the role of the inactivation of the channel's conductance in intracellular calcium regulation was assessed in an identified class of FRMRamide sensitive neurons in a marine snail, Hermisenda crassicornis. Two calcium channel subtype (low and high-voltage activated channels) may be present in the neurons. However, under the conditions examined here, the high-voltage activated channel predominated.

Calcium current appeared at potentials positive to -30 mV and peaked at +20 mV, from holding potentials ranging from -70 to -50 mV. Current activation was voltage dependent, with a sigmoidal relationship, which could be fitted with an H-H formalism of m^2 . However, the inactivation kinetics were dependent on calcium influx and voltage with the voltage range of inactivation lying between -100 and -20 mV. The time course of inactivation was biphasic (at 0 mV in 10 mM $[Ca]_o$, τ_{fast} (τ_1) = 20 - 29 ms, τ_{slow} (τ_2) = 410 - 536 ms). But at -30, +40 and +50 mV step voltages the current waveform decayed monotonically with voltage.

The channel was reversibly blocked by lanthanum (350 μ M) and cadmium (350 μ M) but was less sensitive to nickel and cobalt ions. While nanomolar concentrations of the organic calcium channel blocker, ω -Conotoxin, irreversibly blocked the

channels even micromolar doses of the dihydropyridines (DHP) had little effect on the channels. If anything, the effects of the DHPs could only be described as non-specific.

It is suggested in this thesis that the inactivation of calcium conductance is regulated by voltage and current. Both mechanisms work in concert to fine tune calcium influx following activation of voltage-dependent calcium channels.

Acknowledgments

What as been accomplished was made possible by God and I am thankful for His unfailing love and grace.

In retrospect, I find a dichotomy in the case history of this project. While others have gone their way to support and encourage this work, others made me go through the emotions of a Phd. thesis the hard way. I am glad I had both ways: it made science exceedingly complex and exciting. I wish to thank the members of my committee for their advice in their fields of expertise. Dr. James Russell provided invaluable scientific and emotional support: he was always there when I needed encouragement. Also, I wish to thank Dr. Joy Steele and Jan Przysiezniak for their helpful discussions on the project.

I am deeply grateful for my friends and family for their unfailing support throughout my education and especially during the final throes of the project.

This thesis is dedicated to the late Sophia Yamoah.

Table of Contents

| | | |
|---|--|----|
| Abstract | | iv |
| Acknowledgments | | vi |
| List of Figures | | ix |
| List of Tables | | x |
| Physical constants | | x |
| Abbreviations | | x |
| | | |
| 1. INTRODUCTION | | 1 |
| 1.1 Intracellular calcium..... | | 1 |
| 1.1.1 Functions & Regulation in neurons | | 1 |
| 1.2 Calcium currents..... | | 4 |
| 1.3 Molluscan Neurons..... | | 15 |
| 1.4 Objectives for this Project..... | | 18 |
| | | |
| 2. THE PREPARATION | | 20 |
| 2.1 Systematics..... | | 20 |
| 2.2 Introduction..... | | 21 |
| 2.3 Materials and Methods..... | | 22 |
| 2.3.1 Dissection..... | | 23 |
| 2.3.2 Electrophysiology..... | | 23 |
| 2.3.3 Axonal Backfilling..... | | 24 |
| 2.3.4 Cell Culture..... | | 25 |
| 2.3.4.1 Dissociation & Plating... | | 25 |
| 2.3.4.2 S.E.M..... | | 27 |
| 2.3.5 Immunocytochemistry..... | | 27 |
| 2.4 Results..... | | 30 |
| 2.4.1 Electrophysiology..... | | 30 |
| 2.4.2 Immunocytochemistry..... | | 31 |
| 2.4.3 Cell Culture..... | | 41 |
| 2.5 Discussion..... | | 48 |
| | | |
| 3 CALCIUM CURRENT | | 50 |
| 3.1 Preparation..... | | 50 |
| 3.2 Chemicals & Solutions..... | | 50 |
| 3.3 Experimental chamber..... | | 50 |
| 3.4 Patch clamp..... | | 51 |
| 3.5 Accuracy of voltage clamp..... | | 52 |

| | | |
|----------|---|------------|
| 3.6 | Isolation of I_{Ca} | 53 |
| 3.7 | Evidence for I_{Ca} | 54 |
| 3.8 | Results..... | 54 |
| 3.8.1 | Calcium Current Activation.... | 55 |
| 3.8.2 | Inactivation of Ca^{2+} current.. | 76 |
| 3.8.3 | Effect of $[Ca^{2+}]_e$ | 77 |
| 3.8.4 | Effect of V_m & Elevated $[Ca^{2+}]_i$ | 78 |
| 3.8.5 | Ba^{2+} Ca^{2+} & Sr^{2+} Currents..... | 79 |
| 3.8.6 | Effect of chelators..... | 88 |
| 3.8.7 | Ca^{2+} influx and inactivation.. | 95 |
| 3.8.8 | Time constant of inactivation. | 96 |
| 3.9 | Pharmacology of the channel..... | 100 |
| 3.9.1 | La^{3+} and Divalent Cations..... | 100 |
| 3.9.2 | Organic Blockers..... | 101 |
| 3.9.2.1 | Dihydropyridines..... | 101 |
| 3.9.2.2 | ω -Conotoxin..... | 106 |
| 3.10 | Discussion on Calcium Current..... | 110 |
| 3.10.1 | Identification of the Current. | 112 |
| 3.10.2 | Number of Channel/s..... | 115 |
| 3.10.3 | Low-voltage-activated channel. | 117 |
| 3.10.4 | Pharmacology of the Channel... | 118 |
| 3.10.5 | Activation of Ca current..... | 121 |
| 3.10.6 | Inactivation of Ca channel.... | 122 |
| 3.11 | Model of Inactivation..... | 126 |
| 3.12 | Physiological Considerations..... | 129 |
| 3.13 | Conclusive Remarks..... | 130 |
| 4 | APPENDIX (Voltage clamp)..... | 133 |
| 1. | Voltage clamp..... | 133 |
| 2. | Circuit (A-1)..... | 134 |
| 3. | Series resistance (A-2)..... | 135 |
| 4. | Series resistance measurement (A-3)..... | 138 |
| 5. | Electrical analogy of cells (A-4)..... | 140 |
| 5. | Theoretical error measurement..... | 146 |
| 6. | Error profile..... | 146 |
| 7. | Conductance curve..... | 149 |
| 8. | Space clamp error table (1A)..... | 150 |
| 9. | Appendix B (figure)..... | 153 |
| 10. | Appendix B..... | 154 |
| 11. | Appendix C..... | 155 |
| 12 | Appendix D..... | 157 |
| 5 | REFERENCES..... | 158 |

List of Figures

FIGURES

| | | |
|-----|---|-----|
| 1. | Schematic diagram of Ca_i dynamics..... | 18 |
| 2. | Effect of FMRFamide..... | 32 |
| 3. | Effect of FMRFamide on spikes..... | 33 |
| 4. | Spike waveforms..... | 35 |
| 5a. | Lucifer Yellow injected FSN..... | 36 |
| 5b. | Nickel-Lysine backfilling..... | 36 |
| 6. | Diagram of labelled cells | 38 |
| 7. | FMRFamide-like immunocytochemistry..... | 40 |
| 8. | Neurons in culture (a-e)..... | 44 |
| 9. | Enzymatic dissociation of neurons (a & b).... | 47 |
| 10. | Total membrane current traces..... | 56 |
| 11. | Pharmacology of outward currents..... | 57 |
| 12. | Raw data Ca -current traces..... | 58 |
| 13. | Evidence for uncontaminated I_{Ca} | 60 |
| 14. | Current traces & IVs..... | 61 |
| 15. | Instantaneous I-V curve..... | 63 |
| 16. | IVs for different $[Ca]_e$ | 67 |
| 17. | Activation curves $[Ca]_e$ | 68 |
| 18. | Activation curves Ca , Ba , Sr | 70 |
| 19. | Activation profile & time constant..... | 74 |
| 20. | Time constant & voltage curves..... | 75 |
| 21. | Effect of bathed calcium..... | 80 |
| 22. | $[Ca]_e$ & % inactivation..... | 82 |
| 23. | Current profiles in 5 & 10 mM Ca | 83 |
| 24. | Effect of holding potential..... | 84 |
| 25. | Effect of high $[Ca]_i$ | 86 |
| 26. | Effect of Ca , Sr , & Ba on inactivation..... | 89 |
| 27. | Sr & Ba currents..... | 92 |
| 28. | Effect of chelators..... | 93 |
| 29. | Ca influx & inactivation..... | 97 |
| 30. | Time constant as function of voltage..... | 99 |
| 31. | Effect of lanthanum..... | 102 |
| 32. | Effect of Cd , Co , & Ni | 104 |
| 33. | Effect of the dihydropyridines..... | 107 |
| 34. | Effect of Conotoxin..... | 109 |

List of Tables

TABLES

| | | |
|----|--|-----|
| 1. | Properties of three classes of VDCC..... | 7 |
| 2. | Composition of Solutions..... | 29 |
| 3. | Spike analysis (Control & FMRFamide)..... | 33 |
| 4. | Spike analysis (FSN)..... | 34 |
| 5. | Spike width of intact & cultured neuron..... | 34 |
| 6. | Time to peak (I_{Ca} , I_{Sr} & I_{Ba})..... | 73 |
| 7. | Time constants of inactivation..... | 98 |
| 8. | Properties of Ca-channel..... | 112 |

Physical Constants.

| | | |
|----------------------|--------|---|
| Absolute temperature | T(K) = | 273.16 + T(^o Celsius). |
| Faraday's constant | F = | 9.648 x 10 ⁴ Cmol ⁻¹ |
| Gas constant | R = | 8.314 VCK ⁻¹ mol ⁻¹ . |

Abbreviations.

| | |
|----------------|---|
| 4-AP | 4-aminopyridine. |
| ATP | Adenosine triphosphate |
| C_m/C | Membrane capacitance (F) |
| $[Ca]_e$ | Extracellular calcium concentration. |
| $[Ca]_i$ | Intracellular calcium concentration. |
| DHP | Dihydropyridine. |
| I_x | X current (general abbreviation for Ca, Sr, Ba, Na & K currents). |
| NMDA | N-methyl-D-aspartate. |
| P_{Ca} | Permeability of calcium. |
| Q | Charge (Coulombs) |
| R_i | Volume resistivity (Ω -cm) |
| R_{in} | Input resistance (Ω) |
| R_m | Specific membrane resistance (Ω -cm ²) |
| Tau (τ) | Time constant (s) |
| TEA | Tetraethylammonium. |
| TTX | Tetrodotoxin. |
| V_x | Reversal potential of X. |
| VDCC | Voltage-dependent calcium channels. |

CHAPTER I

INTRODUCTION

Ever since the introduction of techniques for recording electrical activities of neurons, it has become clear that the movement of calcium ions (Ca^{2+}), from the extracellular to intracellular compartments, is of central importance to neuronal function. Intracellular free calcium (Ca_i^{2+}) serves as a second messenger and a rise in cytoplasmic calcium ion concentration initiates several biochemical activities. Paradoxically, it has been shown that a rise in Ca_i^{2+} beyond a certain concentration can cause neuronal death. Thus, neurons must maintain a balance between the influx and efflux of calcium. This thesis describes calcium channel properties and the inactivation mechanisms of the channel. Inactivation of calcium channel conductance is one of the mechanisms by which neurons regulate intracellular free calcium concentration (Eckert & Chad, 1984). An identified class of neurons in the nudibranch mollusc, Hermissenda crassicornis was studied.

INTRACELLULAR CALCIUM

Functions and Regulation in Neurons.

Calcium plays an important role in signalling and processing of information in the nervous system. This

includes the transduction of sensory stimuli (e.g. mechanical, chemical into electrical impulses), the transmission of chemical signals across synapses and the integration and storage of information to effect coordinated motor responses.

Calcium based action potentials were first observed in crustacean muscle (Fatt & Katz, 1953) and later in other invertebrate and vertebrate neurons (Horn, 1978, Llinas & Hess, 1976). Even during pure sodium spikes (Hodgkin & Huxley, 1952), $^{45}\text{Ca}^{2+}$ flux experiments show that intracellular calcium rises to about 3 times that of baseline level (Bianchi & Shanes, 1959) as a result of activation of calcium channels and deactivation following the repolarization phase of the action potential. Thus, Ca^{2+} influx through voltage-sensitive calcium channels (VSCC) down its electrochemical gradient serves to raise $[\text{Ca}_i^{2+}]$. Furthermore, some calcium channels open in response to membrane receptor agonists -receptor operated channels-, namely the binding of ATP in smooth muscle preparations and NMDA receptors in central neurons (ROC Bolton, 1979; Adams et al., 1980; Thomson et al., 1985; MacDermott et al., 1986; Brenner & Eisenberg, 1986). Aside from the extracellular supply, the intracellular free calcium level can be raised by release from calcium stores (Berridge & Irvine, 1984; Spat et al., 1986). All these events can result in an increase in Ca_i^{2+} from, less than 10^{-7} M to about 10^{-4} M (Brinley, 1978; Miller, 1987).

Many intracellular second messengers and enzymes are

activated with a rise in $[Ca_i^{2+}]$; these include cyclic nucleotides, diacylglycerol, inositol phosphates, and protein kinases (Cheung, 1980; Berridge, 1987; Kennedy, 1989). Presumably, transient events, like neuro-secretion and adaptive reactions including regenerative processes following injury or diseases (Van der Zee et al., 1989), as well as long-term storage of memory are directly (Alkon et al., 1990) or indirectly (Lederhendler et al., 1990) effected through the second messenger systems. The regulation of intracellular second messengers therefore depends, partly, on Ca_i^{2+} homeostasis.

A rise in intracellular calcium is known to activate certain classes of potassium channels (Meech, 1974; Swandulla & Lux, 1985) and chloride channels (Byrne & Large, 1987) to repolarize the membrane to limit calcium entry. In addition, the inactivation of calcium currents, in ciliates, Aplysia neurons and insect muscles (Brehm & Eckert, 1978; Brehm et al., 1980; Tillotson, 1979; Eckert et al., 1981; Chad et al., 1984; Ashcroft & Stanfield, 1981), Helix neurons, sympathetic ganglion cells, adenohipophysial cells and cardiac myocytes (Brown et al., 1981; Adams, 1981; Thornton, 1982; Hume & Giles, 1983; Brown et al., 1984; Mitchell et al., 1983) are dependent wholly or in part on calcium influx. Hence, calcium participates in a negative feedback mechanism to regulate the free Ca_i^{2+} level. Other mechanisms known, in principle, to prevent calcium overload are; (1) sequestration of calcium

into intracellular stores, e. g. endoplasmic reticulum (2) an energy dependent pump which extrudes calcium out of cells (3) a carrier protein known to extrude one ion of calcium in exchange for at least three sodium ions (Na^+ - Ca^{2+} exchanger) and (4) intracellular calcium buffers (Brinley, 1978; DiPolo & Beauge, 1983). In neurons, direct electrophysiological evidence for the presence of either the calcium pump or the carrier system has not been obtained, even though biochemical data from experiments performed on the squid axon suggest the presence of such mechanisms. However, a number of laboratories have shown that the absence of extracellular sodium or the presence of ATP generation inhibitors result in an increase in $^{45}\text{Ca}^{2+}$ flux in the squid axon, suggesting that a sodium dependent calcium-efflux mechanism and an ATP-dependent Ca^{2+} pump may be present (DiPolo & Beauge, 1983; Baker & Dipolo, 1984).

CALCIUM CURRENTS

Within the past few years, the kinetics, pharmacology and functional properties of calcium channels have been intensely studied, but our knowledge of these characteristics is incomplete. It is clear that the activation of calcium channels, with few exceptions, is voltage dependent and the time course is slow compared with that of the tetrodotoxin (TTX) sensitive sodium channels. The voltage range of

activation of calcium currents varies both, between and within neurons (Tsien et al., 1987; Fox et al., 1987). Similarly, the inactivation profiles of calcium currents are variable and it is as a result of these observations together with pharmacological differences of I_{Ca} that three distinct calcium channels have been categorized in vertebrate neurons (Fox et al., 1987). Tsien and coworkers demonstrated, at macroscopic and microscopic levels, that in chick sensory neurons, at a holding potential of -100 mV, a transient (T) calcium channel was activated at potentials positive to -70 mV. The T channel had a steady state inactivated potential range between -100 and -60 mV and was found to be insensitive to the dihydropyridines, weakly blocked by cadmium ions and reversibly blocked by Omega-conotoxin (ω -CgTX). With positive step potentials (> -20 mV), Nowycky et al., (1985) found another transient channel (N type). This channel was similar to the T type in its insensitivity towards the dihydropyridines but unlike the T channel, it was highly sensitive and irreversibly blocked by cadmium and ω -CgTX, respectively. A slowly inactivating channel which activates at -10 mv (L type) and which is sensitive to the dihydropyridines has also been described (see table 1: Tsien, 1987; Nowycky et al., 1985; Fox et al., 1987). Not all the three calcium channels are expressed in every cell. For example, only the T and L are seen in canine atrial cells (Bean, 1985), and in sympathetic neurons only N and L have

been recorded (Marchetti et al., 1986). In adrenal medullary chromaffin cells only the L type channel is expressed (Fenwick et al., 1982; Cena et al., 1989) while only the T type is observed in B lymphocytes (Fukushima & Hagiwara, 1985).

The physiological functions of the three calcium channels are not fully understood. In the presence of nickel ions, a blocker of T channels, cardiac myocytes were reported to decrease their frequency of contraction which was enhanced with hyperpolarization (Hagiwara et al., 1988). Such observations together with ones made in vertebrate neurons (Llinas & Yarom, 1981; Burlhis & Aghajanian, 1988) strongly suggest that the T channel is responsible for the generation of pacemaker depolarization in the heart and neurons, but even so, this cannot entirely exclude the possible contribution of other types of calcium channels because the inorganic calcium channel blockers used in those experiments all have some effect on other calcium channels (Tsien et al., 1987). The use of ω -CgTX, a reversible blocker of T channels but irreversible antagonist of N-type, and the dihydropyridine antagonist for blockade of L type channels may help clarify this issue. However, such an experiment is yet to be reported. Speculation on the T channel involvement in contraction of muscles (Perney et al., 1986) and secretion in adrenal glomerulosa cells (Cohen et al., 1988) has also been made.

The L channel may be involved in contraction of heart

cells (Tsien et al., 1989) and release of noradrenaline from synaptosomes, based on the inhibitory role of the dihydropyridines on these events (Hofmann et al., 1987). Neurotransmitter release at the synaptic terminal of the squid axon and the neuromuscular junction of frog (Augustine et al., 1987) and in sympathetic neurons are resistant to the dihydropyridines and cadmium but sensitive to ω -CGTX (Miller, 1987; Hirning et al., 1988).

Table 1. Properties of three classes of voltage-dependent calcium channels.

| Properties | T | N | L |
|--|---|---|--------------------------------|
| Activation range (10 mM Ca^{2+}) | Positive to -70 mV | Positive to -10 mV | Positive to -10 mV |
| Steady state Inactivation range | -100 to -60 mV | >-100 to -40 mV | -60 to -10 mV |
| Relaxation rate (0 mV, 10 Ca^{2+} or Ba^{2+}) | Moderate (τ \approx 20-50 msec) | Moderate (τ \approx 20-50 msec) | Very slow (τ > 500 msec) |
| Single channel conductance | 8 - 10 pS | 11 -15 pS | 23 - 27 pS |
| Single channel kinetics | Late opening, brief burst, inactivation | Long burst, inactivation | Hardly any inactivation |
| Cadmium block | Resistant | Sensitive | Sensitive |
| Cobalt block | Sensitive | Less sensitive | Less sensitive |
| Dihydropyridine sensitivity | No | No | Yes |
| ω -CGTX block | Weak, reversible | Persistent | Weak (Aosaki & Kasia, 1989) |

Consequently, it is common to see the N-type channel being associated with transmitter release (Tsien et al., 1989). This is a bit misleading because most of the calcium currents recorded close to synaptic terminals fall outside the description of an N-type channel. For example, I_{Ca}^{2+} at the synaptic terminal of the squid axon and frog neuromuscular junction activate at potentials around -50 mV and shows little or no inactivation (Augustine et al., 1987). Such kinetics are far from the properties of an N-type channel (see table 1).

The classification of calcium channels formulated by Tsien and coworkers is by no means complete. Invertebrate calcium channels are similar but not identical to the vertebrate T, N, or L channels. For example, Aplysia bag cells and Helix pacemaker neurons exhibit non-inactivating calcium currents that are sensitive to the dihydropyridine antagonists but resistant to Bay K 8644 and ω -CgTX (Eckert & Lux, 1976; Strong et al., 1987). Similarly, the squid axon displays both dihydropyridine and ω -CgTX insensitive calcium currents (Augustine et al., 1987). Even in some vertebrate sensory neurons, ω -CgTX has been found to block predominantly the L-type current which activated from a holding potential around -30 mV (Scott et al., 1990). Recently, Aosaki and Kasai (1989) have reported that the L and N type channels in chick sensory neurons are differentially sensitive to the DHPS and ω -conotoxin respectively. Other laboratories, using the

same preparation (sensory neurons), have reported results which are completely opposite to the selective inhibitory action known for ω -conotoxin on L and N-type channels, i. e. inhibition of N- type current and not L-type current (Plummer et al., 1989). For one thing, we cannot attribute the apparent confusion to differences in preparation and for another, the variation of responses are not likely to result from differences in the use of divalent ions which may modify ω -conotoxin binding (Scott et al., 1991). However, species variations, differences in the preparation of the toxin and the interpretation of experimental data are likely to cause these variations (Hess, 1990).

Other calcium channel blockers e.g. Amiloride (Scott et al., 1991), 1-octanol and gadolinium (Takahashi et al., 1989) have been used by other investigators but they do not appear to have any specific inhibitory actions and hence are not useful for pharmacological separation of channels.

Purkinje cells (cerebellum) have distinct voltage-activated calcium channels which cannot be grouped with the T-, N- and L- type channel classifications. Though similar to the N- type channel, the channel which has been named P channel (Llinas et al., 1989), activate around -50 mV and is insensitive to ω -conotoxin. It is becoming apparent that the N-type channel may consist of several sub-types which might have undergone some evolutionary modification based on function. Calcium channels close to the squid giant synapse

and synaptic calcium channels at cholinergic pre-synaptic terminals (Stanley & Goping, 1991) and the jellyfish, Polyorchis penicillatus, neurons (Przysieznik & Spencer, 1991), have some common properties (they begin to activate at very high positive voltages; $\geq +20$ mV) which are similar to the N-type channels, though they differ in their sensitivities towards pharmacological blockers. Calcium channels in cholinergic neurons are sensitive to ω -conotoxin but insensitive to the DHPs. On the other hand Ca-channels in jellyfish neurons are blocked by the DHP antagonists.

At the single channel level, B-type channel (from bovine cardiac sarcolemma) has been recorded from planar lipid bilayers. It has a single channel conductance of 10 pS (maximum conductance) at hyperpolarizing voltages (-100 mV), has long open times (> 100 ms) and is insensitive to Bay K8644 (Rosenberg et al., 1988). The cardiac cell has a high demand for calcium ions and it is likely that this channel is restricted to serve this purpose but this has yet to be shown.

The observations made, so far, on calcium channels rule out the possibility that only three sub-types of calcium currents exist in the animal kingdom. Several divergent populations of calcium channel sub-types may have evolved and only when an extensive screening of the animal phyla for calcium channels has been made can this categorization be made complete.

In voltage-clamped neurons in which sodium and the fast

and slow potassium currents have been blocked or eliminated, assessment of the kinetics of calcium current activation have been less problematic than inactivation. Calcium current activation occurs at a relatively faster time scale than outwardly directed currents, except the transient outward current, I_A , which is readily blocked by 4-AP. Following calcium influx, the activation of outward currents (e. g. calcium activated potassium current, I_{KCa} : Meech & Standen, (1975)) serves to contaminate the calcium current. Hence, the apparent inactivation of calcium current may be the result of an increasing outward potassium current. Okamoto et al., (1976) showed evidence that, in tunicate eggs, at potential ranges in which little or no potassium current was activated, inactivation of calcium current occurred. Subsequent inward tail current measurement, in molluscan neurons, at the reversal potential of the potassium current by Connor (1977), supported this conclusion, and demonstrated that the calcium current was sustained with slow kinetics of decay. Prior to Connor's report on Archidoris, Katz & Miledi (1971) had observed that sustained depolarization, beyond the reversal potential, by the injection of current into the squid pre-synaptic terminal resulted in cessation of transmitter release. However, transmitter release was regained briefly after current injection was stopped. The conclusion was that the activation of calcium conductance persisted during depolarization and the tail current associated with

repolarization, following current turn-off, resulted in further transmitter release. Subsequent voltage clamp experiments (Llinas et al., 1976, 1981a & 1981b) have confirmed the non-inactivating kinetics of calcium current in the squid axon. These authors (Llinas et al., 1976, 1981a & b) have suggested, therefore, that two types of calcium conductances exist; one which inactivates with prolonged depolarization and the other which does not.

The presence of I_{Ca}^{2+} inactivation and non-inactivation have been ascertained using voltage-clamp recording from dialysed cells (Kostyuk et al., 1975) and the tight-seal whole-cell technique (see chapter 3). In both methods, intracellular calcium is buffered with a chelator (e.g. EGTA) to prevent Ca^{2+} elevation, and outward current activation eliminated with impermeable cations. The use of intracellular calcium chelator and replacement of extracellular calcium with barium or strontium have revealed yet another mechanism of I_{Ca} inactivation; calcium-dependent inactivation. Tillotson, (1979) showed that with a conventional twin-pulse paradigm, calcium current in Aplysia, R-15, R-2 and R-14 neurons exhibited reduced inactivation at pre-pulse potentials close to the equilibrium potential for calcium (E_{Ca}) and that I_{Ca} inactivation decreased when extracellular calcium was replaced with an equimolar concentration of barium. It was further demonstrated that the calcium influx, obtained by integrating the area above the current, correlated with the degree of

inactivation curve (Tillotson, 1980; Eckert et al., 1981). In addition, calcium mediated I_{Ca} inactivation was ascertained using the calcium sensitive dye, Arsenazo III, as an optical calcium indicator (Tillotson, 1980). In this experiment the optical signals were of the type expected according to the postulate of calcium dependent inactivation. Eckert and co-workers, after a series of experiments (Chad et al., 1984; Eckert et al., 1982; Eckert & Ewald, 1983) and in an extensive review Eckert and Chad 1984, concluded that the inactivation of calcium current in most cells and in particular, in invertebrates, can be explained solely as a calcium dependent phenomenon. They illustrated this hypothesis with a kinetic model (Chad et al., 1984). Ca-dependent inactivation of calcium conductance has also been demonstrated in insect muscles (Ashcroft & Stanfield, 1982), ciliates (Brehm et al., 1980), cardiac cells (Giles et al., 1980; Hume & Giles, 1983; Campbell et al., 1988) and sympathetic ganglion cells (Adams, 1981).

The evidence for calcium-mediated inactivation of calcium channels stated by Eckert and colleagues were quite strong. However, there were some fundamental questions which were left unanswered. If inactivation mechanisms of calcium current were exclusively calcium dependent, then, substitution of extracellular calcium with barium should remove the I_{Ca} turn-off. Brown et al., (1981) reported that, in Helix neurons, calcium channel inactivation was not obliterated when barium

ion was used as the charge carrier and even in the initial reported case of this phenomenon (Tillotson, 1979), I_{Ca} inactivation was reduced but not removed with extracellular barium. It is conceivable that barium substitutes for calcium in a calcium-dependent process, however the evidence is not clear-cut (Hille, 1984). Several authors (Brown et al., 1981; Brown et al., 1984; Akaike et al., 1988; Campbell et al., 1988) have demonstrated that the inactivation of calcium current is dependent on Ca^{2+} influx, yet, at certain voltages, the contribution of voltage cannot be ruled out. Thus the inactivation of some calcium channels may depend on both current and voltage. The degree of inactivation at a post-pulse and calcium influx measured from the integral of I_{Ca} , elicited from pre-pulses, may be expected to show parallel relations if the inactivation were Ca-mediated, but this has not been observed in some cases (Brown et al., 1981). Moreover, rapid buffering of Ca^{2+} by intracellular proteins can result in this apparent discrepancy.

Earlier data presented by Eckert et al., (1983), showed convincing evidence to demonstrate the relative absence of any outward current contamination of their calcium current records. Nonetheless, in the kinetic model for calcium-mediated calcium current inactivation, Chad et al., (1984) restricted it to voltages between -26 and 0 mV with the suggestion that beyond 0 mV outward current contamination might affect the model. Thus, the model begged the

fundamental question it was supposed to answer and gave an apparent hint that the inactivation of calcium channels may be partly calcium and voltage dependent.

MOLLUSCAN NEURONS

Molluscs are suitable for physiological studies of individual cells in the nervous system. Not only do their large sized-neurons permit single and multiple microelectrode penetrations but the ability to use identified neurons make molluscs a valuable model system for research in electrophysiology. Studies of ionic currents using the voltage clamp technique (Cole, 1949) are feasible in molluscan neurons. However, one important technical problem in working with molluscan neurons is attaining good spatial control of voltage. To circumvent this problem, relatively small cells or multiple electrode voltage clamp (Llinas et al., 1981a; Connor, 1977; Augustine et al., 1985a) or other methods (Kostyuk et al., 1975) have been used to study ionic currents.

Studies on the ionic currents responsible for the generation of action potentials in Hermissenda neurons have been, largely, restricted to the peripheral nervous system (e.g. photoreceptor). Most of the neurons in the central nervous system which have been investigated (e.g. LP1) are large (approx. 80 - 100 μm . diameter) and hence are not suitable for single electrode voltage clamp studies (see chap.

3). However, smaller diameter neurons which are suitable for voltage clamp have been found in the pedal ganglia. These neurons (25 - 35 μm in diameter) are homogenous in their electrical properties and are sensitive to the neuropeptide, FMRFamide. They supply the visceral organs of the animal (Yamashita, et al., 1991). The neurons, (FMRFamide sensitive neurons; FSN), are relatively easy to isolate and they can grow in culture made from artificial sea water, for several days (see chap. 2).

In the mollusc, Hermissenda, classical conditioning appears to produce both anatomical and biophysical changes characterized by reduction of dendritic volume (Alkon et al., 1990), increase in somatic area (Lederhendler et al., 1990) and reduction of potassium currents (Farley & Auerbach, 1986). These structural and biophysical correlates of learning-related changes have generally been found to be calcium dependent. For example, in the membrane of the type B photoreceptor in Hermissenda, one of the loci for long-term modulation of potassium channels, the conditioning-specific reduction of K^+ currents could not be induced without extracellular calcium or when calcium chelators were injected into the cells in calcium bathed media (Alkon, 1987). Similar results have been found with the anatomical changes associated with conditioning (Lederhendler et al., 1990). It has been suggested that Ca^{2+}_i in conjunction with protein kinase C, mediate the phosphorylation of a 20-kDa G-protein which,

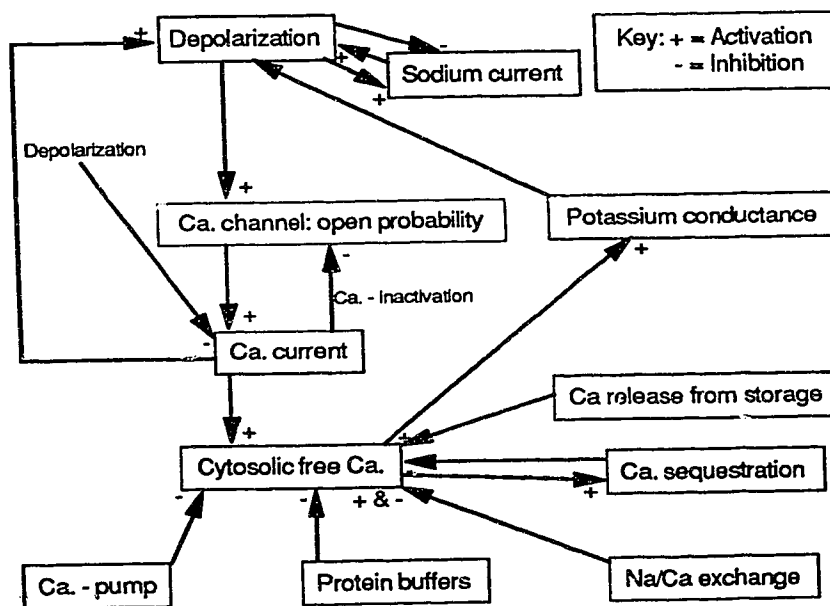
initiates both the anatomical and biophysical changes (Matzel et al., 1990; Nelson et al., 1990). Therefore, it seemed reasonable to begin to address questions related to intracellular calcium regulation in Hermisenda neurons.

Several attempts have been made to measure calcium currents, in Hermisenda, but only that of Collin et al., 1988 was successful. Even that work had its problems because outward current contamination of the calcium current, especially, at positive voltage steps prevented any useful kinetic study. The present project was intended to measure calcium currents in FSNs. This group of neurons were selected for two reasons: (1) They are small in size and hence are suitable for single electrode voltage clamp studies. (2) They are light sensitive (elicit burst activities with light) and have a repetitive firing pattern (FMRFamide response) comparable to that seen in the type B photoreceptor with light, though less robust. It is appreciated that the detail dynamics of calcium channel/s properties in FSN may be different from that of the B photoreceptor. However, it is presumed that the basic mechanisms of the channel's kinetics will be similar in both cells.

Objectives for this project

The regulation of intracellular free calcium depends on membrane bound phenomena and intracellular sequestration mechanisms. The scheme below is a summary of the phenomena entailed in the maintenance of a low intracellular calcium concentration (see caption underneath for detail).

Figure 1. Schematic diagram of intracellular calcium dynamics.



Membrane depolarization opens calcium channels and calcium flow inward along the electrochemical gradient. Increase in Ca^{2+}_i , activates potassium conductance to reverse membrane polarity and inactivates calcium conductance to reduce calcium inflow. An ATP-dependent pump extrudes calcium outside and a carrier-mediated exchanger operates to minimized intracellular calcium overload. In addition, protein buffers in the cell and intracellular calcium pumps in organelles work in concert to ensure homeostatic calcium activity.

The aim of this project is to advance our present knowledge on calcium channel/s properties in Hermisenda crassicornis with emphasis on the voltage-dependent activation, inactivation mechanisms and the pharmacology of the channel/s. The whole-cell variant of the patch clamp technique will be used.

Within the framework of the objectives of this project, I wish to develop stable experimental conditions under which calcium channels in Hermisenda neurons can be studied. The existing problems associated with calcium current measurements (e. g. difficulty in isolating a pure calcium current) in Hermisenda neurons make it quite difficult to study the channel's properties in any meaningful form. It is believed however, that intracellular calcium influx initiates several biophysical changes in some H. C. neurons. Studies of calcium currents may help us to understand, at least in part, the mechanisms of those biophysical changes.

The aim of this project, therefore, was to measure for the first time in Hermisenda neurons, calcium currents. First, the preparation will be described from anatomical and electrophysiological standpoints. The second section will be on calcium channel kinetics and pharmacology. The quality of the space clamp is assessed in the appendix. Last, a qualitative description of the contribution of calcium channel inactivation in maintenance of resting cytosolic Ca^{2+} is given.

CHAPTER 2
THE PREPARATION

SYSTEMATICS (MacFarland, 1966).

| | |
|---------------------|-----------------------|
| Phylum | MOLLUSCA |
| CLASS | GASTROPODA |
| ORDER | ACOELA |
| SUB-ORDER | NUDIBRANCHIATA |
| SUPER FAMILY | AEOLIDIIDAE |
| SUB-FAMILY | FAVORINAE |
| GENUS | HERMISSENDA |
| SPECIES | CRASSICORNIS |

Introduction

In the mollusc, Hermisenda, classical conditioning seems to produce biophysical changes characterized by reduction of potassium currents (Alkon, 1987). The long term modulation of potassium channels appears to depend on Ca^{2+} and phosphorylation of a 20-kDa G-protein (CP20) mediated by a Ca^{2+} -dependent protein kinase C (PKC: Alkon, 1987; Nelson et al., 1989). Therefore, it seemed reasonable to begin to ask questions related to cytosolic calcium regulation in Hermisenda neurons. I have selected a group of FMRFamide sensitive neurons to study calcium channel properties in Hermisenda. These neurons are amenable for the whole cell variant of the patch clamp method (Hamill et al., 1981). They are sensitive to light stimulus; a property common to the type B photoreceptors in Hermisenda, a specific locus for potassium channel modulation.

Since the discovery of FMRFamide in the ganglia of the clam, Macrocallista nimbosa (Price & Greenberg, 1977), this peptide or its homologues have been identified in a variety of invertebrate and vertebrate nervous systems (Callaway et al., 1987; Chronwall et al., 1984; Buchanan, et al., 1987; Cottrell et al., 1984; Norris & Calabrese, 1987). The physiological effects of FMRFamide appear to be variable. It is cardio-excitatory in the mollusc (Price and Greenberg, 1977; Brezina

et al., 1987a & b), increases the conductance of S-channels and decreases calcium currents in Aplysia neurons (Brezina et al., 1987a). As well, it modulates synaptic transmitter release in Helisoma (Man-Son-Hing et al., 1989) and in vertebrates, there is evidence to suggest that FRMFamide or its related peptides are antagonistic to the actions of exogenous opiates (Kavaliers et al., 1985).

FRMFamide increases the firing frequency of an identified class of neurons in H. C. (Yamoah et al., submitted to Bio. bull.). This cluster of neurons (5 - 8) is located in the lower one-quarter of the pedal ganglia. The FRMFamide sensitive neurons (FSN) are homogeneous in their electrical properties. The question of whether FRMFamide-like neurons are present in the nervous system of H. C. was asked and answered with immunohistochemical techniques. Presented here are data which describe the distribution of FRMFamide-like neurons in the nervous system of H. C. In addition, development of a primary culture of the FRMFamide sensitive neurons has been described in this paper.

MATERIALS and METHODS.

Hermissenda crassicornis were obtained from Seacology, Vancouver, Sea Life Supplies, Sand City CA., or Marine Biological Laboratory, Woods Hole, MA. and housed in an aquarium. Animals were fed on Tubularia sp.

DISSECTION

Animals were anaesthetized with 3% MgCl₂ and pinned to the bottom of a petri dish lined with Sylgard (Dow Corning, Midland, MI) under a dissecting microscope. The nervous systems were removed using scissors and tweezers. Specimens were incubated at room temperature for 10 minutes in artificial sea water (ASW) containing 1 mg/ml protease (Type VII, Sigma Chemical Co. St. Louis, Mo.) to facilitate penetration of microelectrodes or whole mount immunocytochemistry.

ELECTROPHYSIOLOGY - Intracellular recording.

The nervous systems were held on microscope slides with minutin pins (Cal. Biochem. CA.). The preparations were bathed with 1 ml artificial sea water (see table 2). Microelectrodes were pulled from thick walled capillary glass (1.2 mm. outer and 0.6 mm. inner diameters: FHC, Brunswick, ME) and filled with either 2 M potassium acetate or 5% Lucifer Yellow (LY-Sigma Chem. CO.) in 1 M LiCl₂. Electrode resistances were 30-80 M Ω. The preamplifiers (Dagan 8800; Minneapolis, Mn) incorporated a bridge circuit to allow current injection through the recording electrode. Current injection was monitored using a current to voltage converter placed between the indifferent electrode, made from 3 M KCl

agar bridge, and earth. Signals were stored on tape and displayed using an oscilloscope and pen-recorder. Neurons clustered at the lower quadrant of the pedal ganglia were penetrated.

Spike activity and passive electrical properties, e.g. input resistance, were measured. Hyperpolarizing current pulses of 1-7 nA and 500 ms duration were applied for at least 20 minutes to inject the dye. Following LY injection, the microelectrodes were carefully drawn out of the cells and the preparations were viewed directly under ultraviolet light with fluorescein isothiocyanate filters. When the background noise from leakage of the dye in the interstitial space was significant, preparations were dehydrated through an alcohol series (30% 70% 95% and 100% ethanol) and cleared with 100% methyl salicylate before photographs were taken.

AXONAL BACKFILLING

The nerve fibre which contained the axons from the neurons stained with LY was backfilled with nickel-lysine (Fredman, 1987). A stock solution consisting of 1.0 M NiCl_2 and 4.0 M L-Lysine was made and stored at 4°C. After dissection, the nerve fibre of interest was placed in small vaseline-wells which contained hypo-osmotic solution (75% tonicity) of the stock solution. The preparations were

incubated at 4°C for 48 hours. 50 mg. dithiooximide was dissolved in 3 ml 100% dimethyl sulfoxide (DMSO, Sigma Chemical Co.) to form rubeanic acid. Nickel was precipitated by adding 2 drops of the rubeanic acid solution to a dish containing the preparation and 1 ml ASW. After 30 minutes, specimens were fixed with 4% paraformaldehyde in PBS, dehydrated in an alcohol series and cleared with methyl salicylate. Specimens were mounted and photographs were taken through a Nikon inverted microscope.

CELL CULTURE

DISSOCIATION and PLATING of NEURONS

The nervous systems were isolated and treated with protease and collagenase to loosen the surrounding connective tissue. Several methods of digesting connective tissue were employed depending on the study. When cultures were intended for longer experimental procedures, the nervous system was incubated at 20°C in 3 mg/ml protease (Sigma P8038) in ASW for 25-35 minutes. FSN were then isolated. This was done by removing the large neurons on the superficial aspects of the brain and then the clustered neurons were sucked with a pipette. Identified neurons were triturated with a fire-polished-tip pipette and plated in Corning culture dishes with 1.5-2 ml filtered ASW. Initially, dishes were

pre-treated with 0.3 mg/ml. polylysine (Sigma Chem. Co.), but this step could be omitted, for it was observed later that cells attached to polylysine-free dishes. Not only did neurons remain viable in culture but they regenerated neurites. Cultures were kept at 8°C. The ASW was changed every 48 hours.

The method described above did not remove glial cells from the neurons. However, it was noted that cells treated this way could be maintained longer in culture (12-14 days) than glial cell-free neurons. For removal of glial cells, dissected nervous systems were incubated in 1 mg/ml. protease in ASW overnight at 4°C. Following incubation, the tissues were treated with fresh enzyme solution (1-2 mg/ml.) for 15-20 minutes at room temperature. Alternatively, brains were digested in an enzyme solution with 16 mg/ml. dispase (Boehringer Mannheim GmbH) and 1 mg/ml protease in ASW for 25-30 minutes at room temperature. The preparations were washed with ASW and FSN were isolated, triturated, and plated in culture dishes. Cultures were stored as described previously. They remained viable for 7 to 8 days. Pictures were taken with a Nikon camera attached to an inverted microscope equipped with phase contrast optics.

SCANNING ELECTRON MICROSCOPY

To assess the quality of the dissociation procedure, neurons in culture were observed under the scanning electron microscope. Cells were plated on cover slips and fixed overnight in a solution made from 2.5% glutaraldehyde, 1.5% paraformaldehyde, 5 mM EGTA, 2.5% sucrose in 0.1 M cacodylate buffer. Following fixation, cells were dehydrated with 100% dimethoxypropane, incubated in 100% hexamethyl desilozone and allowed to air-dry. Cover slips were mounted and sputter coated with gold palladium. Scanning electron microscope (SEM) facilities of the Surgical Medical Research Institute (PHILIPS SEM 505) and Marine Biological Laboratory (JEOL SM.840) were used.

IMMUNOCYTOCHEMISTRY of NERVOUS SYSTEM

The nervous systems were pre-fixed by adding 2 drops of 10% paraformaldehyde in phosphate buffer saline (PBS) for 10 minutes and transferred to 4% paraformaldehyde in PBS overnight at 4°C. Following 30 minutes of washing in 4% Triton X-100 in PBS and then blocking solution for 20 minutes, to reduce non-specific binding, tissues were incubated for 72 hours at 4°C in antibody raised against RFamide peptide (a polyclonal antibody obtained from Spencer, A. N.; University

of Alberta) or against FRMFamide-monoclone (ICN Immunonuclear Corp, Stillwater, MN) in PBS (dilution 1:100). The blocking solution was made from 1% bovine serum albumin- fraction V (ICN ImmunoBiol. IL) and 2-3 drops of horse serum (Vector Labs. Inc. CA) in PBS. The primary antibody was washed for 20 minutes in PBS and the slide then transferred into PBS for 15 minutes. Fluorescein isothiocyanate (FITC) labelled secondary antibody, goat anti rabbit IgG, was diluted in the blocking solution 1:200. Specimens were incubated in the secondary antibody solution for 5 hours in the dark after which they were washed in PBS for 30 minutes before mounting with poly aqua mount on microscope slides. Slides were stored in the dark at 4°C, overnight, before pictures were taken on a Zeiss microscope equipped with excitation barrier filter and reflector combination cubes containing an excitation of 440 to 490 nm wavelength and a selective barrier filter from 520 to 560 nm.

Control experiments were conducted. The primary antibody was pre-incubated in FMRFamide (.5 mg./ml. Sigma Chemical Co.) for 6 hours, centrifuged and the supernatant used as a control for the specificity of the RFamide antibody.

Table 2: Columns 1 & 2 are composition of artificial sea water (ASW) and culture solution (940 - 1000 mosmol) used for the experiments described in this thesis. Columns 3 & 4 are the components of salts used for voltage clamp experiments for measurement of calcium currents (see chap. 4).

| Composition of Solutions | | | | |
|--------------------------|----------------------|------------------|-----------------|---------------------------|
| Chemicals | Concentrations in mM | | | |
| | ASW | Culture solution | External media. | Internal (Pipette) media. |
| NaCl | 420 | 400 | - | 20 |
| Choline-Cl | - | - | 300 | - |
| KCl | 10 | 10 | - | - |
| CaCl ₂ | 10 | 10 | 5, 6, 10, 15. | - |
| MgCl ₂ | 22.9 | 22.9 | 50 | 2 |
| MgSO ₄ | 25.5 | 25.5 | - | - |
| Dextrose | - | 11 | - | - |
| HEPES | 15 | 15 | 15 | 35 - 50 |
| EGTA | - | - | - | 10 |
| Gen. SO ₄ | - | 50 mg/L | - | - |
| TEACl | - | - | 100 | 20 |
| 4AP | - | - | 5 | - |
| BaCl ₂ | - | - | 5, 10. | - |
| SrCl ₂ | - | - | 5, 10. | - |
| CsCl | - | - | - | 400 |
| ATP | - | - | - | 5 |
| GTP | - | - | - | 1 |
| Glutathione | - | - | - | 10 |
| pH | 7.8 NaOH | 7.8 NaOH | 7.8 TEAOH | 7.4 TEAOH |

KEY: Gen. SO₄ = Gentamycin sulphate.

RESULTS

Electrophysiology

When viewed from the dorsal side of the nervous system, on the lower right quadrant of the right pedal ganglia of H.C., ventral to the giant neurons, there is a cluster of 5 - 8 neurons (25 - 35 μm diameter). Very little is known about these neurons except that they are sensitive to micromolar concentrations of exogenously applied FMRFamide (figure 2). This cluster of neurons which we tentatively call FMRFamide sensitive neurons (FSN) are, in general, electrically silent with occasional spikes (Yamoah et al., submitted to *Bio. Bull.*). However, in the presence of 5 μM FMRFamide, the cells became tonically active with intermittent after-hyperpolarizations. A typical effect of FMRFamide on FSN is presented in figure 2. In addition, FMRFamide depolarized the membrane and caused a slight decrease in spike amplitude but with no significant change in the slope of the action potentials (figure 3 & table 3). The resting membrane potentials of the cells were around -70 to -50 mV (see table 4). Usually, potentials above -40 mV were recorded on initial impalement but cells sealed off in 5 to 10 minutes and the resting membrane potential became more hyperpolarized. The resting potential in figure 2 was -66 mV and the spike amplitude was about 90 mV high. To ascertain the homogeneity of this classes of neurons, I performed spike waveform

analysis on 3 different FSN neurons from different animals (see table 4a & b). The properties of the neurons were quite similar, both within and between neurons. Figure 4 depicts action potentials recorded from three different FSNs.

Shown in figure 5a is Lucifer Yellow injected soma of a FSN. When allowed to diffuse into the axon, the dye could be seen in a nerve fibre which supply the visceral organs (the gut and the heart). Anterograde Lucifer Yellow filling of the soma could not be used to identify all the neurons so, the nerve fibre which contained LY-filled axons was retrogradely filled with nickel-lysine. Backfilling with nickel-lysine showed several stained soma in the nervous system (fig 5b). In figure 6 a scheme for the location of FSNs and their relation to other identified neurons in the nervous system has been illustrated. Only the FSN were isolated and studied. The arrows show the location of FSN. The action of FRMFamide on these neurons had a short delay. Is FRMFamide or any of its homologue present in the nervous system of H.C. ?

Immunocytochemistry of Nervous System

Consistent labelling of FRMFamide-like cells were obtained in all the experiments (n > 40 for whole mount nervous system). Both ipsilateral and contralateral cells in the cerebropleural and pedal ganglia stained positive to FRMFamide and RFamide antibodies.

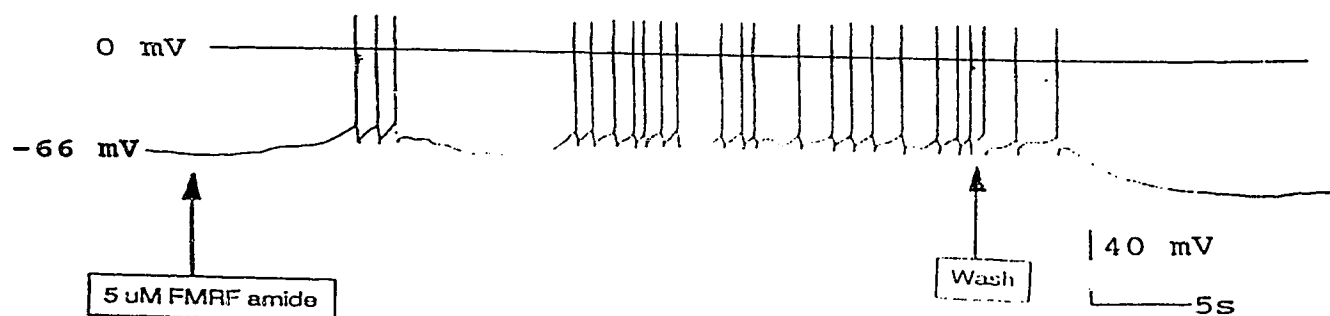


Figure 2. Effect of FMRFamide on the cluster of the identified neurons.

The identified neurons in the pedal ganglia were penetrated with 2M potassium acetate containing microelectrodes (50 - 80 MΩ). After stabilization (seal formation) the resting potential of this group of cells ranged between -70 to -50 mV. These neurons were normally silent. On application of 5 μM FMRFamide, however, they became active, firing repetitively with intermittent after-hyperpolarization. The effect of the neuropeptide had a short delay of and lasted until of wash-out with the control solution.

Figure 3

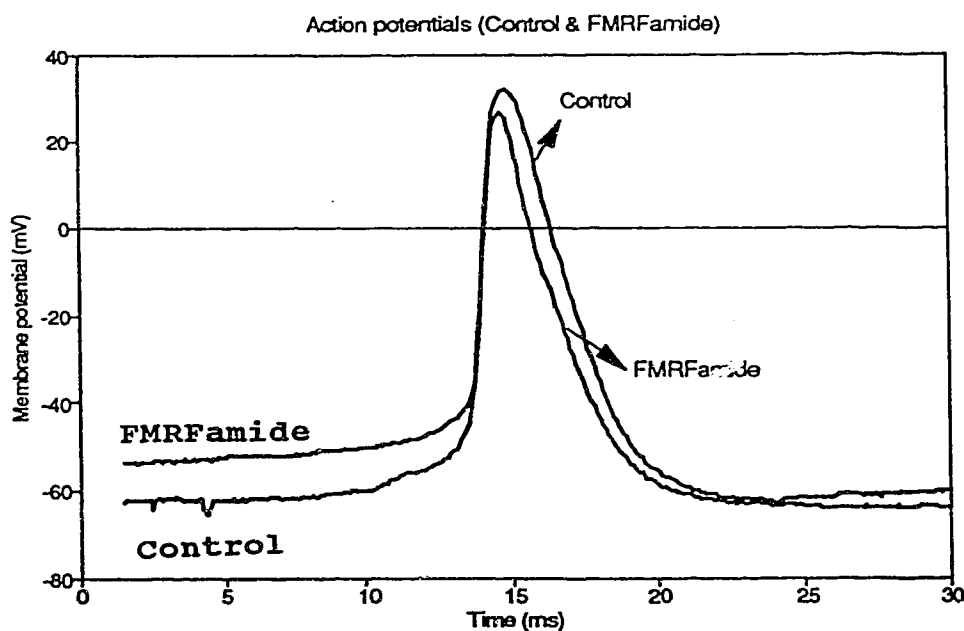


Figure 3. Effect of FMRFamide on spike width.

Superimposed on each other are control action potential and that recorded in the presence of the neuropeptide, FMRFamide. Table 3 indicates the means in resting potential, spike amplitude and half-width.

Table 3. Means of action potential properties of control and FMRF-amide applied cells. (means \pm std deviation: n = 3 cells).

| Properties | Control cells | FMRF-amide application |
|------------------------|----------------|------------------------|
| Resting potential (mV) | 60.3 \pm 7.0 | 42.4 \pm 6.8 |
| Spike Amplitude (mV) | 90.9 \pm 3.9 | 79.6 \pm 4.9 |
| Spike half width (ms) | 2.3 \pm 0.4 | 1.9 \pm 0.2 |

Table 4a. Spike analysis within a single neuron.

Properties of action potentials from five different FSN. The numbers are means \pm standard deviations (std; n = 50 samples).

| Properties | Cell 1 | Cell 2 | Cell 3 | Cell 4 | Cell 5 |
|--------------------------|-----------------|-----------------|-----------------|-----------------|-----------------|
| Resting potential (mV) | 60.5 \pm 3.3 | 60.2 \pm 4.7 | 60.3 \pm 7.0 | 60.4 \pm 5.5 | 60.2 \pm 4.71 |
| Spike amplitude (mV) | 90.9 \pm 2.9 | 90.9 \pm 3.4 | 90.9 \pm 3.9 | 91.2 \pm 3.1 | 91.1 \pm 3.5 |
| Half width of spike (ms) | 2.2 \pm 0.3 | 2.2 \pm 0.4 | 2.3 \pm 0.4 | 2.3 \pm 0.2 | 2.3 \pm 0.1 |
| Rise time (ms) | 1.9 \pm 0.3 | 1.8 \pm 0.2 | 1.7 \pm 0.2 | 1.8 \pm 0.3 | 1.8 \pm 0.4 |
| Maximum slope (V/s) | 107.0 \pm 2.7 | 106.5 \pm 2.9 | 103.3 \pm 3.2 | 106.0 \pm 3.3 | 107.0 \pm 2.2 |

Table 4b. Table of action potential properties of 3 different FSNs (cells were from different animals) means \pm std deviation: n = 10 samples.

| Properties | FSN1 | FSN2 | FSN3 |
|--------------------------|-----------------|----------------|----------------|
| Resting potential (mV) | 40.9 \pm 10.1 | 62.7 \pm 4.9 | 52.5 \pm 8.3 |
| Spike amplitude (mV) | 98.1 \pm 7.7 | 89 \pm 6.8 | 90.3 \pm 6.5 |
| Half width of spike (ms) | 2.4 \pm 0.5 | 2.2 \pm 0.3 | 2.5 \pm 0.6 |
| Maximum slope (V/s) | 107 \pm 2.7 | 104 \pm 5.8 | 102 \pm 4.6 |

Table 5. Means of spike widths of action potentials in intact ganglia and cultured cells (means \pm std deviation: n = 5 cells).

| Properties | Intact neuron | Cultured neuron |
|--------------------------|---------------|-----------------|
| Half width of spike (ms) | 2.3 \pm 0.3 | 2.7 \pm 0.2 |

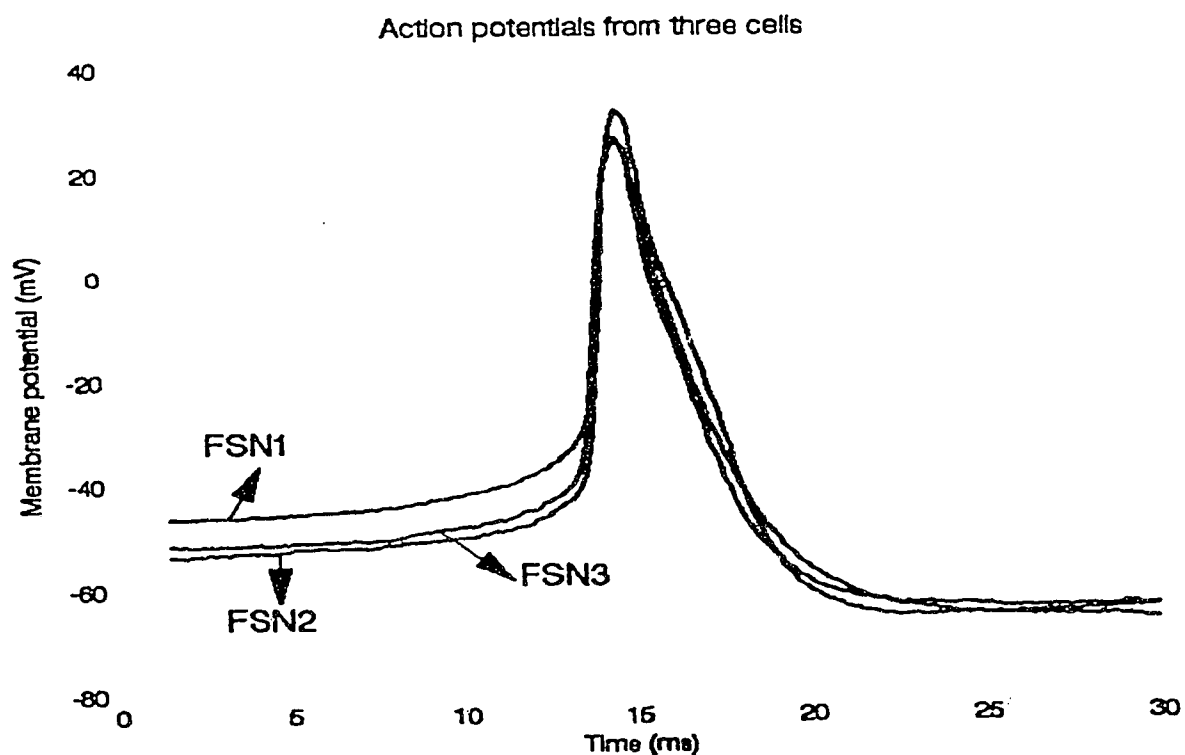
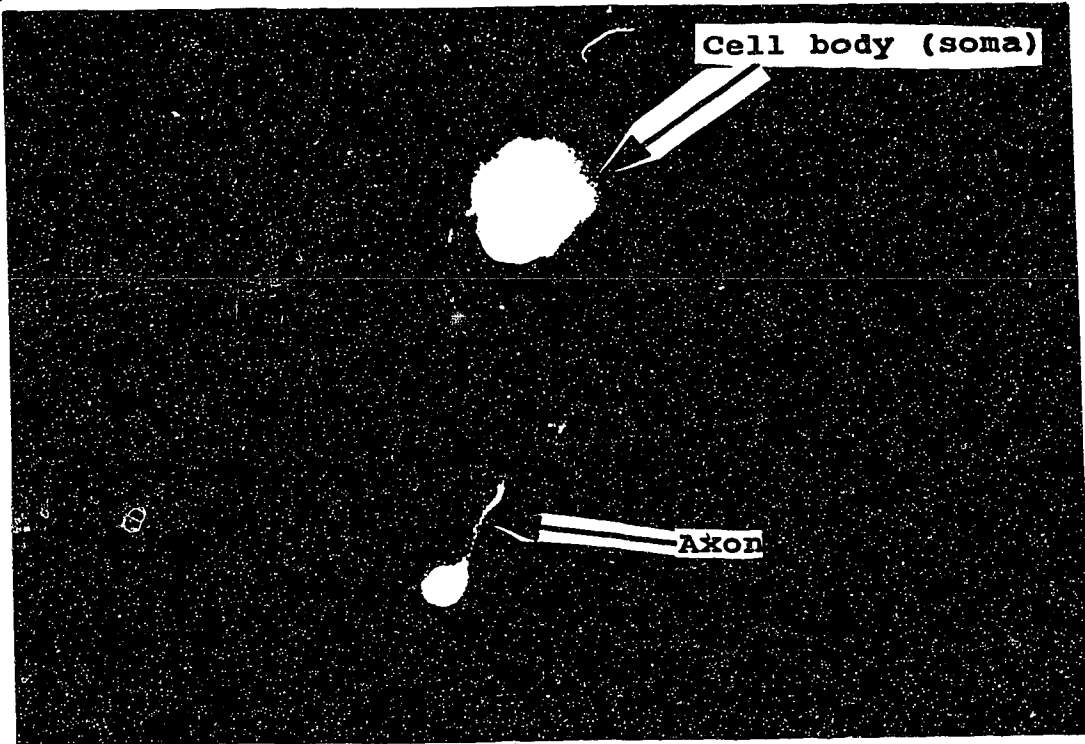


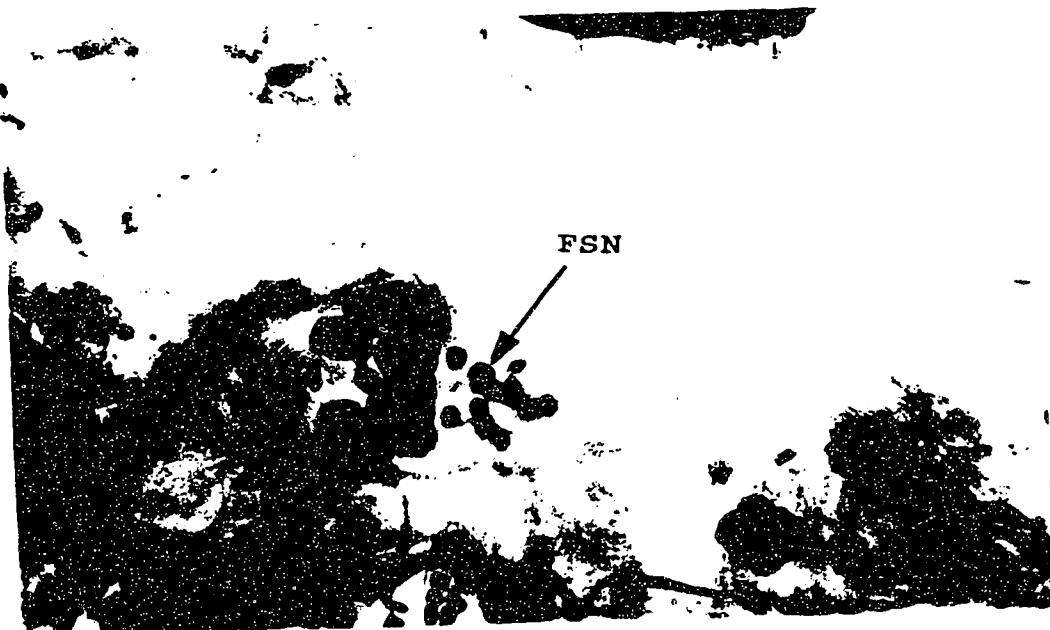
Figure 4. Spike waveforms from the FMRamide sensitive neurons (FSN).

Superimposed on each other are action potentials recorded from three different cells. Apart from the slight variation at the basal potentials the spike shapes were similar (see table 4). Though not evident here, there was usually a long period of hyperpolarization after the spike.

5a



5b

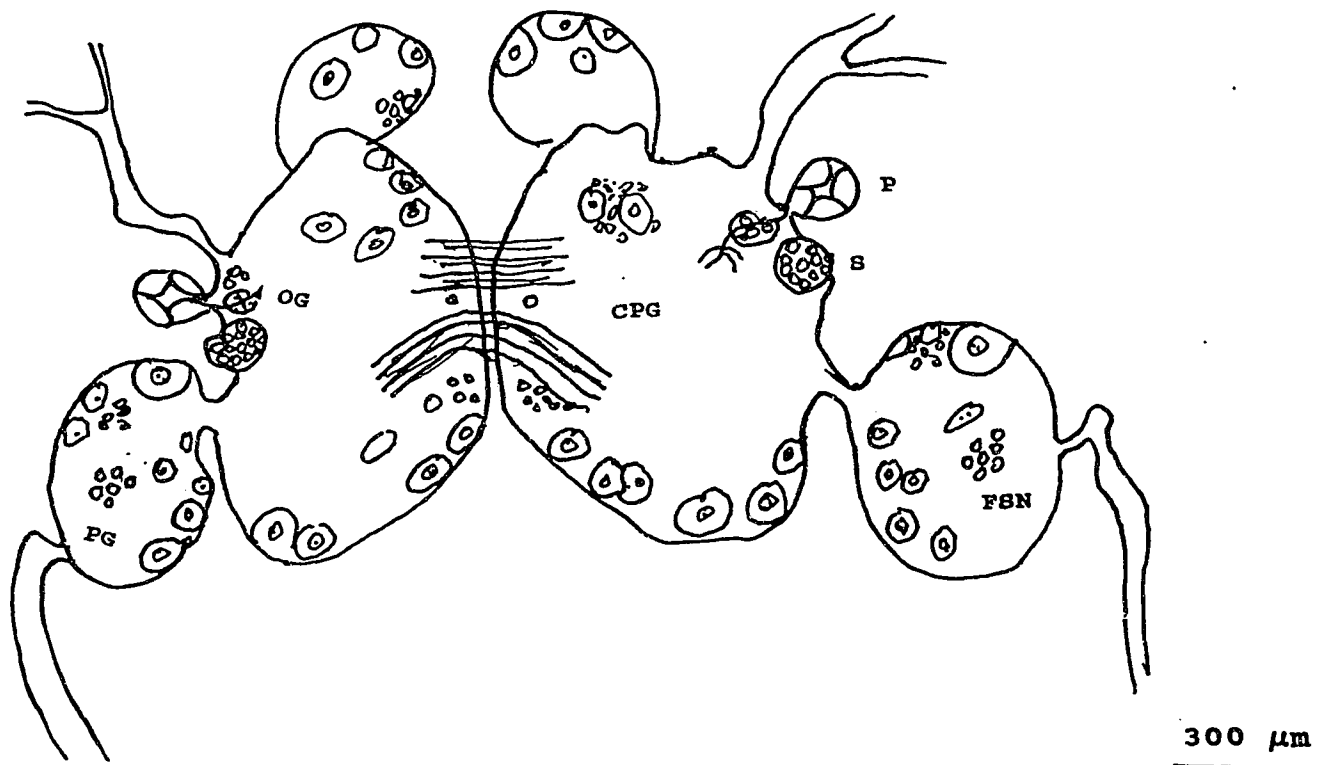


Figures 5a & 5b.**5a. Lucifer Yellow injected FSN**

Neurons were penetrated with an electrode with 5% Lucifer yellow in 1 M LiCl. The dye was injected into the cell with hyperpolarizing square pulses (1 - 7 nA) of 500 ms duration for about 20 minutes. The brains were then kept in a 4° refrigerator for about an hour for the dye to diffuse into the axons. The preparation were viewed using UV light and the appropriate filters. Picture shows the soma (s) and axon (a), with arrows.

5b. Nickel-Lysine backfilling

The nerve fibres which carry axons of the FMRFamide sensitive neurons were backfilled with a solution of nickel-lysine. The soma of the FSNS (see arrow) were labelled together with other large neurons in the pedal ganglia. As well, other neurons in the cerebropleural ganglia were labelled. Shown here are the studied neurons. Note, in this picture the pedal ganglion has been orientated in such a way as to make FSNS visible. Normally they lie underneath the layer of large superficial neurons.



6. Schematic diagram of labelled cells.

Shown here is a diagram of the nervous system of *Hermissenda crassicornis* and the labelled cells with nickel-lysine.

Key: CPG = Cerebro-pleural ganglia
 FSN = FMRamide sensitive neurons
 OG = optic ganglion
 P = photoreceptors
 PG = pedal ganglion
 S = statocyst

Stained axons from positively-stained cells were seen making their way into regions of unstained neurons. In the buccal ganglia immunoreactivity could be observed in the neuropil and few cells.

Figure 7a shows whole mount nervous system with RFamide labelling. The arrow points to two contralateral cells in the cerebropleural ganglia which showed consistent labelling. Axons from these cells terminated in the pedal ganglion where neuronal soma, together with varicose endings of the nerve fibres which stained positive to RFamide could be identified. None of the previously identified neurons in the cerebropleural ganglia (e.g. metacerebral giant neuron MGN), photoreceptor or the hair cells (Collin et al., 1988; Alkon, 1987) showed positive staining. I also was unable to match any of the identified adrenergic or dopaminergic neurons in H. C. (Sakakibara, et al., 1987) with the reactive cells in the cerebropleural ganglia. Interestingly, reactive cells were observed in the region between the photoreceptors and the hair cells. This region, contains the optic ganglia and has neuropil which is serotonergic (Land & Crow, 1985; Auerbach et al., 1989).

Positively stained cells and neuropil could be identified in the pedal ganglia (fig 7a). Invariably, contralateral immunoreactive cells were seen with neuropile around them exhibiting positive staining.

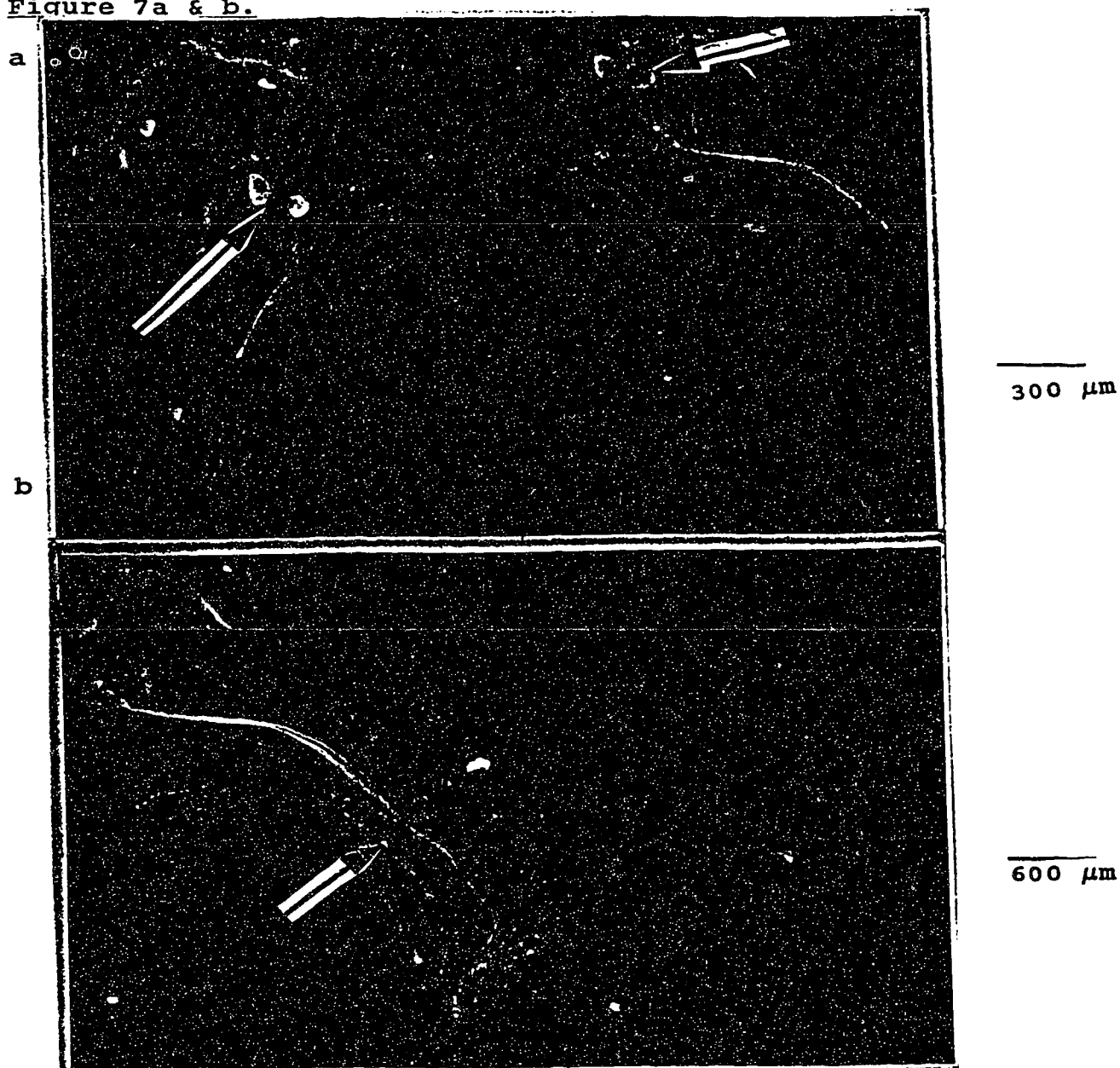
Figure 7a & b.

Figure 7. FMRFamide-like immunocytochemistry.

7a. Neurons which were reactive to polyclonal antibodies against FMRFamide are shown here. Cells in the cerebropleural ganglia were stained and axons from these neurons could be seen projecting into the pedal ganglia.

7b. In the pedal ganglia, few cells were labelled but several parts of the neuropile in the central region of the ganglia had intense labelling.

As seen in a more detailed picture (higher magnification: fig. 7b) several varicosities could be identified with FMRFamide like immunoreactivity. Stained cells were clustered and appeared to be smaller in diameter (30-60 μm). Even with whole mount preparations, stained axons were, occasionally, identified leaving the pedal ganglia (not evident in figure 7b). What was not seen, was immunoreactivity in the identified giant neurons in the ganglia (e.g. LP1). However, neuropil close to the giant neurons were occasionally seen with positive staining.

Cell Culture

The technique (ASW culture) employed in this study, for culturing neurons, has not previously been used for H. C. neurons. Sombati et al., 1989, have described a method for culturing H. C. neurons in ASW with 15 - 20 % fetal calf serum but it was found necessary to reduce the media to only ASW in order to eliminate, as much as possible, exogenous factors which influence neuronal growth. Neurons adhered to culture dishes and began to extend growth cones in about 3 - 5 hours after plating. Previous studies on primary cell culture of neurons from invertebrate species, such as Aplysia californica (Kaczmarek et al., 1979), Helisoma Trivolvis (Wong et al., 1981), Loligo Pealea (Parsons and Chow, 1989) and the leech Hirudo Medicinalis (Ready and Nicholls, 1979) have

indicated that the tips of growing neurites have growth cones and other growth-associated structures like filopodia and lamellapodia. However, neural fibres have been observed to elongate without any structural specialization of their growing tips (Lopresti et al., 1973). Presumably, neurite extension without growth cones is dependent on the level of localized calcium fluxes in growing neurons, because such growth can be induced in growing neurons of Helisoma Trivolvis by manipulation of extracellular calcium concentrations (Kater et al., 1988). I observed both forms of neuronal growth in H.C. pedal neurons.

Depicted in figure 8a. is a neuron (FSN), 4 hours after isolation from a pedal ganglion. The caption on the right compares the spike waveform in culture and that in the intact ganglia. In general, cultured cells had action potentials which were broader (see table 5). Presumably, this results from the removal of synaptic inputs in culture.

The soma of neurons sent out growth cones which subsequently gave out filopodia to probe the environment before the movement of cytosolic domains. This process has been described in other systems as well. Axons which were attached to their soma after trituration usually underwent the classical 'wallerian' degeneration before extending growth cones (fig 8b). Moreover, axons which failed to degenerate were capable of giving out growth cones and extending neurites. An SEM illustration of a retained axon in its

initial stage of growth is shown in figure 8c. Variations in the branching pattern of growing neurons were observed. There were usually a primary axon which branched into several neurites and the branching occurred until about the sixth day when recognizable growth ceased. The growth pattern described occurred in neurons with growth cone-associated neurites and those without (fig 8d & e). While neurons were usually unipolar, there were a few bipolar and multipolar cells as well. In addition, neurites of growing neurons could form anatomical synapses. Furthermore, in densely plated dishes, axo-somatic and soma-somatic synapses were observed.

Despite the heterogeneity in branching pattern and synapses seen in culture, I do not attribute these observations to the culture media. Rather, it is believed that such morphological complexity in growth may be typical of H. C. pedal neurons, for similar observations have been reported in Hermisenda neurons cultured in defined media (Sombati et al., 1989) and in other systems as well.

SEM pictures illustrating cells prepared using the two methods used for dissociation of neurons are shown in figure 9a & b). Removal of glial cells was more effective with dissociation method 2 than method 1.

Caption of fig 8a.

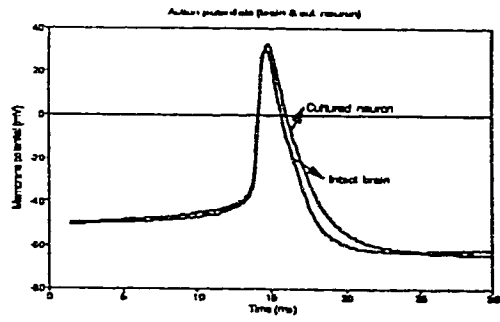
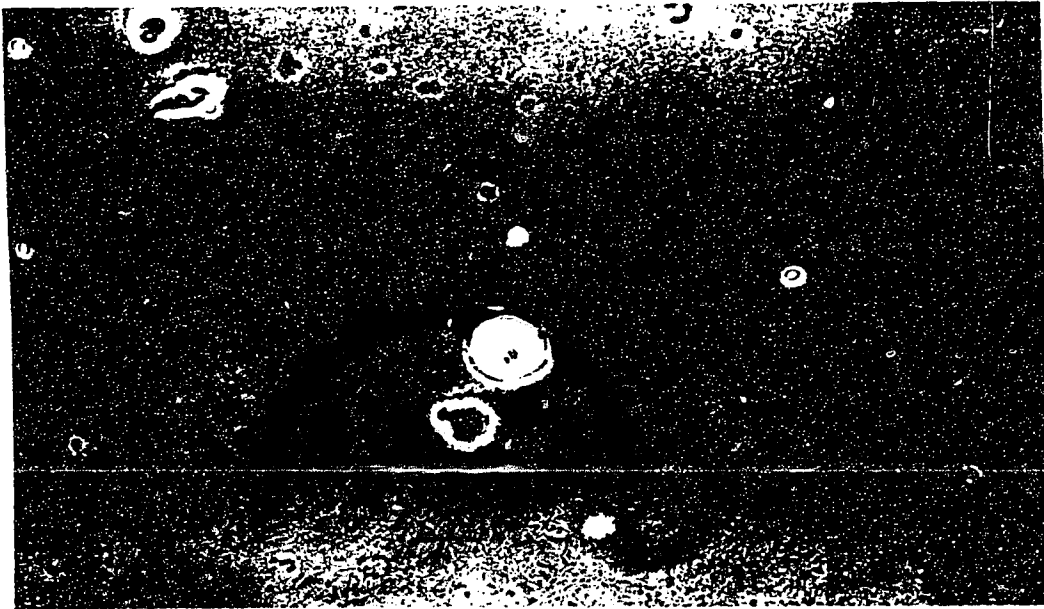
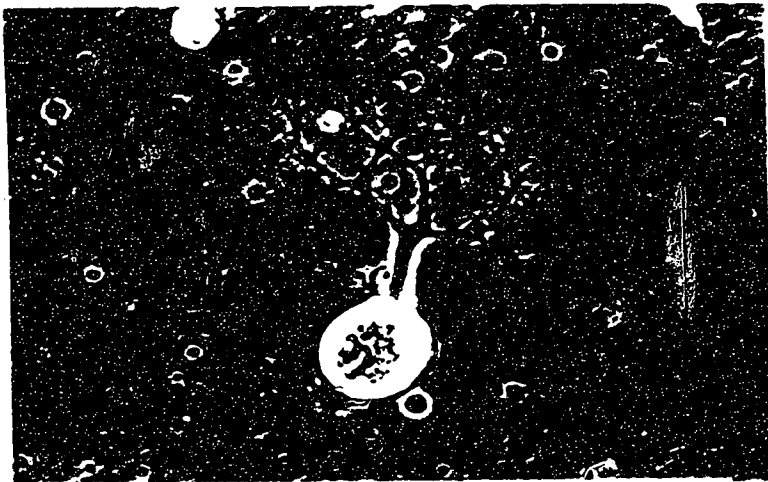


Figure 8a



40 μm

Figure 8b



30 μm

Figure 8c

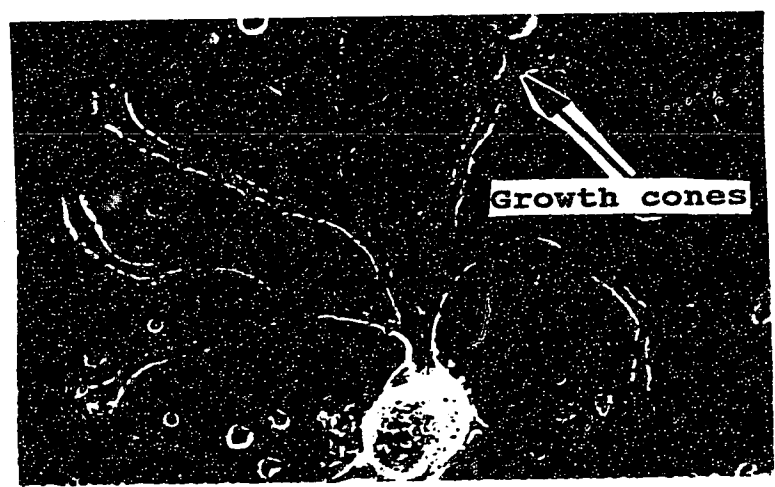


Figure 8d

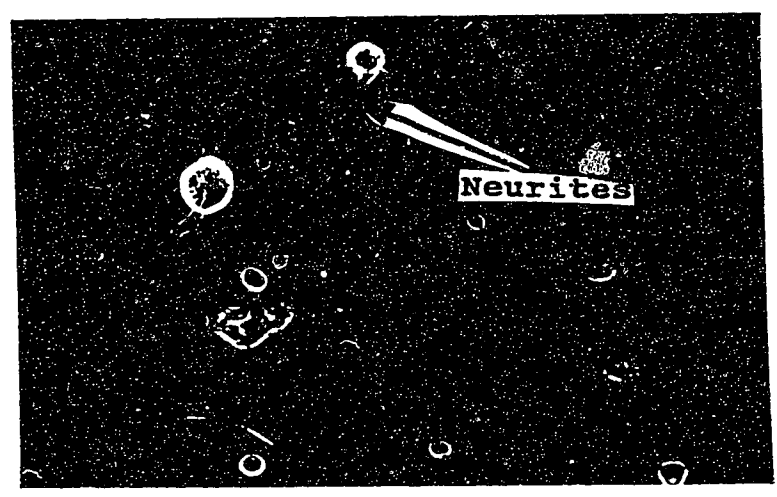


Figure 8e

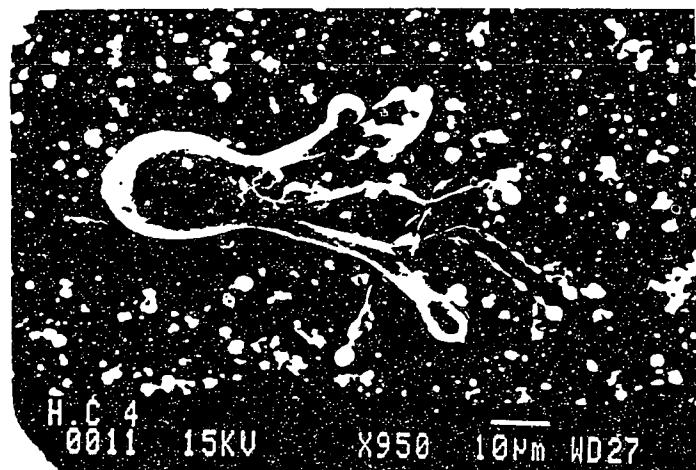


Figure 8a - e. Neurons in culture.

a. FSNs were isolated from the brain with a fire-polished-tipped pipette then triturated and plated in culture dishes. A 4 hour old neuron in culture is shown. The neurons began to grow at about 6-8 hours after plating. The caption shows action potentials recorded from neurons in intact brain and culture. In general however, spikes from cultured cells were broader.

b. Depicted here is a neuron which has been in culture for 48 hours. c & d. The two forms of growth patterns, one in which the extension of neurites were via growth cone and the other without. e. Scanning electron microscopic illustration of a neuron beginning to grow without the initial degeneration of a broken axon.

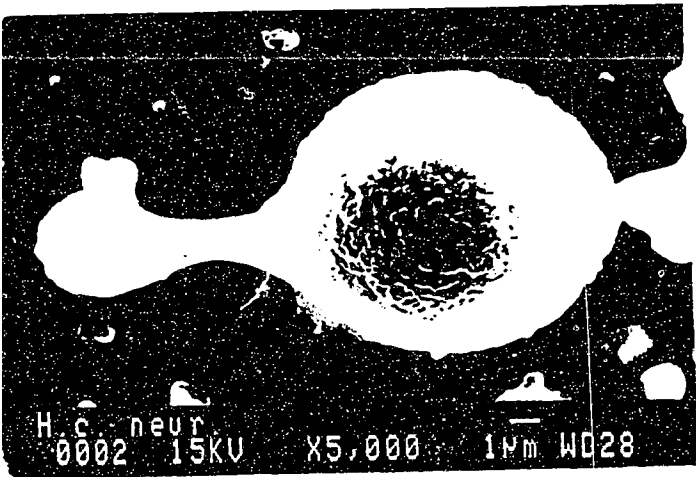


Fig. 9a & b. Enzymatic dissociation of neurons.

The two methods used for dissociation were assessed by scanning electron microscopy. Method 2 (b) removed surrounding connective tissue and glial cells while method 1 (a) did not.

DISCUSSION

In this section, I have demonstrated the physiological effect of FMRFamide on a cluster of neurons in the pedal ganglia of Hermissenda and have shown that these neurons have homogenous electrical properties. In addition, the presence of FMRFamide-like peptides in the nervous system has been shown.

Whereas the effects of FMRFamide and or its homologue have been described as excitatory in muscles (see Greenberg & Price, 1983 for review), the action of the peptides on neurons has been mostly inhibitory (Mackey et al., 1987; Piomelli et al., 1987; Cottrell & Davies, 1987; Kobayashi & Muneoka, 1989). The inhibitory actions of FMRFamide and its related peptides on neurons have been investigated and, almost invariably, the enhancement of potassium conductance of some sort and reduction in calcium currents have been implicated (Brezina et al., 1987a; Brezina et al., 1987b; Cottrell et al., 1984). In contrast to their inhibitory actions, FMRFamide peptides decrease potassium conductance and increase sodium currents (Cottrell & Davies, 1987) as well. Intuitively, the observation made in the present studies (increase in spike frequency and narrowing of spike width) on the action of FMRFamide can be explained by a reduction of potassium conductance (Yamoah, 1988). Hence, FMRFamide may modulate calcium influx via an action on potassium conductance.

Serotonin (5-HT) and FMRFamide are involved in the modulation of ionic currents, in the same cells in Aplysia, Helisoma and the prosobranch Rapana (Weiss et al., 1984; Kobayashi & Muneoka, 1990; Man-Son-Hing et al., 1989). In Hermisenda, it has been documented extensively that 5-HT may be involved in ionic current changes associated with associative conditioning (Farley & Wu, 1989; Crow & Forrester, 1986). The existence of FMRFamide-like neurons in the vicinity of the optic ganglia may be a good reason to test for the effect of the peptide on H. C. photoreceptors. FMRFamide and its related peptides have been shown to contain the carboxyl terminal sequence Arg-Phe-amide (Greenberg & Price, 1983) and it appears that this is the active terminus. Given that, care must be taken when results obtained from FMRFamide immunoreactive cells are interpreted. The results described only implicates the presence of a FMRFamide group of neuropeptides.

CHAPTER 3

Calcium Current

Preparation

FMRamide sensitive neurons were identified, treated with enzymes and isolated as described in chapter 2. Spherical cells without neurites were used throughout the experiments and to ensure this, only cultures which were less than 12 hours old were used in this section of the project.

Chemicals & Solutions

Nitrendipine, BayK 8644, ω -Conotoxin, BAPTA and Tetrodotoxin (TTX) were obtained from Calbiochem Behring Corp. (La Jolla, Ca.). HEDTA, EGTA, Mg-ATP, HEPES base, CdCl_2 and all other chemicals used were from Sigma Chemical Co. (St. Louis, MO). See table 2 for compositions of solutions.

Experimental Chamber

Cells were transferred to culture dishes (Falcon 1008) with freshly prepared experimental solution (see table of solutions; chap. 2) which was mounted on a mechanical stage on an inverted phase-contrast microscope (Diaphoto-TMD, Nikon, Japan). Mounted on the stage was a temperature-controlling device which used the Peltier effect. The temperature of the

experiments was maintained at 7 - 9°C.

Patch Clamp

Whole-cell calcium currents were recorded using the patch-clamp technique (Hamill et al., 1981). A 3 M-KCl agar electrode was dipped into the recording dish as the reference electrode. Patch pipettes were pulled with a Narishige PP-83 puller from plain haematocrit capillary tubes (Propper, New York, U.S.A) and had resistance of 0.2 - 0.8 M Ω . The series resistance (R_s) obtained with these electrodes varied between 1.7 and 3.5 M Ω (see appendix). Normally, a 20% R_s compensation was made. Seals were established with gentle suction at a tube connected to the pipette after it had touched the surface of the cell. Typically, the seal resistance was about 0.9 G Ω .

An axopatch 1B (Axon Instruments, Burlingame, CA) patch-clamp amplifier was used. Voltage commands were elicited and data collected with pClamp software on a Compaq 286 computer through a TL-1 Labmaster A-D board (Axon Instruments, Burlingame, CA). All recordings were filtered at 2 to 5 kHz after data acquisition. Some records were leak subtracted, averaged ($n = 7$) and scaled hyperpolarization steps of one-fourth amplitude. Leakage currents were subtracted on-line in other records using a proportional pulse (P/N) procedure with positive pulse and $N = 10$. The P/N method improved the

current resolution and reduced the time of the recording session. Also, this method replaced the need for whole-cell capacitance compensation. In a caption in figure 10 a non-leak corrected sodium current trace has been illustrated. This depicts the worst case for current resolution seen in the recordings. In figure 12 non-leakage current corrected calcium current traces have been shown. This can be compared with typical on-line leak current corrected traces in figure 14a. Except where indicated, the holding potential was -60 mV. The voltage traces shown were the protocols and not the actual voltages in the cells. Analyses of the data were made with pClamp (Clampan and Clampfit) and a Quattro-pro version of Lotus 123.

Accuracy of Voltage Clamp

A detailed analysis of series resistance and space clamp problems as pertained to the cells studied have been made and discussed in the appendix. None of the signs of space clamp problems were observed in the experiments. The shape of the current-voltage relationship for sodium and calcium current were close to bell-shape: an indication that the space clamp condition were closed to ideal. Taking both the experimental and theoretical assessment (appendix) together, it is reasonable to say that the voltage error associated with the voltage clamp experiments did not change the kinetics of the

calcium current significantly.

Isolation of Calcium Current

Initial experiments were conducted to determine conditions appropriate for measurement of uncontaminated calcium currents. In normal extracellular and pipette media the total membrane current recorded showed a transient followed by a slow inward current and then an outward current (figure 10). In the absence of extracellular sodium (choline replacement) and low calcium no inward currents were recorded but a transient and a delayed outward current became prominent. The transient outward channel was blocked with extracellular 5 mM 4-AP while the delayed current was removed with bath application of TEA (≥ 75 mM: figure 11). Internal dialysis with equimolar concentration of cesium, instead of potassium ions appeared to block all the outward currents, including a calcium activated potassium current. Hence by eliminating the transient inward current (sodium current: tetrodotoxin insensitive channels) with choline and the outward currents with 4-AP, extra and intracellular TEA and cesium, the remaining membrane current was only that of calcium. There were no evidence for the presence of chloride channels in these cells because a change in the extracellular concentration of Cl^- ions did not alter the magnitude of the current.

Evidence for calcium current

After blockage of outward currents and elimination of sodium currents the remaining membrane current had these properties: (a) The magnitude of the current was dependent on extracellular calcium concentration. (b) The channels through which the current was carried was selectively permeable to the divalent cations, strontium and barium. (c) The inorganic cations, cadmium, lanthanum, cobalt, and nickel and the organic compound, ω -conotoxin blocked the current (d) The current-voltage relation predicted a reversal potential of the charge-carrier to be very positive ($> +80$ mV). All these, were indications of the presence of calcium channels.

Results

All experiments were done at $7 - 9^{\circ}$. Shown in figure 12 are calcium current traces before leakage current subtraction. Recordings were obtained under conditions in which I expected close to pure calcium currents. Sodium ions in the external media were replaced with choline ions and outward currents suppressed with 100 mM external TEA, 5 mM 4-AP and potassium ions in the pipettes replaced with cesium and TEA (see table 2). If there were substantial outward current contamination of calcium currents I expected it to have shown up as a resultant increase in the rate of decay of the inward current

at more positive potentials. Figure 13 depicts two current traces generated by holding an identified neuron at -60 mV and jumping to $+10$ and $+40$ mV. At each step potential a similar peak current magnitude was elicited but the inactivation was more pronounced at $+10$ than at $+40$ mV.

Not only did this observation imply that outward current contamination of I_{Ca} was close to absent but it gave evidence to suggest that the decay of the current might not be strictly voltage dependent. Thus the inactivation of the calcium current was real.

Calcium Current Activation

Figure 14a shows a family of calcium current traces generated by holding neurons at -60 mV and stepping to different voltages (step voltages have been indicated on the traces). Each trace was made up of, at least, five runs of recordings. In figure 14b, a current-voltage plot obtained from records of peak and steady state currents, when neurons were held at -80 mV, has been illustrated. Currents activated at about -30 mV, peaked at about 20 mV and declined with increasing voltages.

Figure 10

Total Membrane Current Traces.
Holding Potential = -60 mV

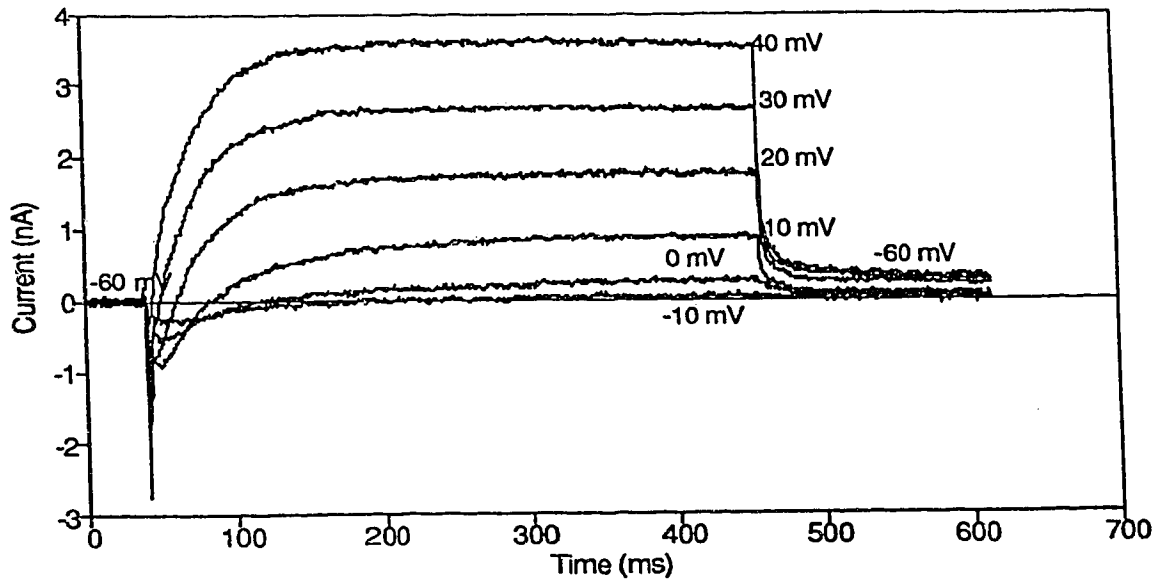


Figure 10 Whole cell membrane current traces.

Total membrane currents recorded with extracellular 300 mM Na^+ , 10 mM Ca^{2+} , and intracellular 300 mM K^+ as charge carriers. The holding potential was -60 mV and current records were filtered at 2 kHz. Leakage and capacitive currents were subtracted on-line. On a caption below are traces of non-leak corrected sodium current traces. Recordings were made in the absence of Ca^{2+} and at conditions in which outward currents have been suppressed with pharmacological blockers. Experimental temperature was 8°C.

Sodium current traces.
No leakage correction

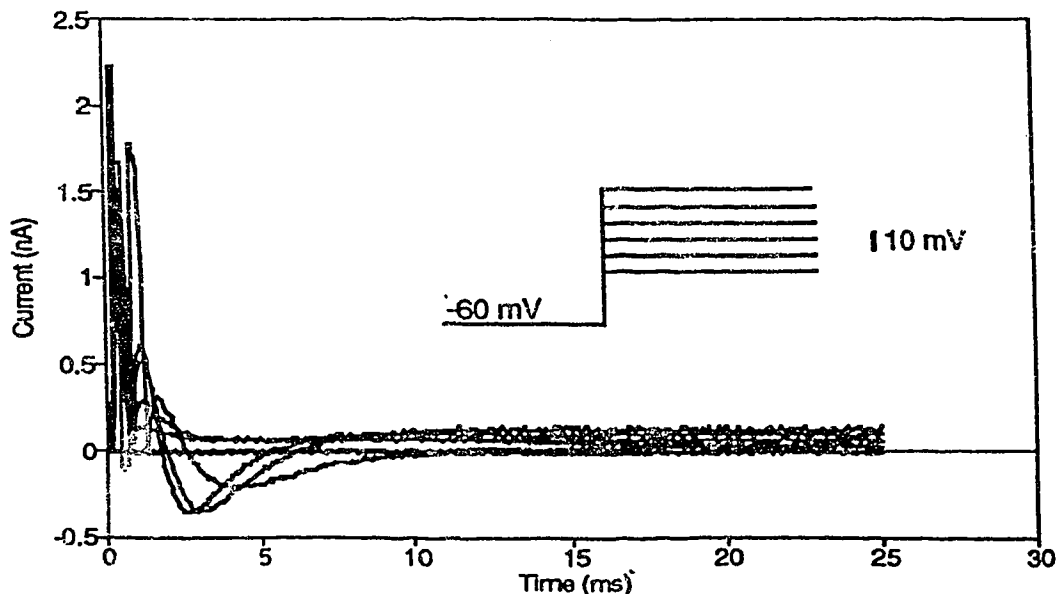


Figure 11 Effect of 4AP & TEA on I_k & I_f
H.P. = -80mV S.P. 5mV.

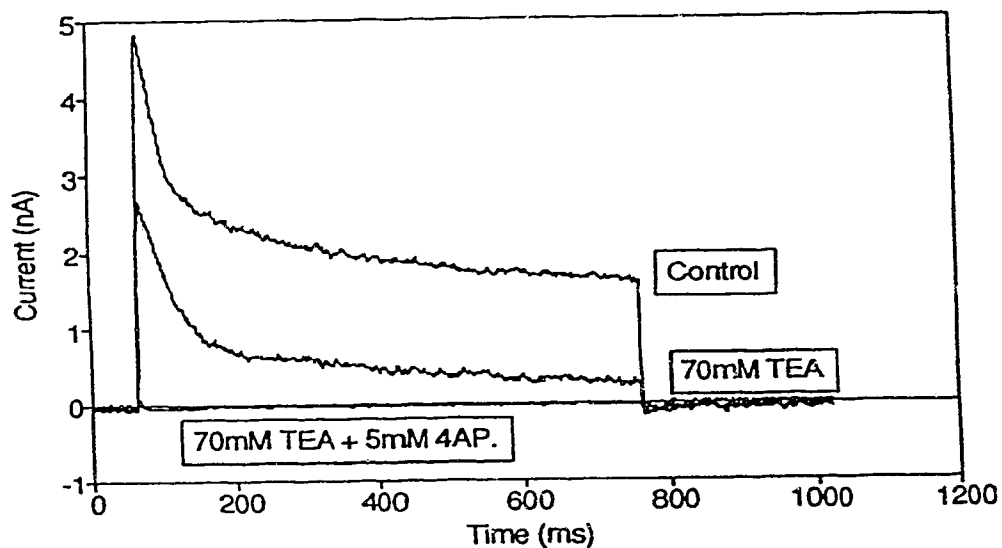


Figure 11. Pharmacology of outward currents.

Membrane currents were recorded in the absence of both sodium and calcium ions (choline substitution). The control trace was elicited from -80 mV holding potential. Typically, a fast transient outward current appeared which was followed by a delayed current. 70 mM TEA, or more, removed the delayed current and 5 mM 4-AP, blocked the fast channel.

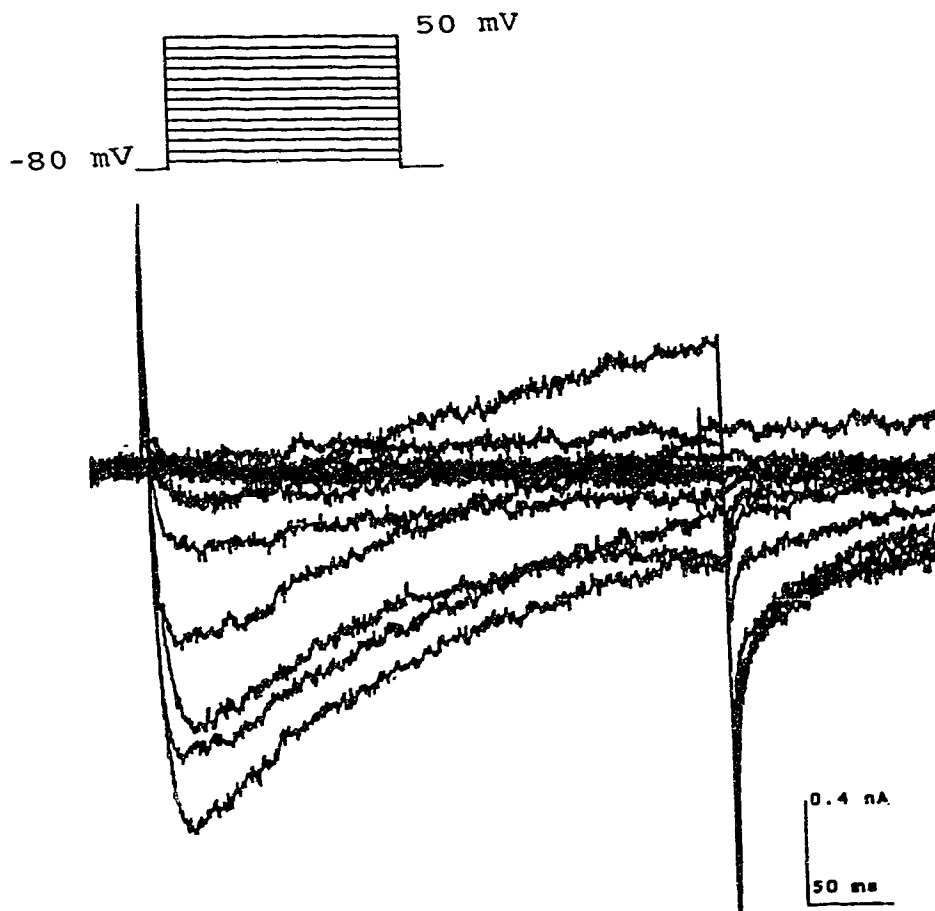


Figure 12 Calcium current traces without leakage-current correction.

Illustrated here are combined traces of active calcium and passive leakage current traces. Cells were held at -80 mV and stepped to test voltages indicated.

When cells were held at potentials more negative than -80 mV, there was no significant change in the maximum current recorded. Superimposed on the same plot is the steady state current voltage relationship. The points are the mean of points between 600 ms and 700 ms after application of 730 ms pulses. Prominent 'shoulders' were not observed in both the peak and steady state IVs. The absence of different peaks on the IV is indicative of the fact that most, if not all, of the channels belong to one population of calcium channels. The other likely explanation will be that there are two calcium channel subtypes with similar steady state current-voltage relations.

The presence of two distinct populations of calcium channels usually results in two phases of the decay of the total current (Armstrong & Matteson, 1985). It will be shown later in the section on current inactivation that, two time constants could be determined for the relaxation of I_{Ca} , however this could only be obtained when the extracellular $[Ca^{2+}]$ was high (≥ 10 mM). Thus, the two time constants were induced by calcium and did not result from two sub-types of channels. Furthermore, based on the sensitivity of a large portion of the channels to cadmium ions and ω -conotoxin I worked with the hypothesis that one type of calcium channel was predominant in the identified neurons. The presence of a small population of a low-voltage-activated channel in FSN would be discussed later.

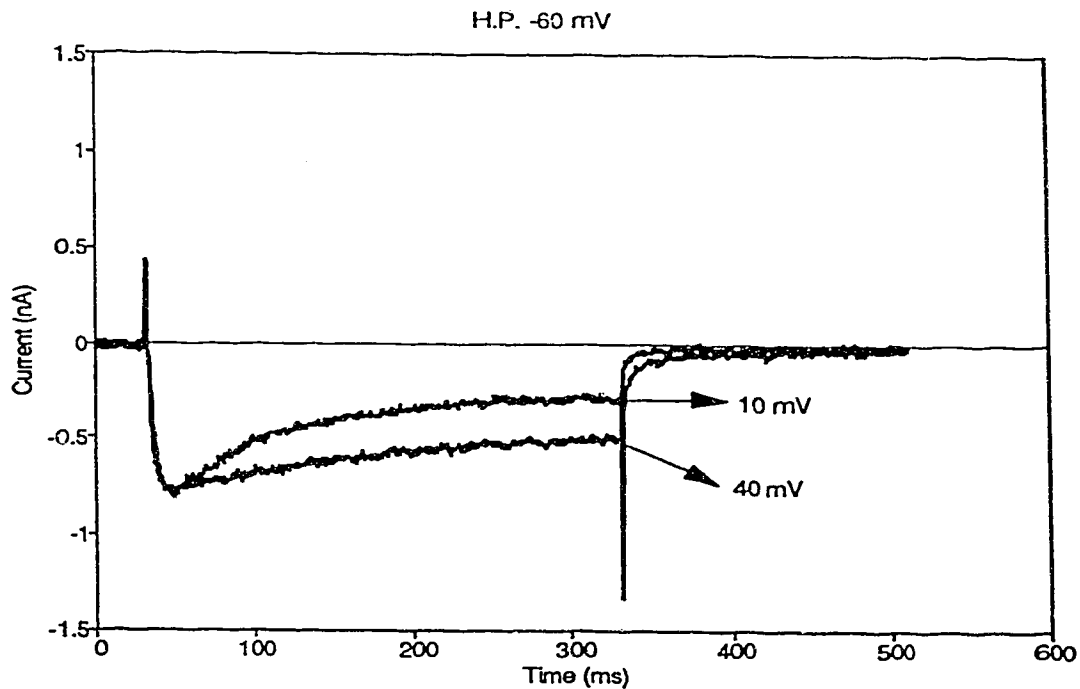
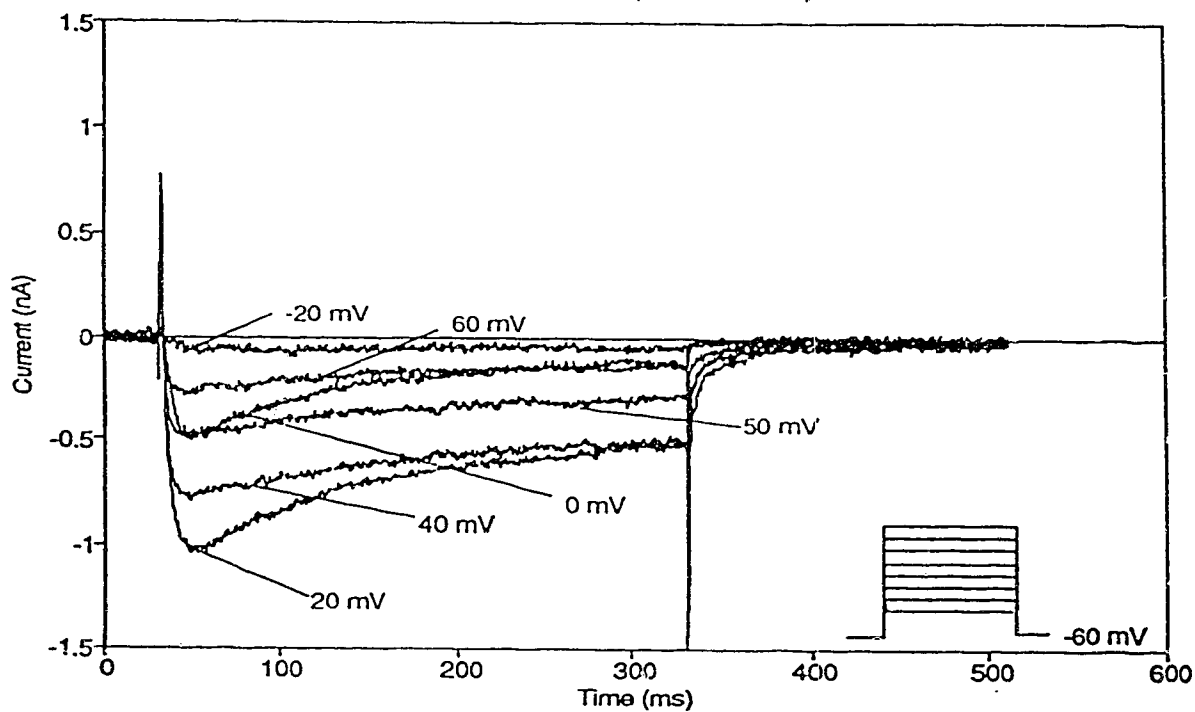


Figure 13. Evidence for uncontaminated calcium current.

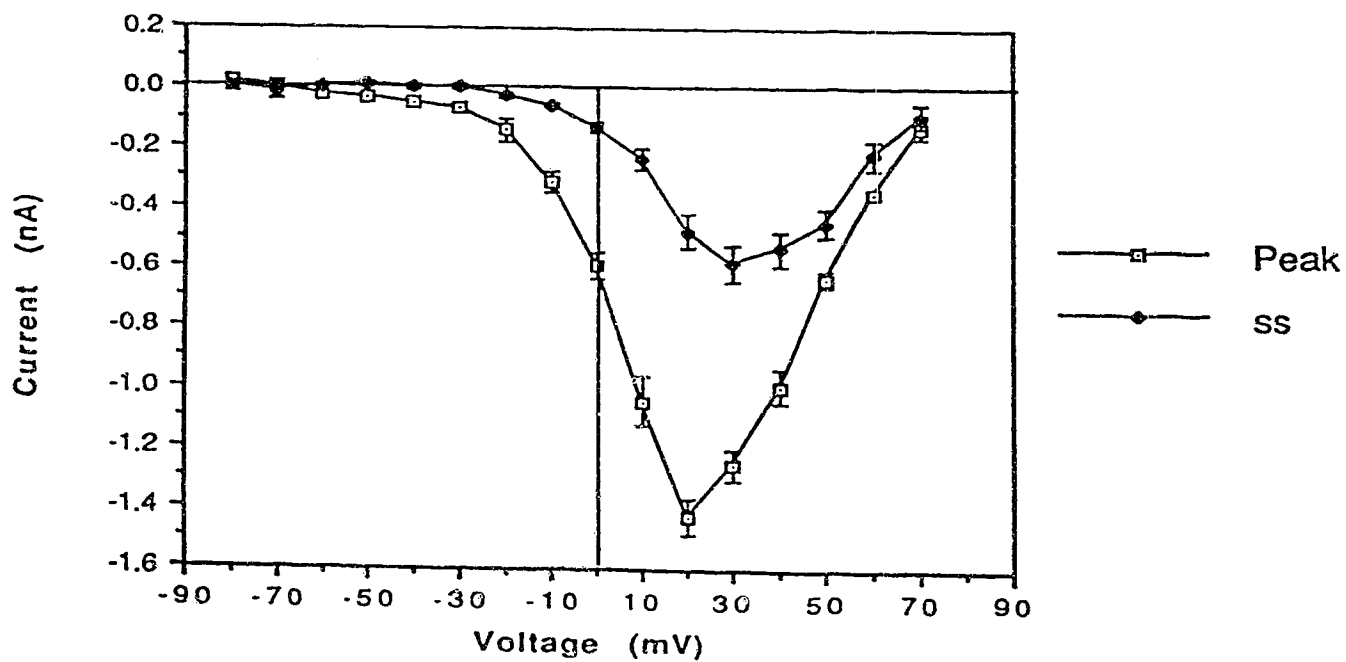
The masking effect of outward currents in calcium current records should be seen at positive potentials when the driving force of I_{Ca} is decreasing but outward currents are increasing in magnitude. Thus at higher positive voltages the decay of I_{Ca} should have been more rapid if there were substantial outward current contamination. Depicted here are two I_{Ca} traces all of which were generated from a holding potential of -60 mV and stepped to +10 and +40 mV. Both voltages elicited currents of similar peaks but different inactivation profiles. Less inactivation was seen at more positive potentials, suggesting that the inward calcium current recorded was close to being pure.

14a

Calcium current traces (HP = -60 mV)



14b

Peak & Steady state I-Vs at H.P. -80 mV
(n = 14 cells for peak & n = 15 cells for ss)

14c

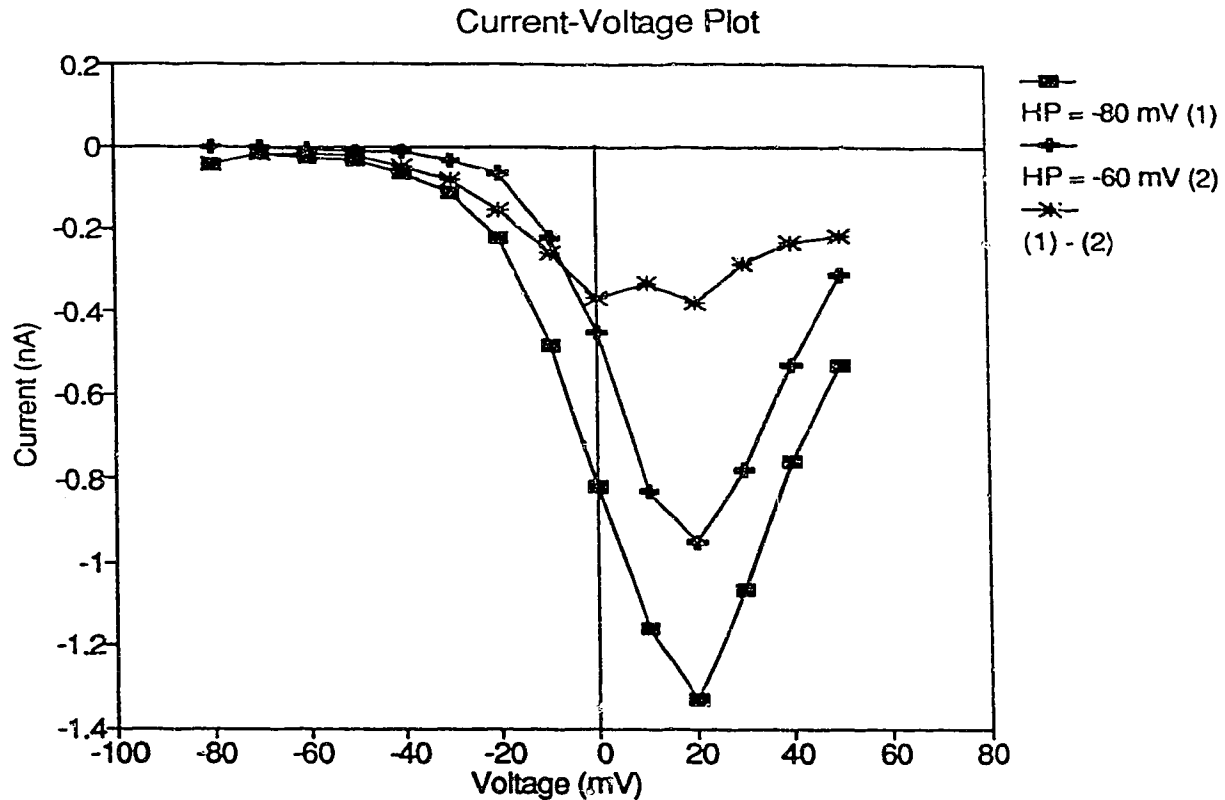


Figure 14a-c. Current traces and I-V relations

Family of calcium current traces obtained from -60 mV to the step potentials shown. Currents were elicited with rectangular pulses and extracellular calcium was 10 mM. Leak currents were subtracted from the traces on-line. Each trace is made of means of at least 5 runs. From -60 mV the current activated around -30 mV, increased till it reached maximum level at +20 mV and declined as the step potential approached the apparent reversal potential of calcium. **b.** A current-voltage curve obtained from holding several cells at -80 mV is shown here ($n = 14$ cells; mean \pm std. error). Note that the steady state IV plotted from points between 600 to 700 ms also peaked around +20 mV. **c.** When cells were held at different voltages and the IVs compared it was clear that at all voltages the profiles of the curves were similar.

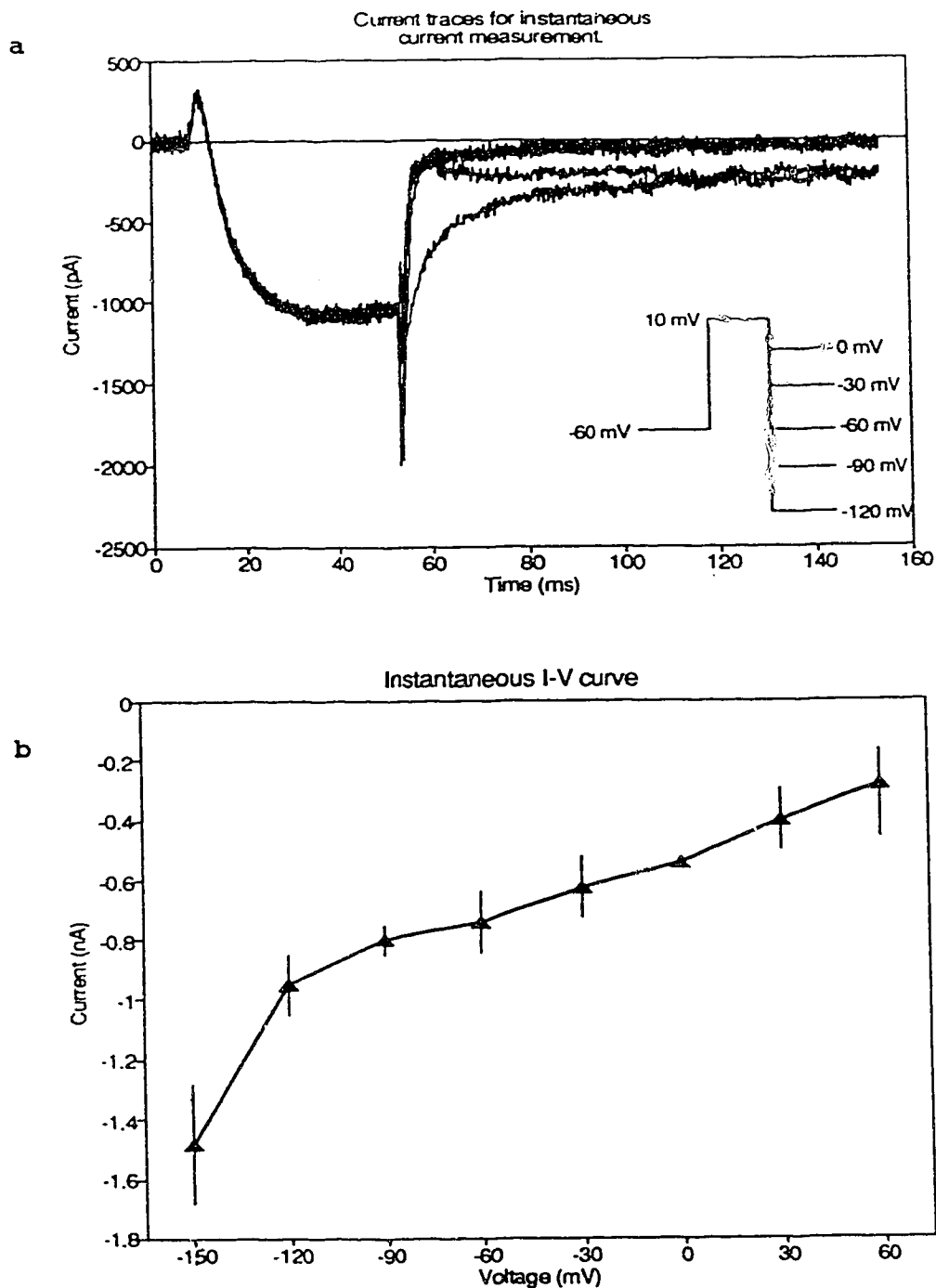


Figure 15a & b Instantaneous current-voltage relation.

A brief voltage pulse was elicited to activate the calcium channel followed by step voltage to different potentials (a) to measure the instantaneous currents. The resulting current-voltage relation is shown (b). The non-linear behaviour of the curve suggests a non-ohmic channel.

As the external calcium concentration was varied from 6 mM to 10 mM, the activation kinetics of the current remained unchanged but the current magnitude increased in accordance with the independence principle and constant field theory (equation 1: Hodgkin & Katz, 1949; Hodgkin & Huxley, 1952). The constant field equation (equation 3-1) is an approximation of the ionic permeation between two asymmetric domains with non-ohmic electro-diffusion properties. Simplified, it may appear, however, this is the only available equation which adequately describes the calcium currents (see figure 15a & b) for the non-linear characteristics of the instantaneous current-voltage relationship). Hence it was adopted to fit the current-voltage relationship.

$$P_{Ca} = I_{Ca} \left(\frac{RT}{4F^2} \right) \left(\frac{1}{[Ca] V} \right) \frac{(e^{2VF/RT} - 1)}{(e^{2(V-V_r)F/RT} - 1)} \dots \dots \dots (3-1)$$

On the assumption that the permeability (P_{Ca}) of Ca^{2+} at any given potential is constant, we expressed equation 1 as:

$$\frac{I_{Ca_1}}{I_{Ca_2}} = \frac{[Ca_1]}{[Ca_2]} \frac{(e^{2(V-V_{r1})F/RT} - 1)}{(e^{2(V-V_{r2})F/RT} - 1)} \dots \dots \dots (3-2)$$

where $[Ca_1]$, V_{r1} , and $[Ca_2]$, V_{r2} , are the concentrations and estimated reversal potentials for 6 mM and 10 mM external calcium respectively. In figure 16 the IV plot of different $[Ca^{2+}]_e$, 6 mM and 10 mM, has been superimposed. As well, the predicted IV for 10 mM external calcium simulated from equation 2 has been plotted with dotted lines.

$$V_r = \frac{RT}{2F} \ln \left(\frac{[Ca^{2+}]_e}{[Ca^{2+}]_i} \right) \dots \dots \dots (3-3)$$

The reversal potentials were calculated from the Nernst equation, (equation 3 - 3). The $[Ca^{2+}]_i$ value was the pipette calcium concentration which was estimated with a computer program which took into consideration all ions present in the internal solution including ATP and EGTA (E. Stanley; personal communication). Also, I considered calcium sensitive electrode measurement of our 'low calcium' solution recorded as 30 - 50 μ M $[Ca^{2+}]_{free}$ from the impure salts used to constitute the intracellular solution. Taken together, the estimated $[Ca^{2+}]_i$ used for the calculation of V_r was 1.2×10^{-9} M. At 9°C, the reversal potential for 6 mM and 10 mM $[Ca^{2+}]_e$ worked out to be 187 mV and 193 mV respectively. The membrane conductance for calcium as estimated from the slope of the linear portion of the ascending limb of IV-plots (figure 15)

was 17.5 nS for 6 mM and 29.0 nS for 10 mM external calcium.

Steady state activation and voltage relationship of the calcium current indicated a right shift of about 2.5 mV as $[Ca^{2+}]_e$ was raised from 6 mM to 10 mM (fig 17a & b). Both barium and strontium ions shifted the steady state-voltage curves in the negative directions (see figure 18a-c). The curves were fitted with a Boltzmann equation using a standard least square regression fit method. A left shift of the steady state activation curve implies an increase in the availability of channels for activation at a given voltage.

The time course of activation for calcium and strontium currents were similar (table 6). However when barium was used as the charge carrier, the channels were more available for activation and the time course faster than in calcium. The two $[Ca^{2+}]_e$ had comparable steady state activation kinetics (fig. 17a & b). Activation of the channel was therefore independent of the divalent ion species, except barium current, or concentration but dependent on the transmembrane potential. Increasing $[Ca]_e$ increased the current magnitude. After allowing for about 1.5 ms delay in the activation profile, I could fit a single exponential to the calcium current. The time constant of I_{Ca} activation ranged between 0.9 and 8 ms, depending on the membrane potential.

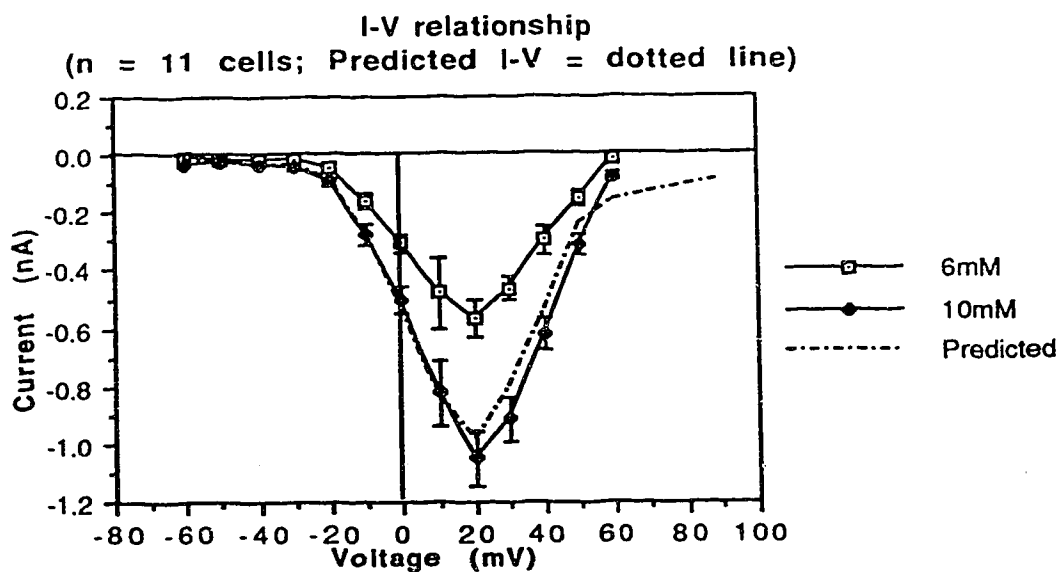


Figure 16. I-Vs at different $[Ca^{2+}]_e$ and a simulated one.

The current magnitude increased as the bath $[Ca^{2+}]$ was raised, however beyond 20 mM the system saturated. The IVs for two different $[Ca^{2+}]_e$ have been shown here (n = 11 cells) and the predicted curve for 10 mM calcium is shown with a dotted line (see text).

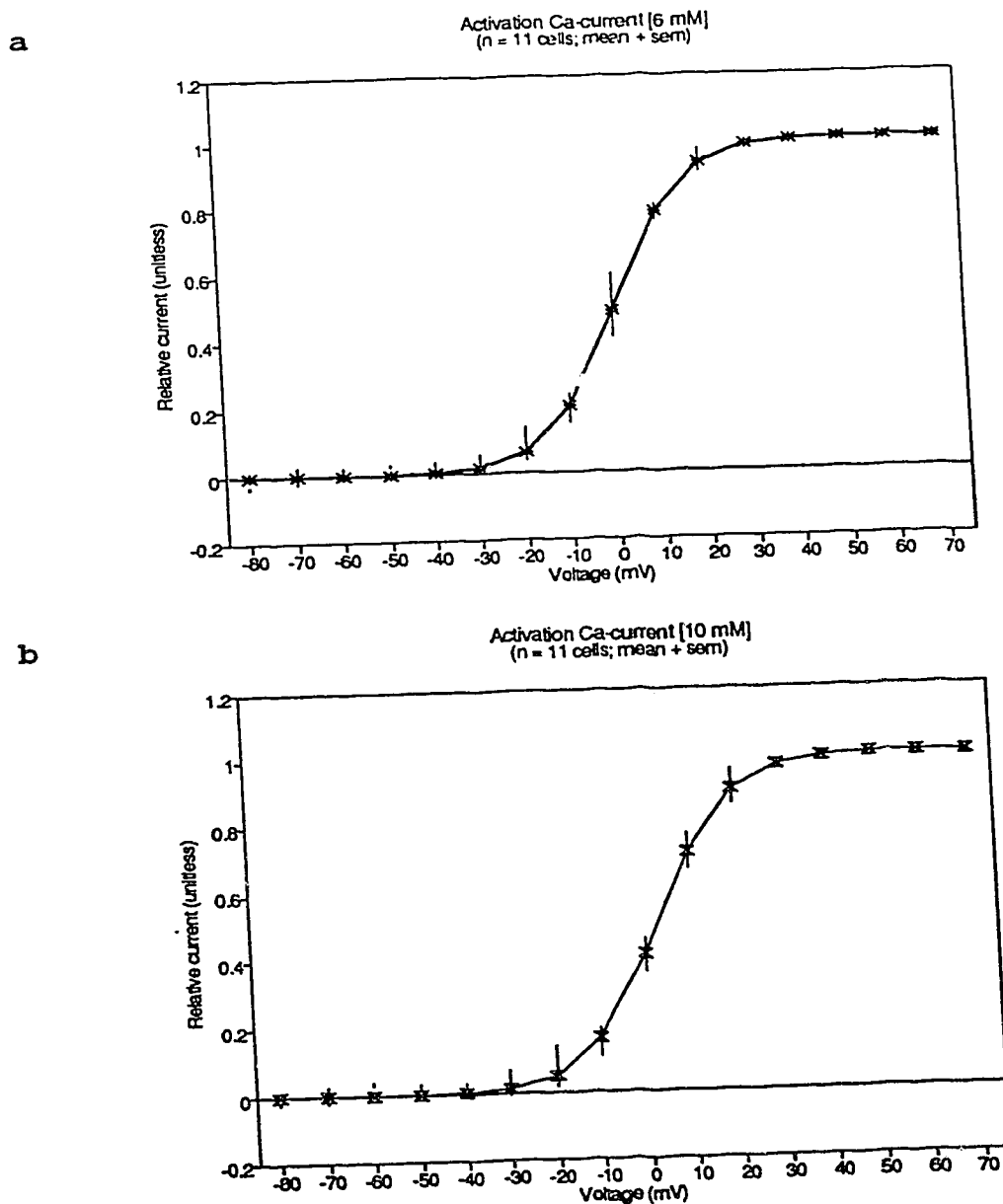


Figure 17a & b. Calcium current activation.

The steady state activation of I_{Ca} was well fitted with the Boltzmann's equation of the form;
 $m_{\infty} = [1 + \exp((V_{1/2} - V) / K_m)]^{-1}$, where $V_{1/2}$ is the half activation voltage and K_m is a slope factor. **a.** $V_{1/2}$ for 6 mM $[Ca^{2+}]_e$ curve was at 0.4 mV and that of **(b)** 10 mM was at 2.9 mV. The slope factors for 6 and 10 mM were 7.9 and 7.7 respectively.

Illustrated at figure 19 is the activation time course of a current trace elicited from -60 mV resting potential to 10 mV and the natural logarithmic plot used to determine the time constant.

The activation of the current was assumed to behave close to the Hodgkin and Huxley-style model. Accordingly, the gating transition of the channel between open and close states were described in terms of the forward (α) and backward (β) rate constants. The α s and β s are functions of voltage and gating of the channel in 6 mM and 10 mM external Ca^{2+} were described as:

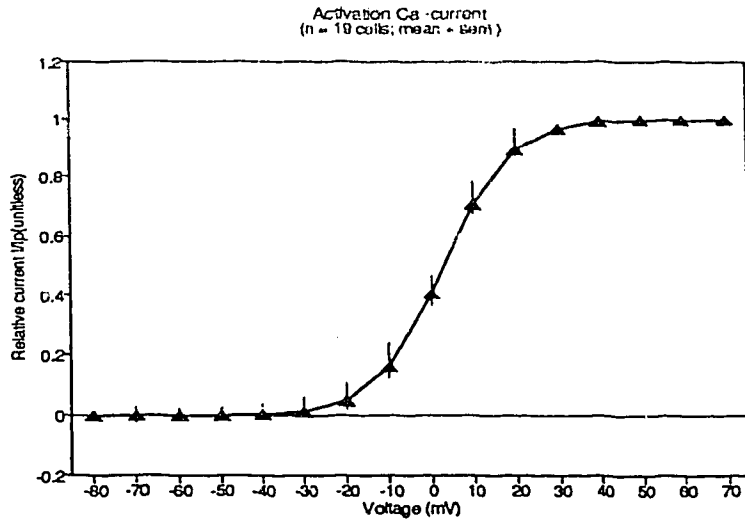
$$\alpha = 500 e^{28.6(V-38)} \dots\dots\dots (3-4) \quad 6mM$$

$$\beta = 27 e^{16.7(0.005-V)} \dots\dots\dots (3-5) \quad 6mM$$

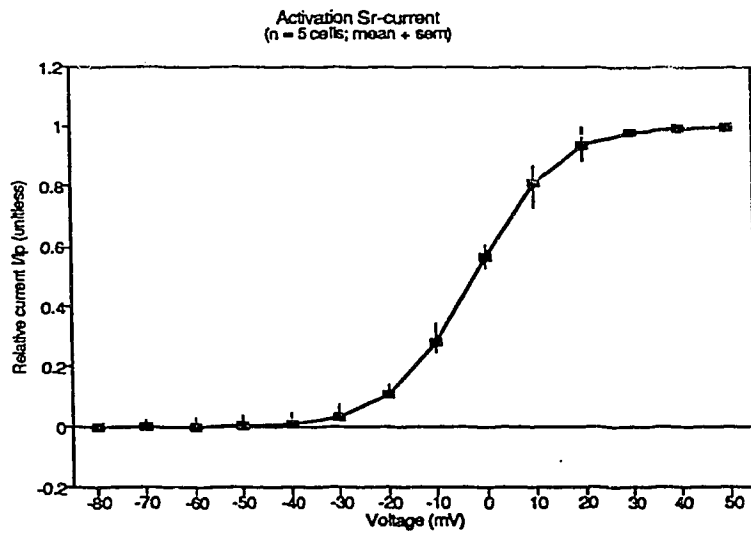
$$\alpha = 515 e^{30.2(V-40)} \dots\dots\dots (3-6) \quad 10mM$$

$$\beta = 42 e^{19.7(0.01-V)} \dots\dots\dots (3-7) \quad 10mM$$

a



b



c

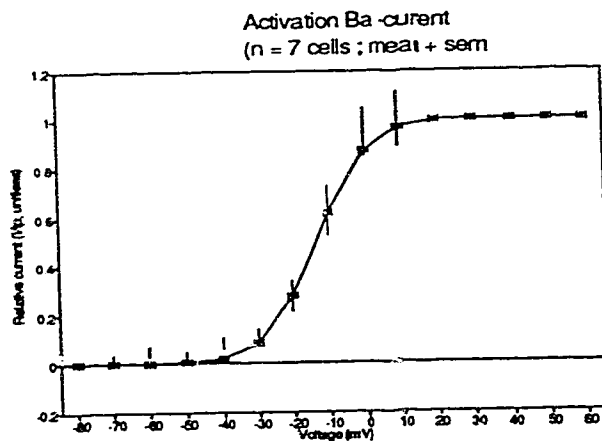


Figure 18a-c. Current activation for Ca²⁺, Sr²⁺ and Ba²⁺.

Other divalent cations, strontium and barium permeate the calcium channel. Illustrated here are the steady state activation curves for the three ions. The *n* (number of cells) for each experiment and the Boltzmann's equation fit have been indicated. The fit was done with a standard least square regression analysis. Both Sr²⁺ and Ba²⁺ shifted the activation curve to the left, with the shift being pronounced in barium solution (≈15 mV).

Table 6. Time-to-peak of calcium, strontium and barium currents. (number of cells = 5: mean \pm error)

| Membrane potential (mV) | I _{Ca} . Time to peak (ms) | I _{Sr} . Time to peak (ms) | I _{Ba} . Time to peak (ms) |
|-------------------------|-------------------------------------|-------------------------------------|-------------------------------------|
| -40 | - | - | 11.5 \pm 2.3 |
| -30 | 9.4 \pm 1.2 | 11.3 \pm 1.5 | 8.4 \pm 2.5 |
| -20 | 12.6 \pm 3.8 | 10.6 \pm 2.2 | 5.7 \pm 1.4 |
| -10 | 8.2 \pm 0.9 | 7.9 \pm 3.4 | 3.1 \pm 1.8 |
| 0 | 6.3 \pm 1.3 | 7.1 \pm 2.6 | 3.0 \pm 2.6 |
| 10 | 4.9 \pm 1.5 | 5.1 \pm 2.0 | 3.2 \pm 1.6 |
| 10 | 4.2 \pm 0.6 | 4.8 \pm 1.0 | 2.9 \pm 0.8 |
| 20 | 2.2 \pm 1.0 | 2.4 \pm 0.7 | 1.1 \pm 0.4 |
| 30 | 2.1 \pm 0.8 | 1.9 \pm 0.9 | 0.9 \pm 0.3 |
| 40 | 1.1 \pm 0.4 | 1.3 \pm 0.6 | 0.7 \pm 0.4 |

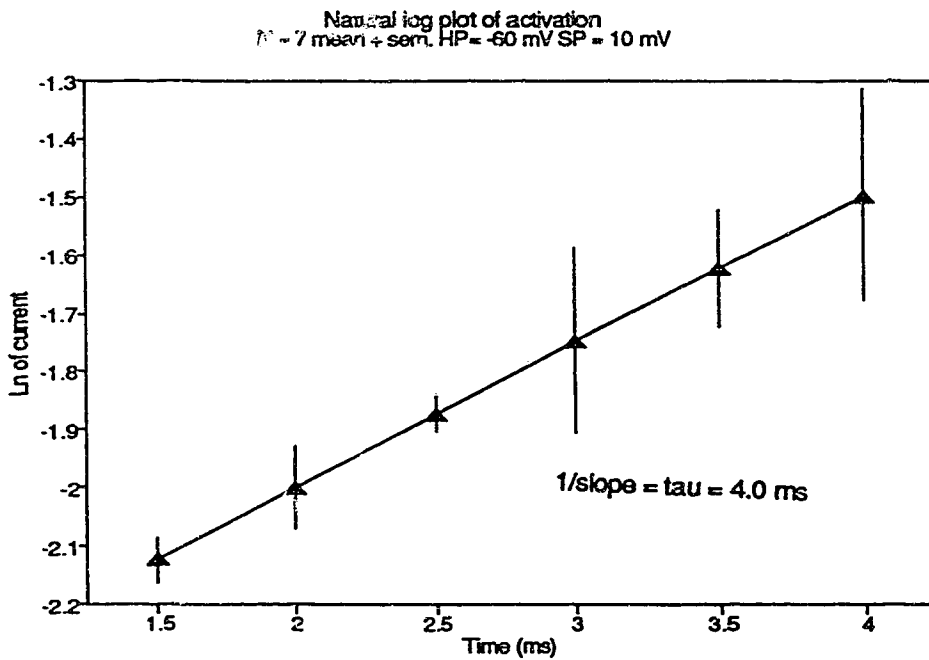
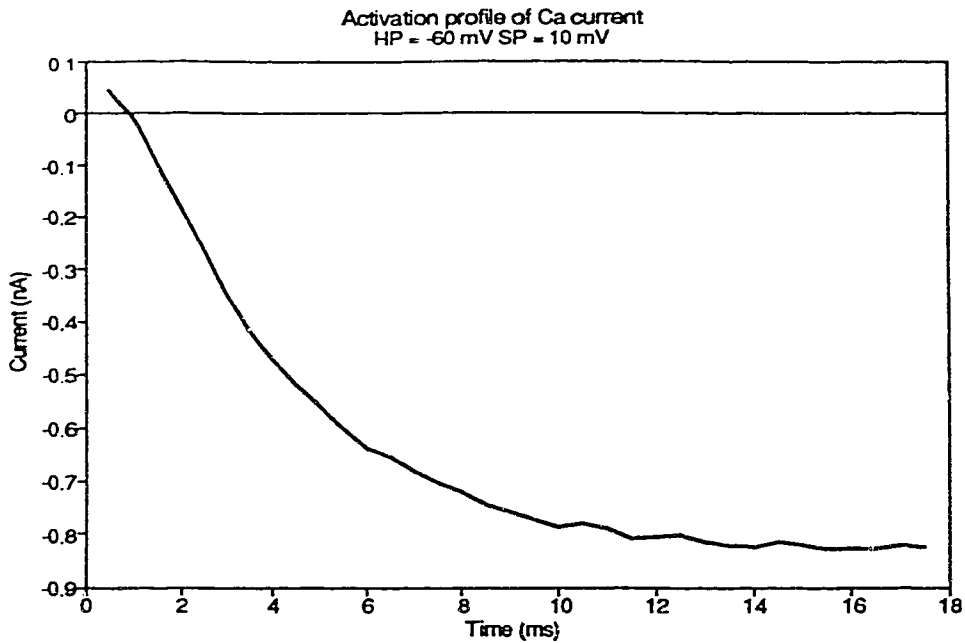


Figure 19. Time constant of activation.

At all step voltages the time course of activation could be fitted well with a single exponential. The profile of activation of a current trace elicited from -60 to +10 mV has been shown and the logarithmic plot to determine the time constant is illustrated underneath.

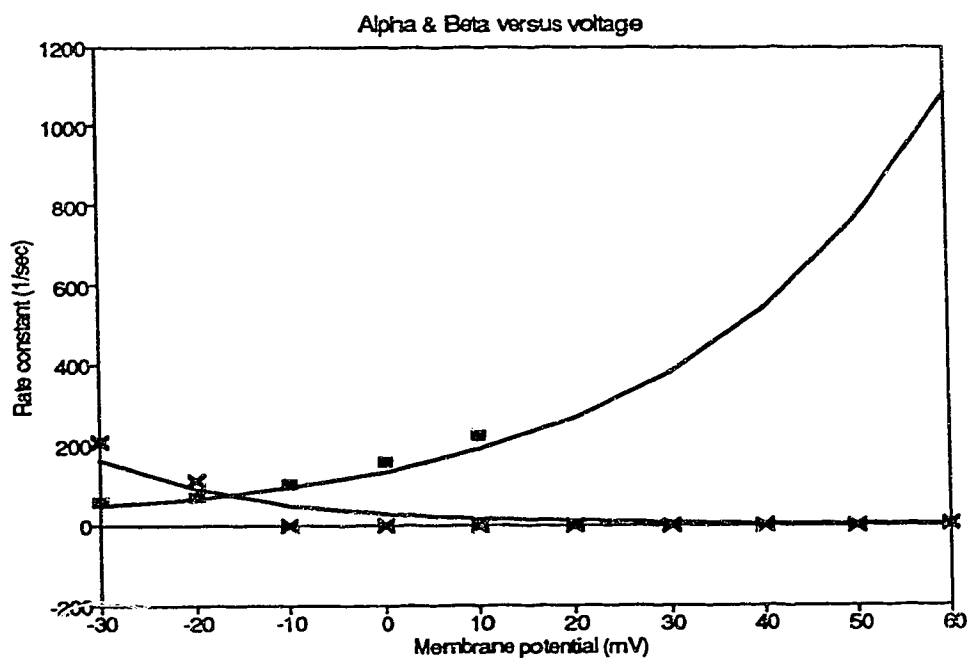
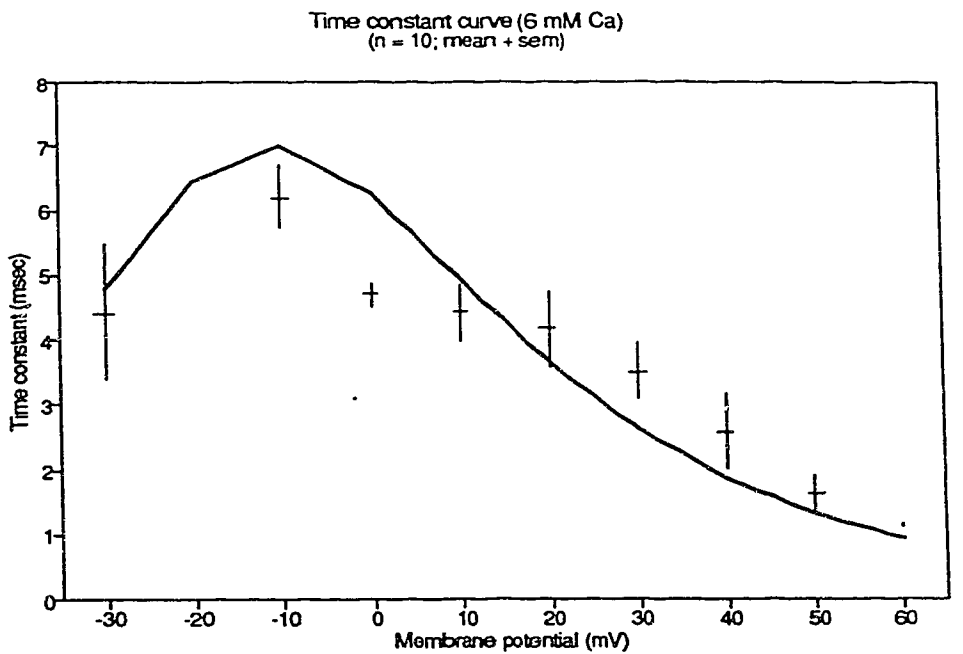


Figure 20. Time constant of activation and voltage.

Time constant curves for I_{Ca} at 6 mM external calcium. The curves were generated from the α s and β s plotted underneath (see text for equations).

Figure 20 shows a plot of the relation between time constant of activation and voltage in 6 mM Ca and the α and β simulated from equations 3-4 and 3-5. The line joining the scattered points was generated with equation 8, from the computed α s and β s.

$$\tau = \frac{1}{\alpha + \beta} \dots \dots \dots (3-8)$$

Inactivation of Calcium Current

The inactivation of calcium currents in excitable cells has been described as either voltage (Fox, 1981) or calcium dependent (Eckert & Chad, 1984) and in some cases both mechanisms seem significant in turning off I_{Ca} . Even a quick glance at the calcium current traces recorded from the snail neurons (see fig. 13) suggests that the inactivation of the current may not be entirely a voltage dependent phenomenon. In this section I show results intended to describe the mechanism of I_{Ca} inactivation. Voltage clamp records of I_{Ca} , along with barium and strontium currents, indicate that the inactivation of the channel is dependent both on voltage and current.

Effect of Extracellular Calcium ions

Calcium ion (5 mM and 10 mM) was tested for its ability to alter the relaxation of I_{Ca} . A change in $[Ca^{2+}]_e$ from 5 mM to 10 mM doubled the degree of inactivation. While the decay of the current at 5 mM was best fitted with a single exponential at all voltages, at 10 mM it was appropriately fitted with two time constants (τ), at some step potentials, (using the pClamp software, clampfit); fast and slow, with the slow τ being similar to the relaxation at 5 mM calcium. An example of two current traces elicited from -60 to 0 mV in 5 mM and 10 mM calcium depicts enhancement of the decay with increased $[Ca^{2+}]_e$ (fig. 21a). This calcium induced inactivation saturated beyond 20 mM (fig. 22). As demonstrated in figure 21b., the decay time constant was biphasic in the presence of 10 mM (also see table 7). In general, however, there was no significant change in the slow time constant for the 10 mM current and the decay of currents in 5 mM $[Ca^{2+}]_e$. The interpretation of this observation could be that the calcium induced effect was prevalent only in the initial 100 ms of the current pulse and that the late events were not dependent on calcium. But with 15 mM and 20 mM external calcium, the slow decay time constants were relatively faster than at 5 mM. For example, from a holding potential of -60 mV and a step pulse of 0 mV the time constant

for the slow decay in 5, 10, 15, and 20 mM $[Ca^{2+}]_e$ were as follows; 370.4, 359.7, 310.5, 276.8 (all in ms) respectively. As $[Ca]_e$ was raised from 5 mM to 10 mM the anomalous behaviour of current decay shown in figure 13 increased without a clear-cut restriction to any distinct phase of the relaxation profile (figure 23a & b). Thus, though the effects of raised extracellular calcium on I_{Ca} inactivation on the early phase of the decay was more drastic than the late phase, I could not fully attribute the slow phase to a calcium independent event. Nor could I implicate calcium influx as the sole regulator of the relaxation of the calcium current.

Effect of Holding Potential and Elevated $[Ca^{2+}]_i$

In order to remove or reduce the Ca-induced component of inactivation, neurons were held at potentials at which there was a steady state influx of calcium. The prediction was that, saturation of the calcium dependent component with steady state Ca influx will make studies of other factors influencing inactivation convenient. As will be expected, recordings were not stable when cells were held at relatively positive potentials. However, in cells in which I could reliably hold for about 5 s or more, at potentials at which I_{Ca} was already activated (> 30 mV), I found that as the holding potential was brought to depolarizing levels, the inactivation of I_{Ca} began to look like what one would expect from a voltage

dependent phenomenon (i.e. a sigmoidal decrease in the relative inactivation curve as the potential of the post-pulse became more positive). Figure 24 illustrates characteristic traces of calcium current records as the holding potential was moved towards positive voltages. Above -20 mV holding potential, increasing step voltages resulted in enhanced inactivation.

If relatively high [Ca] was introduced into the neurons, either by holding the cells at positive potentials or by adding Ca^{2+} into the patch electrode, the voltage dependent component of I_{Ca} relaxation was made prominent (see figure 25). Figures 22 and 25 were generated using a twin-pulse protocol with a gap (< 10 ms) between the pre and test-pulses. The gap allowed for the channels to deactivate after the activating pre-pulses before the test-pulse was elicited (see caption: Brehm & Eckert, 1978; Tillotson, 1979).

Barium, Calcium & Strontium Currents.

Divalent cations which pass through calcium channels have been substituted for calcium ions to study I_{Ca} inactivation (Hagiwara & Ohmori, 1982; Eckert & Tillotson, 1981). The idea is that if calcium channels inactivate primarily via calcium influx, then other ions which permeate the channel, beside calcium, should either remove or reduce the relaxation of the channel.

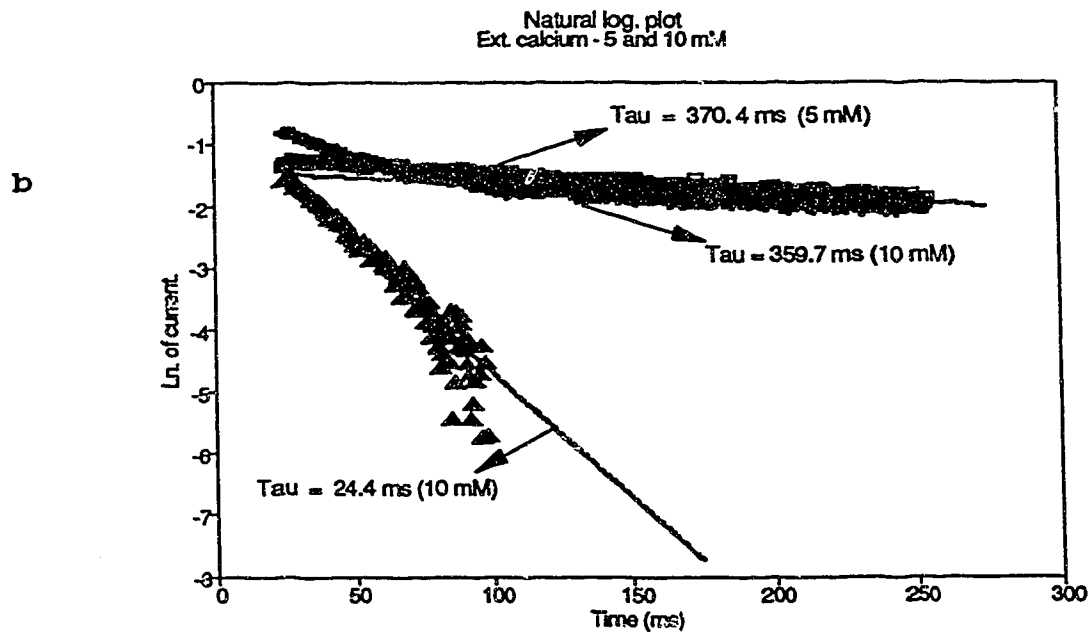
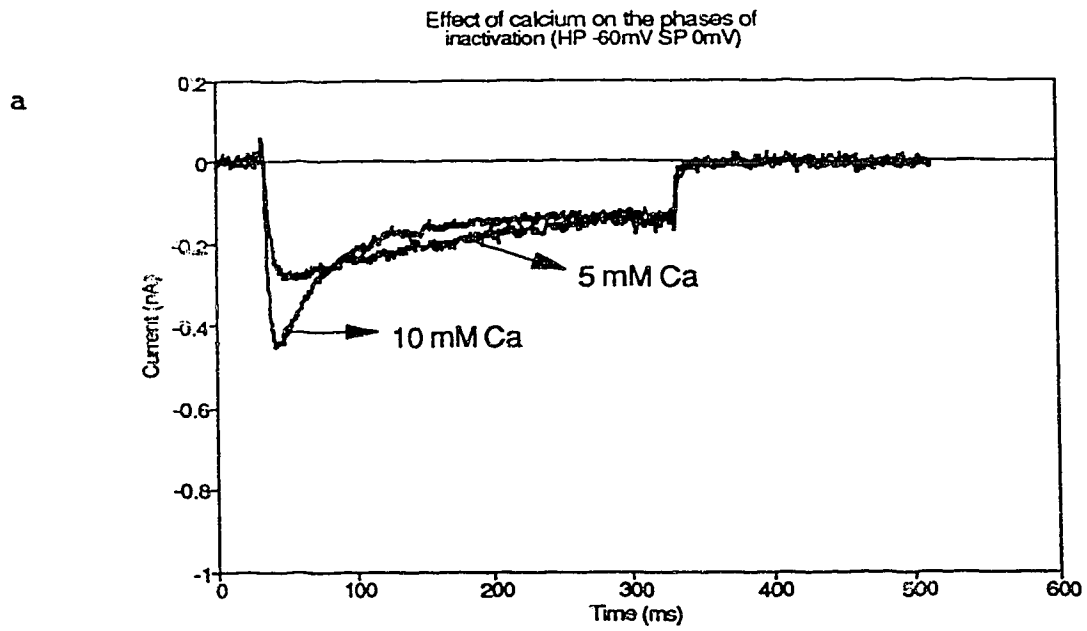


Figure 21a & b. Effect of bath calcium.

a. Increase in bath calcium increased peak current. As the $[Ca^{2+}]_e$ was raised the activation profiles continued to fit well with a single exponential while the inactivation kinetics changed from one to two exponential decays. Illustrated here are two traces generated with identical pulse protocol but with different $[Ca^{2+}]_e$. b. Below is the logarithmic plot for determination of the time constants (see table 7).

Figure 22

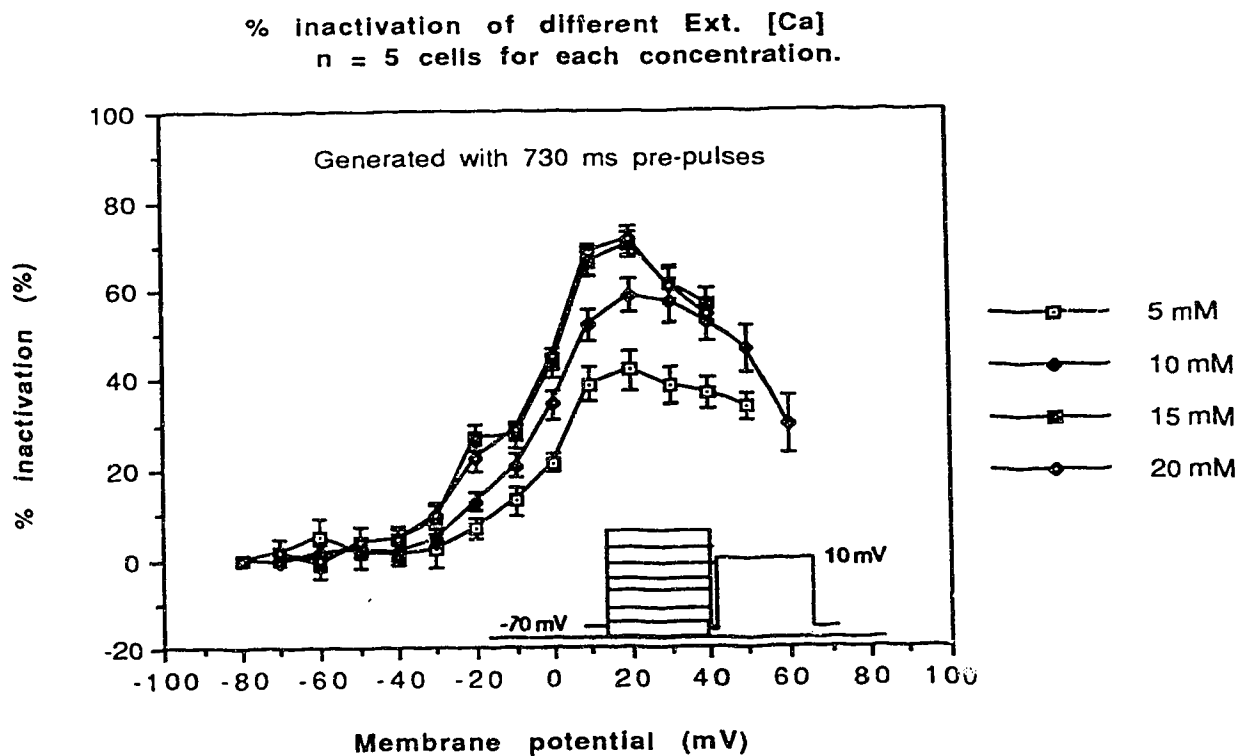
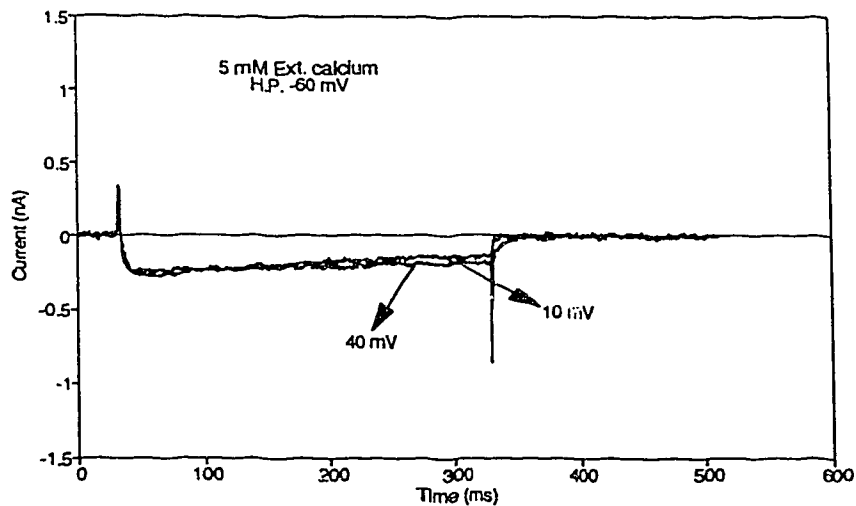


Figure 22. $[Ca^{2+}]_e$ and the % inactivation curves.

With a double-pulse protocol with a gap of 7.3 ms (to allow for recovery from channel activation), a close-to U-shape %inactivation curves were plotted. Such curves are indicative of a current dependent inactivation mechanism. As the $[Ca^{2+}]_e$ was increased, from 5 mM, current magnitude increased until 15 to 20 mM, when the channel saturated. It is not clear whether the saturation in the curves shown here resulted from a limitation imposed by the current magnitude or from saturation of the calcium dependent mechanisms.

a



b

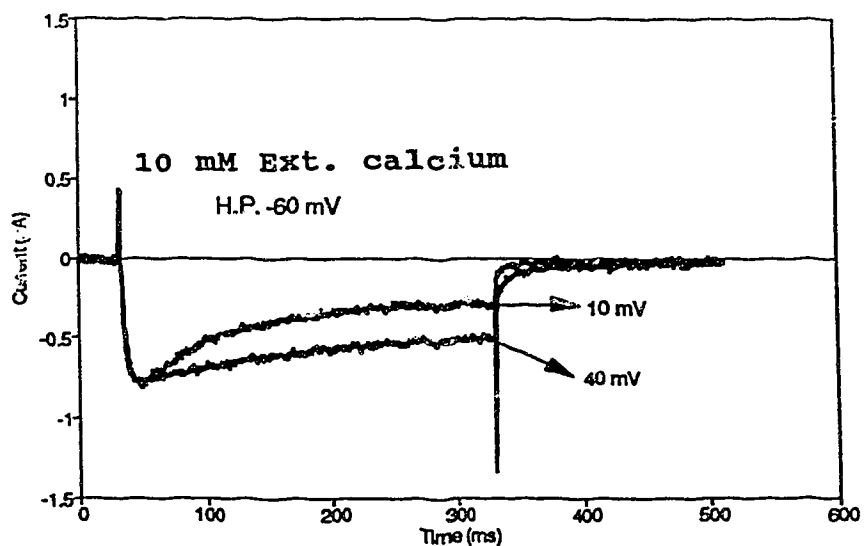


Figure 23a & b. Current profiles in 5 and 10 mM calcium.

Shown here are traces of currents with similar maximum amplitude but different inactivation profiles. **a.** In 5 mM the difference between 10 and 40 mV test pulse currents are not as obvious as in 10 mM (**b**).

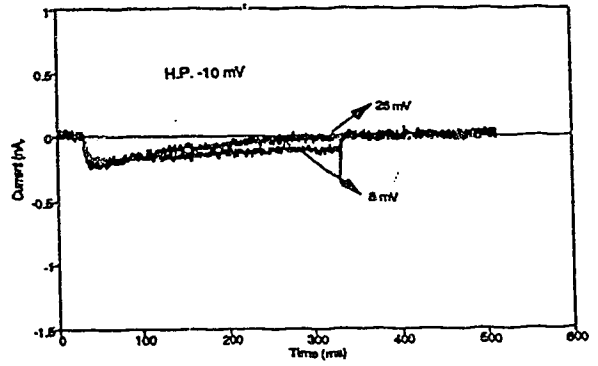
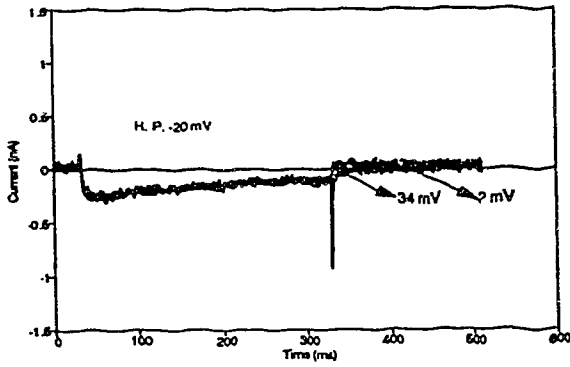
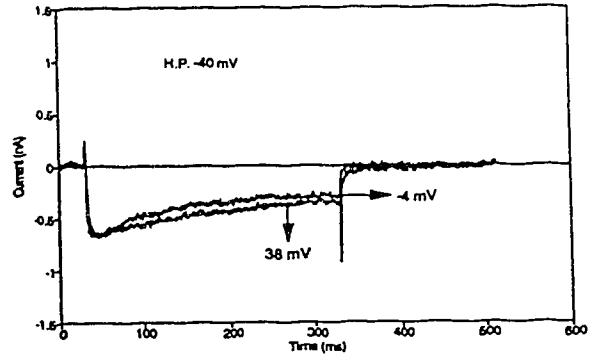
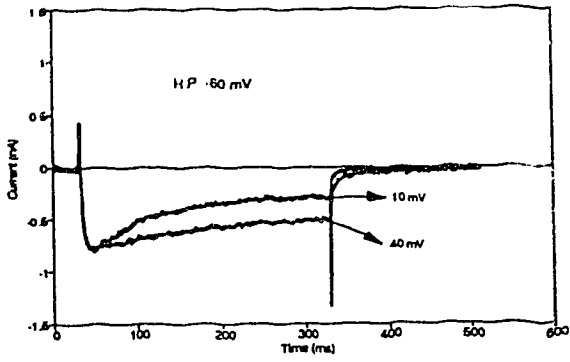


Figure 24. Effect of holding potential.

Different holding voltages had different effects on the characteristic inactivation of the current. As the holding potential became more positive, the decay of I_{Ca} became rapid with increasing step potentials. Opposite results were seen at some voltage ranges when cells were held at negative voltages. Note that at -20 and -10 mV the I_{Ca} is already activated and thus there was a persistent influx of calcium at the steady state potentials.

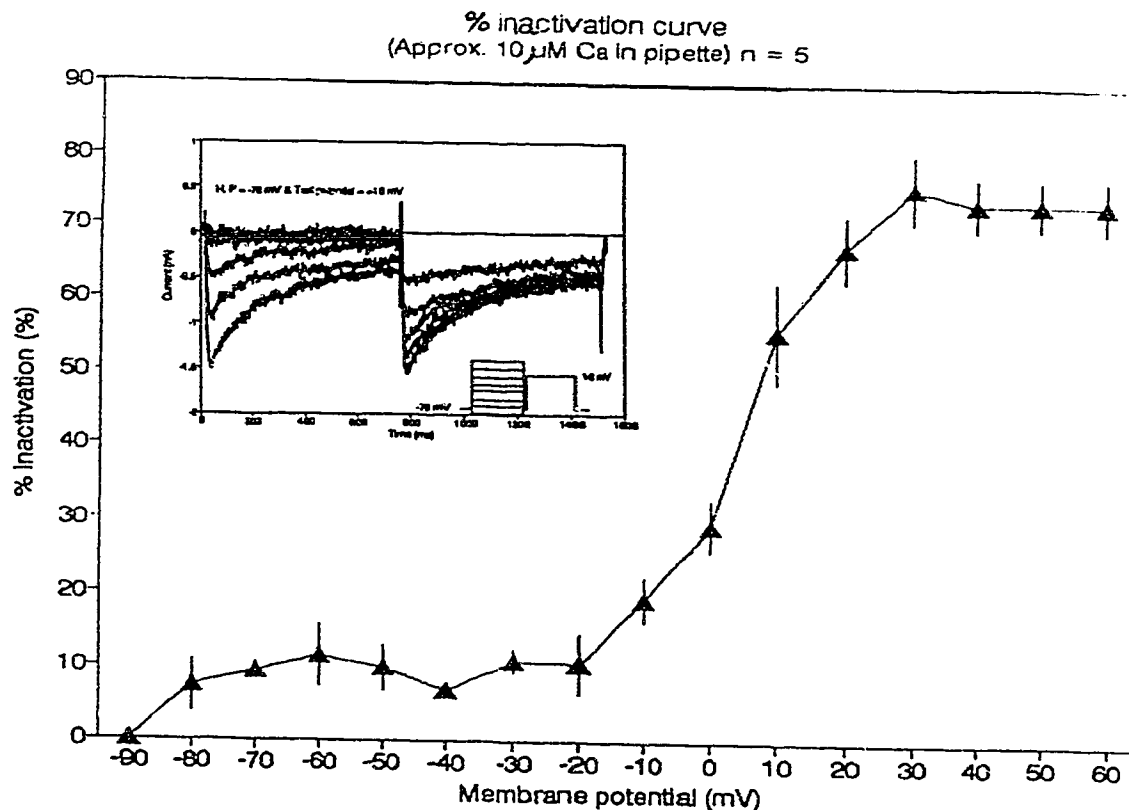


Figure 25. Effect of high intracellular calcium.

In fig. 24 it was shown that if enough calcium were allowed to permeate the neurons before the inactivation profile was assessed, the result was close to that which would be expected from a voltage dependent phenomenon. Here, about $10 \mu\text{M}$ Ca was added to the pipette and the percentage inactivation of the current plotted against voltage. The curve was generated from a double-pulse paradigm (Tillostson, 1979) in which the gap between the pre and test-pulses was 7.3 ms to allow for recovery from deactivation.

Qualitatively, for a step pulse of approximately 350 ms, strontium reduced, while barium removed the relaxation of the channel (see figure 26a). With long duration pulses (> 600 ms) however, barium currents showed inactivation (fig 26 b & d). Therefore, the calcium dependent inactivation is prominent in the first few hundred milliseconds of the current waveform.

Previous reports from pituitary cell lines and other cells (Hagiwara & Ohmori, 1982; Tillotson, 1979) support the present observation. Since barium appears to attenuate I_{Ba} turn-off and since strontium ions reduce the relaxation of the channel, in experiments where short duration pulse protocols are used, it has been common to isolate calcium as the only inducer of I_{Ca} inactivation (Eckert & Chad, 1984). Strontium, to a lesser extent, behaved very much like calcium. For example, current traces recorded when 10 mM strontium was the charge carrier, showed an apparent increase in inactivation at less positive compares to that at more positive potentials (figure 27a). Presumably, strontium, binds to the calcium-binding-site to cause inactivation.

In the case of barium currents, it was observed that slow inactivation occurred at very positive potentials and when long duration pulses were elicited (fig 26), relaxation could be seen at almost all activating step potentials. Thus, strontium, to a greater extent, mimicked the current induced inactivation of the channel while I_{Ba} showed slow inactivation

which was predominantly a voltage dependent event.

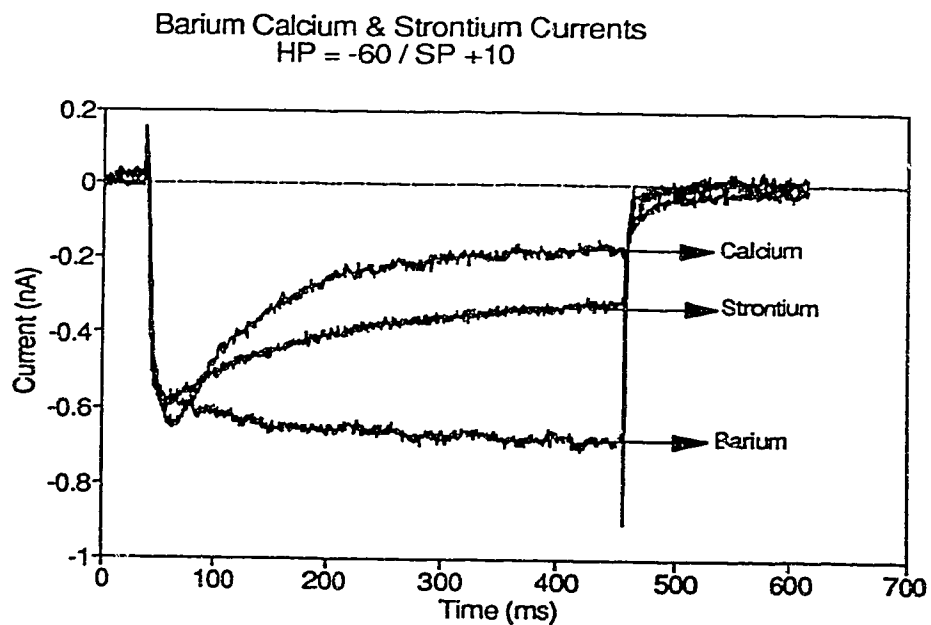
The degree of inactivation caused by the three divalent ions were compared using a double pulse protocol of which the pre-pulse duration was about 730 ms with a gap of 7 ms for the channel to deactivate before the test pulse. The results agree with the observation that inactivation was enhanced with calcium followed by strontium then barium ions (fig. 26a-d).

Effect of Chelators.

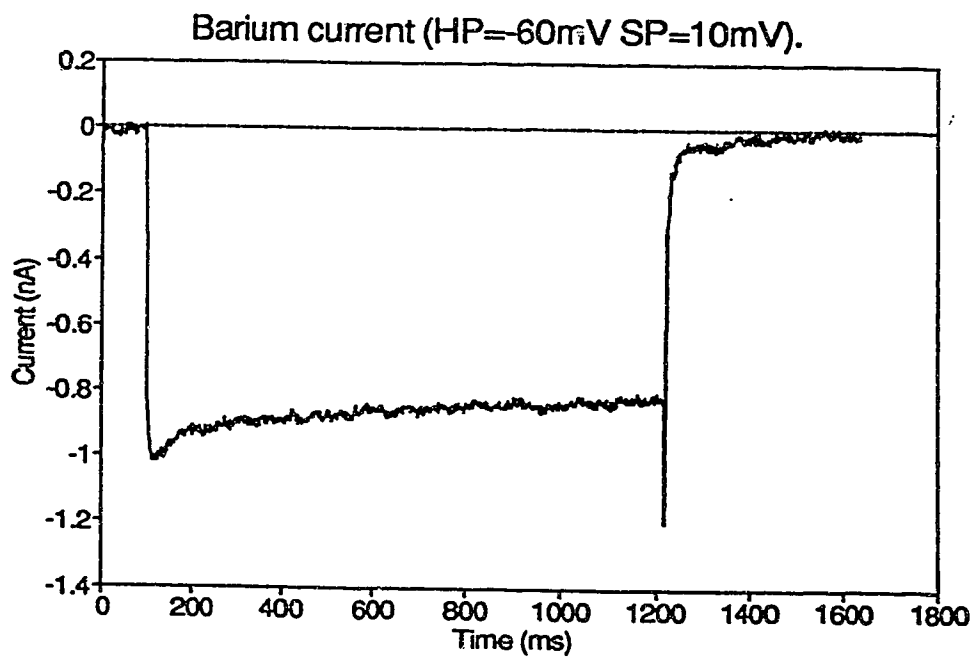
Unless otherwise stated, all current records reported so far were obtained under conditions in which there was approximately 9.8 mM free EGTA (see methods) in the patch pipette. This was used to keep the intracellular free Ca^{2+} buffered at low levels ($\approx 1.3 \times 10^{-9}$ M). In spite of the EGTA, substantial inactivation was observed, most likely as a result of insufficient dialysis (Byerly & Hagiwara, 1984; Gutnick et al., 1989) and inadequate diffusion of the chelator to the sub-membrane spaces (Neher, 1986) or calcium independent mechanism of inactivation.

The use of different and more efficient calcium chelators like BAPTA (Marty & Neher, 1985; Neher, 1986), has been commonly used to assess the extent to which Ca-buffering limits the mechanisms of calcium dependent inactivation (Gutnick et al., 1989; Plant, 1988;).

Figure 26a



26b



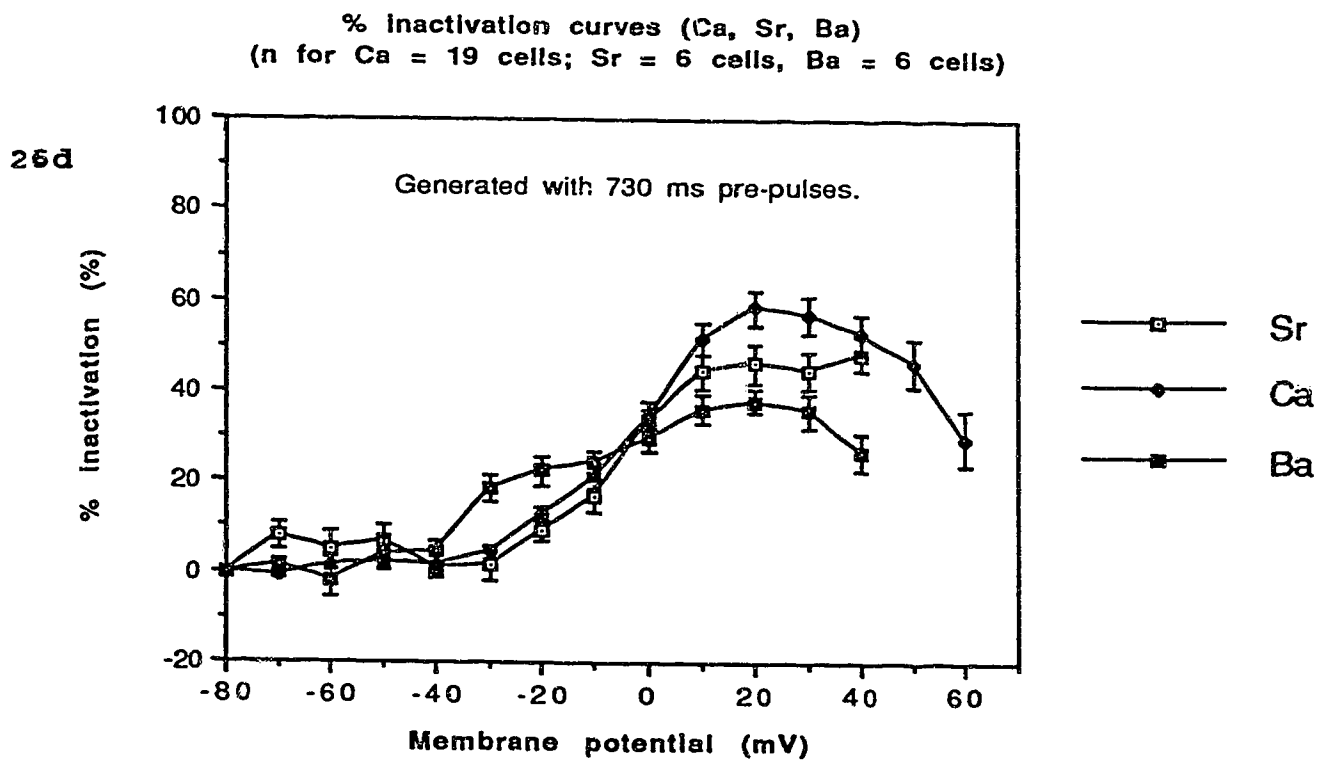
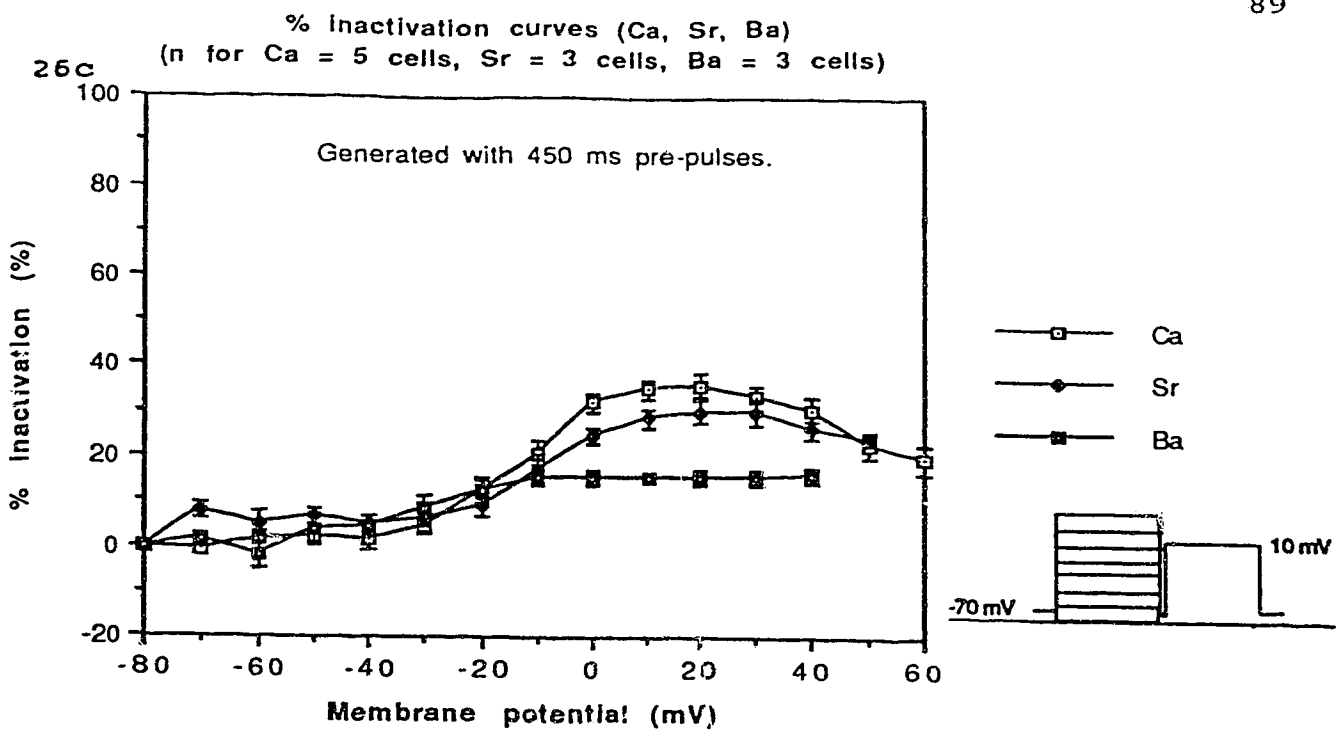
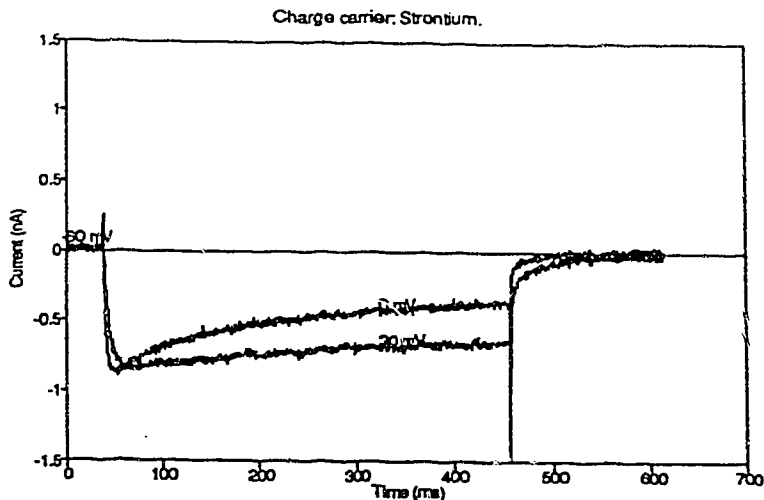


Figure 26a & d. Effect of calcium, strontium and barium on inactivation.

a. Three current traces elicited in Ca^{2+} , Sr^{2+} and Ba^{2+} are superimposed. With this pulse duration (~350 ms) calcium caused a relatively fast relaxation followed by strontium and barium appeared to remove the inactivation entirely. b. Long pulses for barium currents showed some degree of slow inactivation. c. With a twin-pulse protocol (see caption) the percentage inactivation of I_{Ca} , I_{Sr} and I_{Ba} were compared. In general an incomplete or complete U-shaped curve was obtained i. e. maximum inactivation was seen at potentials where the peak currents were elicited and as the pre-pulse voltages approached the apparent V_r (reversal potential), the extent of inactivation decreased. Such observation is typical of a current dependent inactivation phenomenon. With short duration pre-pulses, the current dependent inactivation was more apparent than with long ones (d).

a



b

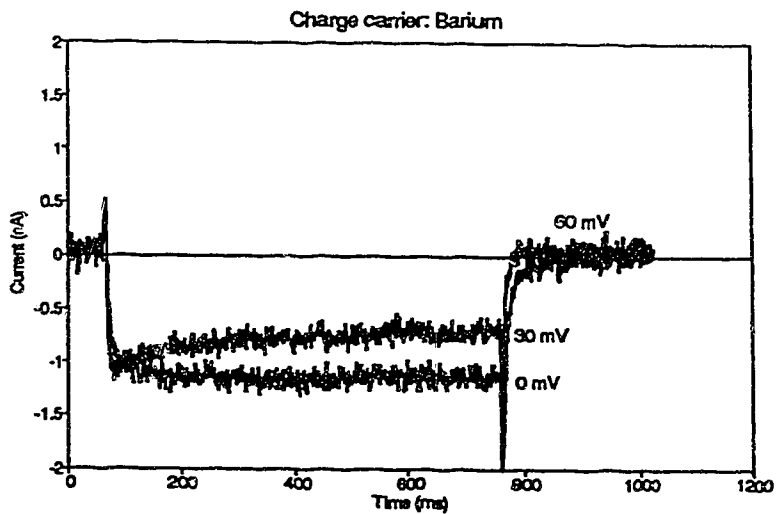
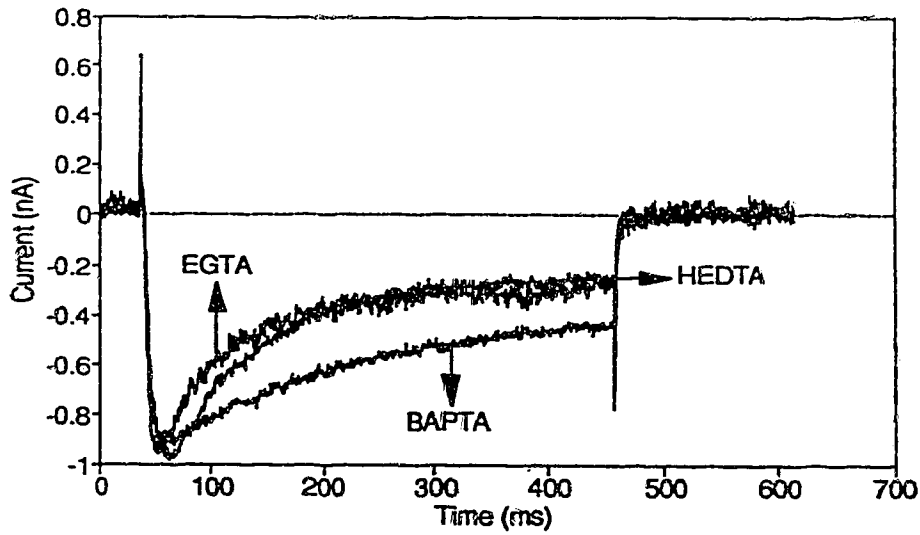


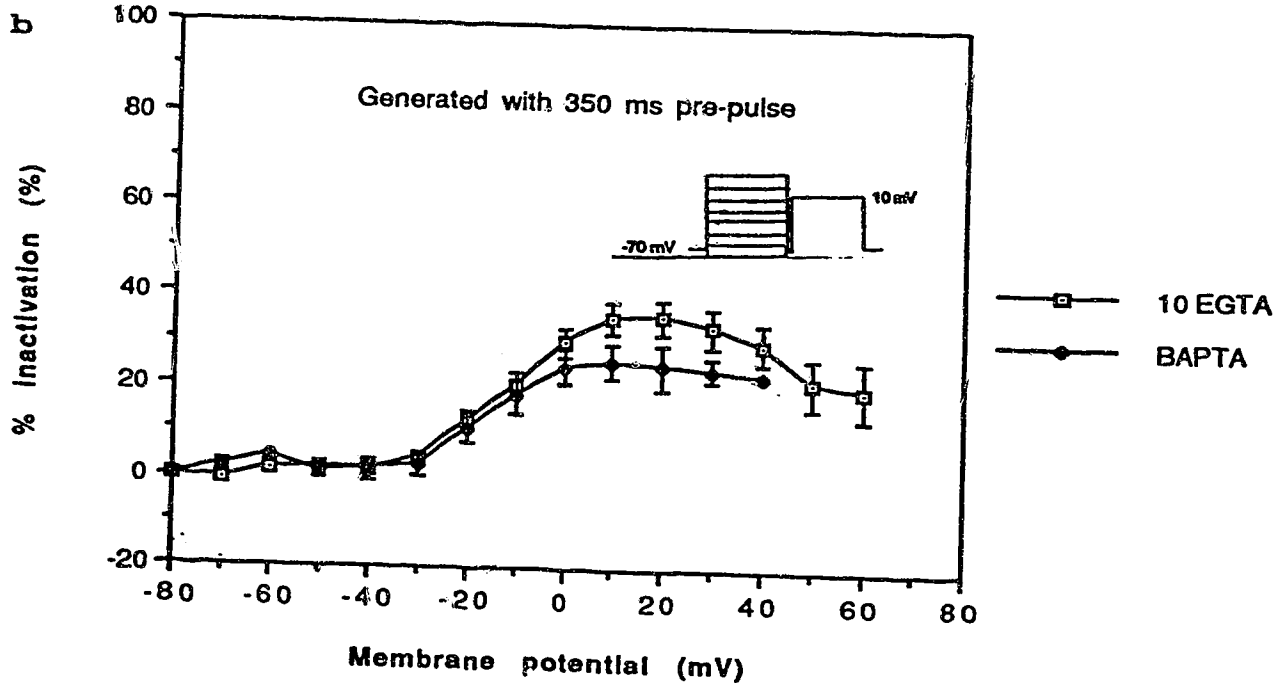
Figure 27 a & b. Strontium and Barium Currents.

a. Two traces of I_{Sr} illustrating the phenomenon whereby currents of similar peaks elicit different inactivation profiles. If the decay of the current was dependent entirely on the current then we should expect currents of the same peak to have comparable relaxation. b. I_{Ba} , on the other hand decayed with increasing voltages.

a Effect of chelators on inact.
10mM EGTA, BAPTA & 12 mM HEDTA



% Inactivation of Ca current: 10 mM EGTA
n = 5 cells; 10 mM BAPTA n = 3 cells.



c

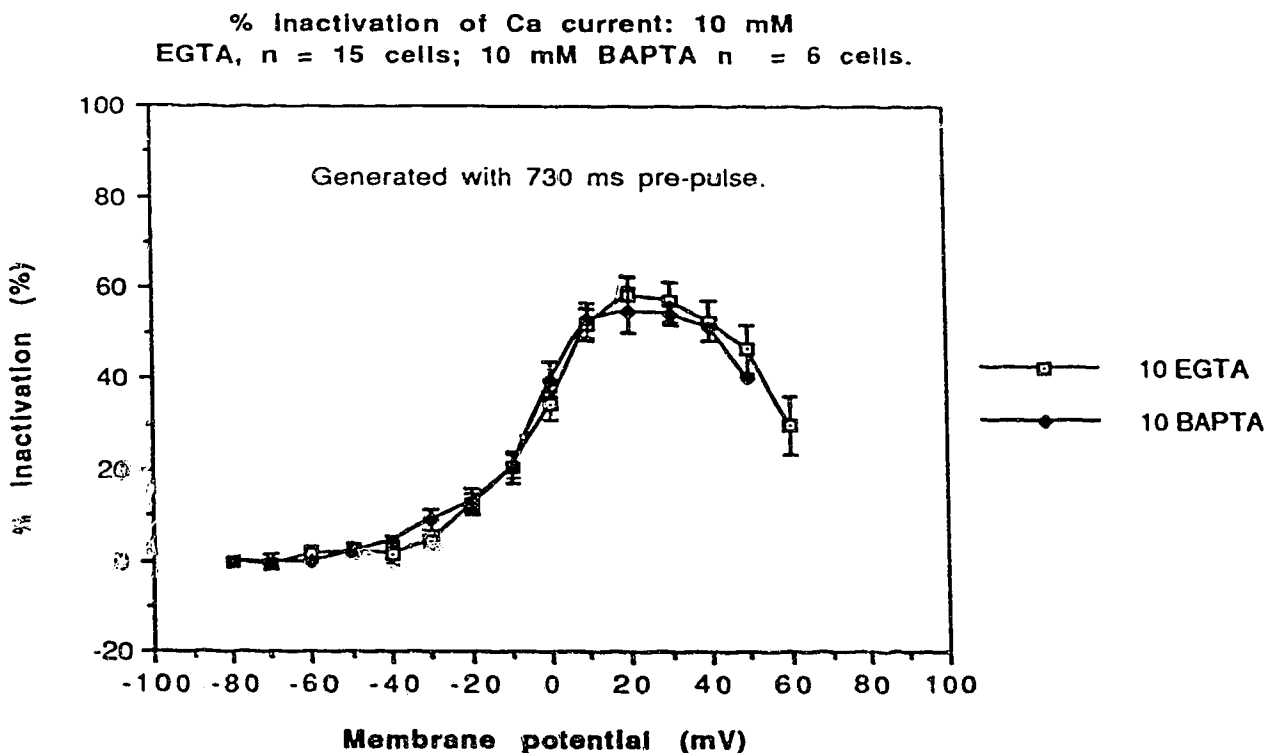


Figure 28a-c. Effects of EGTA, HEDTA and BAPTA.

Different intracellular calcium chelator were used to study the inactivation kinetics of I_{Ca} . The effects of 10 mM EGTA and BAPTA and 15 mM HEDTA are shown at a. BAPTA appeared to reduce the relaxation (b) of the current but the effects of HEDTA and EGTA were quite similar. c. When the percent inactivation caused by EGTA and BAPTA were compared, using long pulses, it was realised that the effect of BAPTA was not all that different from that of EGTA. The number of experiments for each chelator is indicated.

BAPTA, EGTA and HEDTA were used to evaluate the effectiveness of chelation in slowing inactivation of I_{Ca} . While 10 mM EGTA and 12 mM HEDTA showed similar inactivation profiles, 10 mM BAPTA slowed the relaxation of the current (fig. 28a & b). The results with HEDTA were a bit surprising since it appears to be a less effective buffer than EGTA (Thayer et al., 1990). The difference between the effects of EGTA and BAPTA was not outstanding when the pre-pulse duration was increased (> 700 ms: fig. 28c), which agrees with the suggestion that calcium-dependent inactivation is eminent in early section of the current waveform, as reported also in Helix neurons (Gutnick et al., 1989).

Calcium Influx and Inactivation.

If the inactivation of the calcium channel was dependent on calcium entry, then, with a double pulse protocol, the influx of calcium during a test pulse should correspond to the degree of inactivation (i. e. assuming less effective intracellular protein buffers). In pancreatic β -cells (Plant, 1988), a direct relation between inactivation and Ca^{2+} influx has been observed. This was perhaps the best demonstration indicating that the relaxation of the channel, in that system, was strictly calcium dependent since the behaviour was not influenced by voltage.

In the FSN preparation, the results were not

straightforward one. Whereas inactivation at the initial activation voltages (-30 to +10 mV) showed an apparent dependence on Ca^{2+} entry, there was no direct relation between inactivation and calcium influx at more depolarised voltages (fig. 29). Hysteresis of the curve is indicative of the fact that calcium is not the only factor involved in the inactivation process. Similar observations have been made in Helix neurons (Brown et al., 1981; Gutnick et al., 1989) and together with other results, the authors have implicated both voltage and calcium as the factors controlling I_{Ca} inactivation.

Time Constant of Inactivation

In the presence of 5 mM external calcium, the relaxation of I_{Ca} , at all step potentials, could be described by a single exponential. The time constant of inactivation was slow, decreasing from 667 ± 103 ms ($n = 9$) at -30 mV to 170 ± 59 ms ($n = 9$) at +50 mV. As the extracellular calcium was raised to 10 mM or more, I could no longer fit one exponential to the decay of the current, but two time constants were required at most potentials (see table 7: currents were measured in 10 mM external calcium).

Shown in figure 30 is the time constant of inactivation as a function of membrane potential.

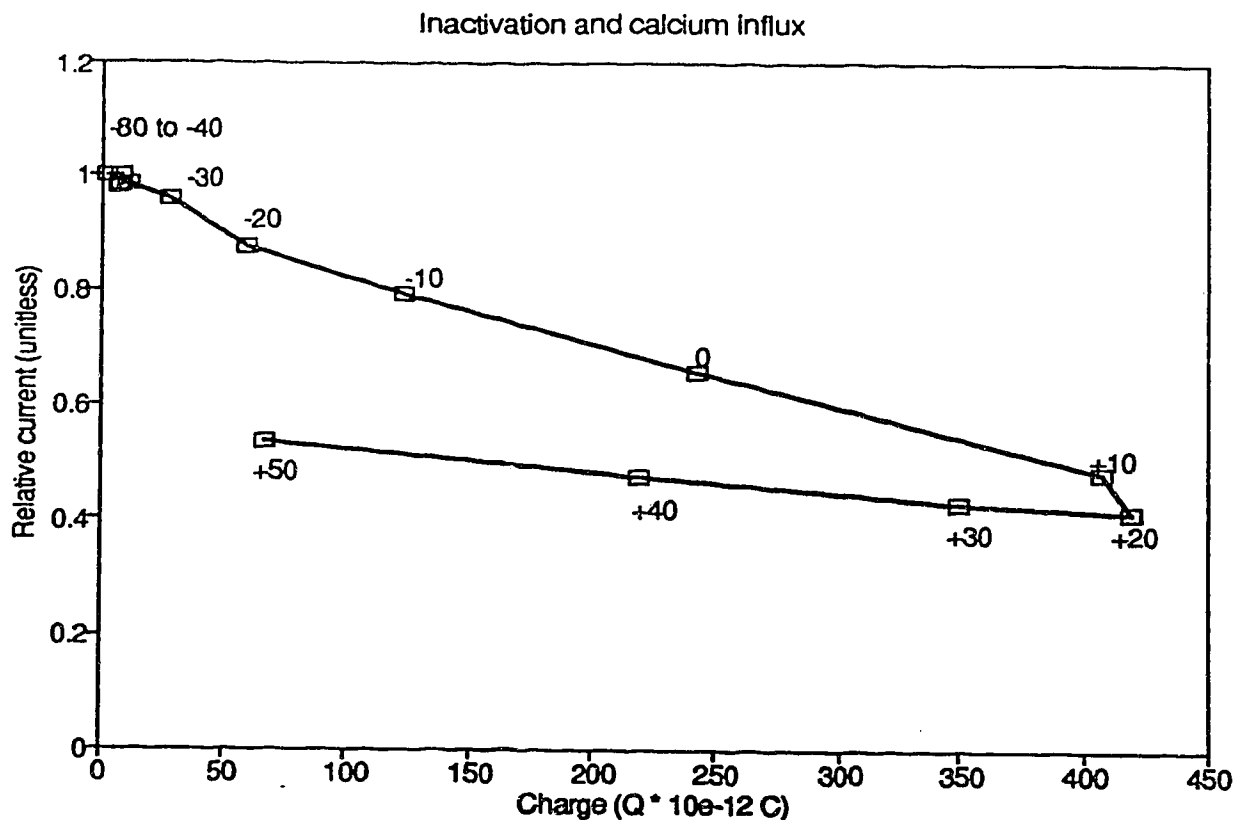


Figure 29. Relationship between Ca^{2+} influx and inactivation.

The relation between calcium entry during a pre-pulse (~750 ms) and the inactivation produced at a test pulse to 10 mV was assessed. The integral of the pre-pulse leaked-subtracted currents give the charge Q , which is directly proportional to calcium influx ($\text{Ca}_{\text{influx}}$): $\text{Ca}_{\text{influx}} = Q/zF$, where z is the charge of Ca^{2+} and F is Faraday's constant. Here, the charge was plotted as a function of inactivation. Inactivation increased with calcium influx but beyond +10 mV the curve exhibited hysteresis. The lack of a uniform decay with calcium entry suggested that the inactivation was not dependent entirely on current.

| Table 7. Time constant of inactivation (mean \pm std. error. n = 9 cells) | | |
|--|---|---|
| Membrane potential (mV) | Fast time constant (ms: τ_{fast}) | Slow time constant (ms: τ_{slow}) |
| -30 | - | 666.7 \pm 102.8 |
| -20 | 56.6 \pm 18.8 | 549.5 \pm 100.0 |
| -10 | 33.5 \pm 13.8 | 502.5 \pm 93.0 |
| 0 | 24.6 \pm 4.3 | 473.9 \pm 63.7 |
| 10 | 36.8 \pm 16.9 | 431.7 \pm 80.1 |
| 20 | 88.8 \pm 21.2 | 384.6 \pm 101.5 |
| 30 | 108.3 \pm 62.7 | 337.1 \pm 73.5 |
| 40 | - | 204.1 \pm 43.0 |
| 50 | - | 169.5 \pm 58.9 |

Though not shown in detail, similar results have been reported from Aplysia neurons (Chad et al., 1984). In that work a calcium dependent inactivation could have resulted in the bi-phasic time constant. Subsequently, a quantitative model which assumed a Ca-mediated inactivation was developed to predict the shape of the calcium current traces in Aplysia neurons for a restricted range of voltage steps (Eckert & Chad, 1984).

In the present case, however, it was not possible to attribute the appearance of a bi-phasic time constant of decay solely to either voltage or calcium. While τ_{slow} declined with voltage, τ_{fast} , after the initial drop with voltage (from -30 to 0 mV), began to increase. Similarly, there was no direct relationship between the τ s and direct calcium influx measurements.

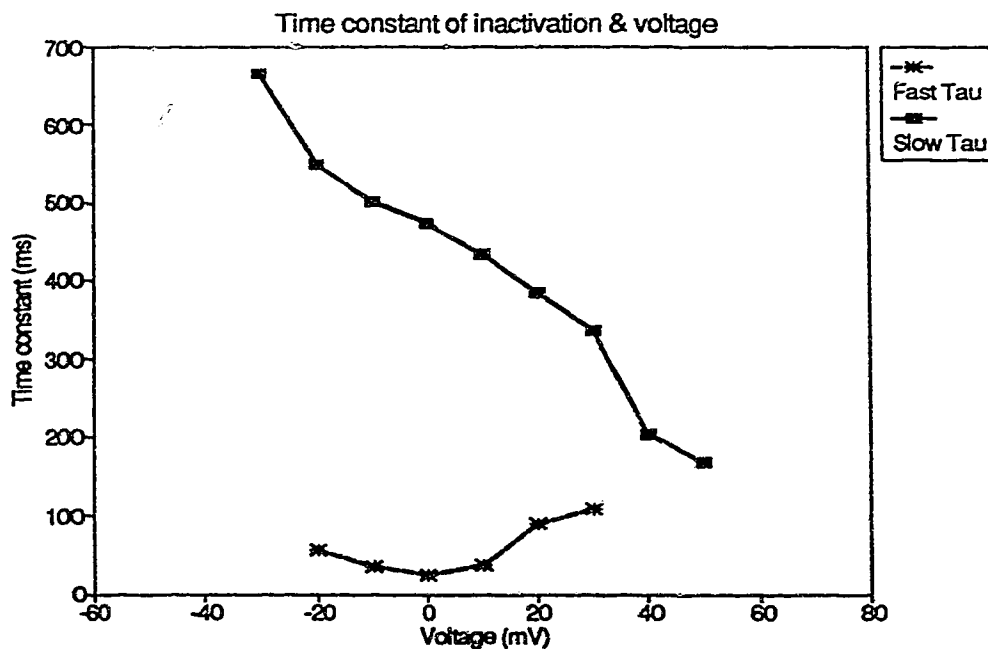


Figure 30. Time constant as function of voltage.

The mean values in table 7 were plotted against membrane potential. At the initial voltage at which the current began to appear the time constant was long and only a single exponential fit the profile appropriately. However, with subsequent positive voltages τ splits into two but becomes single again at 40 and 50 mV.

Pharmacology of the Channel

Lanthanum and Divalent Cations.

Lanthanum at micromolar concentrations quickly and reversibly blocked the inactivating component of the calcium current. Shown in figure 31a are traces depicting the effect of 350 μM lanthanum and recovery after wash-out. Recovery was slow and incomplete. However, with time (≈ 5 minutes) and at higher concentrations ($> 500 \mu\text{M}$) the non-inactivating component which remained unblocked on the trace shown was blocked, but recovery was never achieved under those circumstances. Presumably long exposure to lanthanum caused cell death and this might have resulted in the effect seen on the non-inactivating component. The effect of lanthanum was independent of voltage (fig 31b). At low doses the current was reduced without a shift in the current-voltage relationship. It appeared, at least qualitatively, that the surface charge effect produced on introduction of La^{3+} was insignificant.

While cadmium (Cd^{2+}) completely and irreversibly blocked the calcium current at concentrations similar to that of lanthanum, higher doses of nickel ions (Ni^{2+} 1-2 mM) and even more cobalt ($\text{Co}^{2+} > 5 \text{ mM}$: fig 32b) were required to block the current. Representative records of control and the experimental effect of Cd^{2+} are shown in figure 31a.

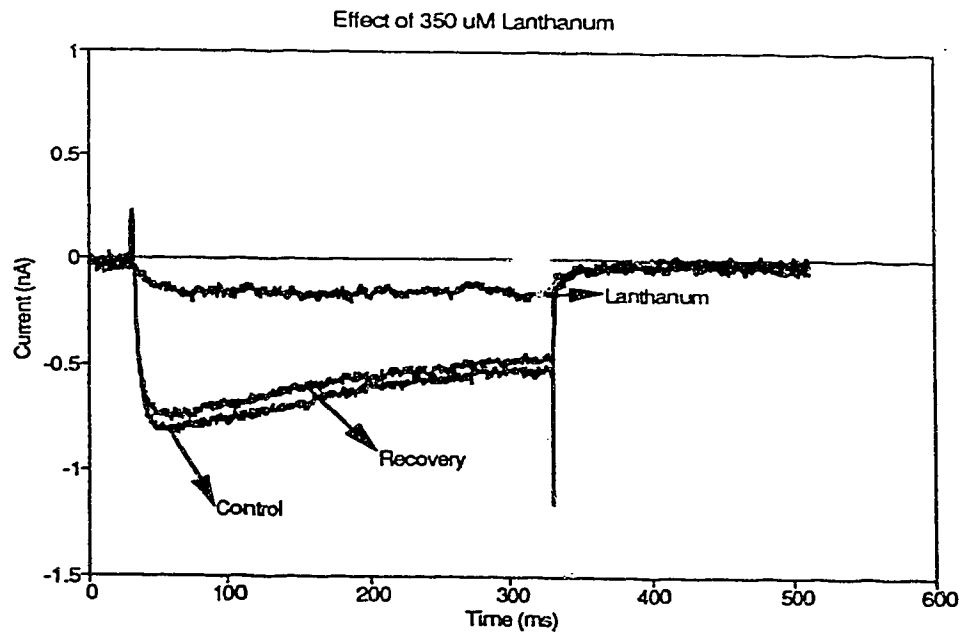
Spontaneous action potentials recorded from the neurons (not shown) under current clamp conditions, were often abolished in the presence of 500 μM Cd^{2+} . This was not surprising since the threshold voltage for activation of I_{Ca} was at potentials (-40 to -30 mV) which were closer to the resting membrane potential (60.28 ± 9.94 mV; see chap. 2, table 4) than that of the sodium current (≈ -20 mV). Blockade of a non-inactivating calcium channel with Cd^{2+} in the photoreceptors of H. C. has been reported (Collins et al., 1989). However, the effect was observed at very high concentrations. This may reflect diffusional problems associated with drug applications on semi-intact nervous systems.

Organic Calcium Channel Blockers.

Dihydropyridines.

Most neurones especially invertebrate ones, appear to be insensitive to the dihydropyridines (DHP) or if they were sensitive, the doses required to cause any effect were considerably higher than that needed for calcium channels in muscles. It was unclear whether the DHPs acted only on one population of channels (L-type; Tsien et al., 1988) because at higher concentrations nifedipine partially blocked the N-type channel as well (Jones & Jacobs, 1990).

a



b

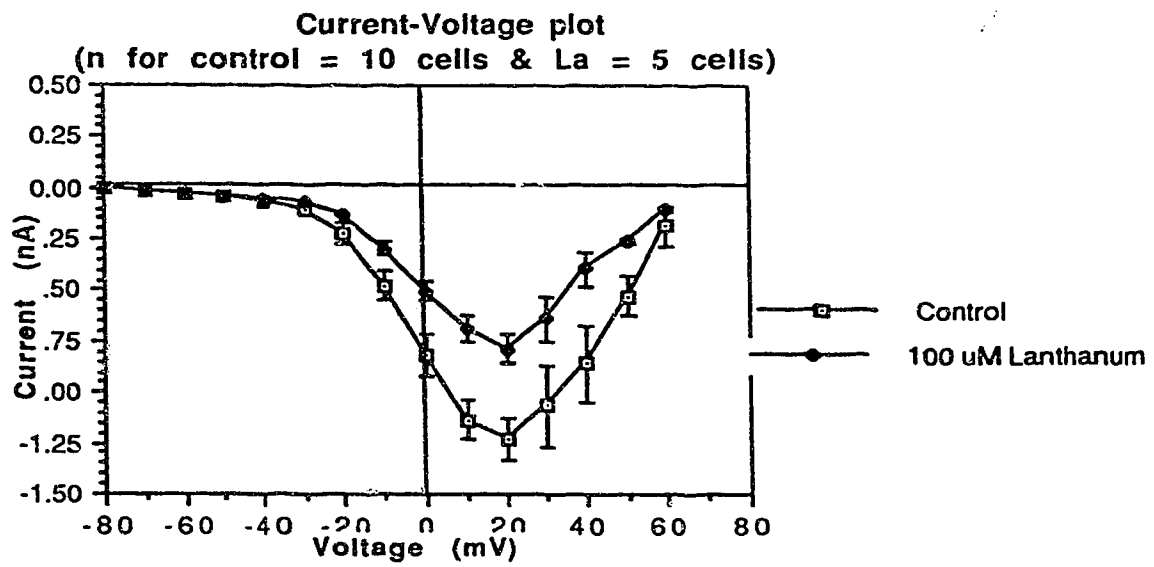
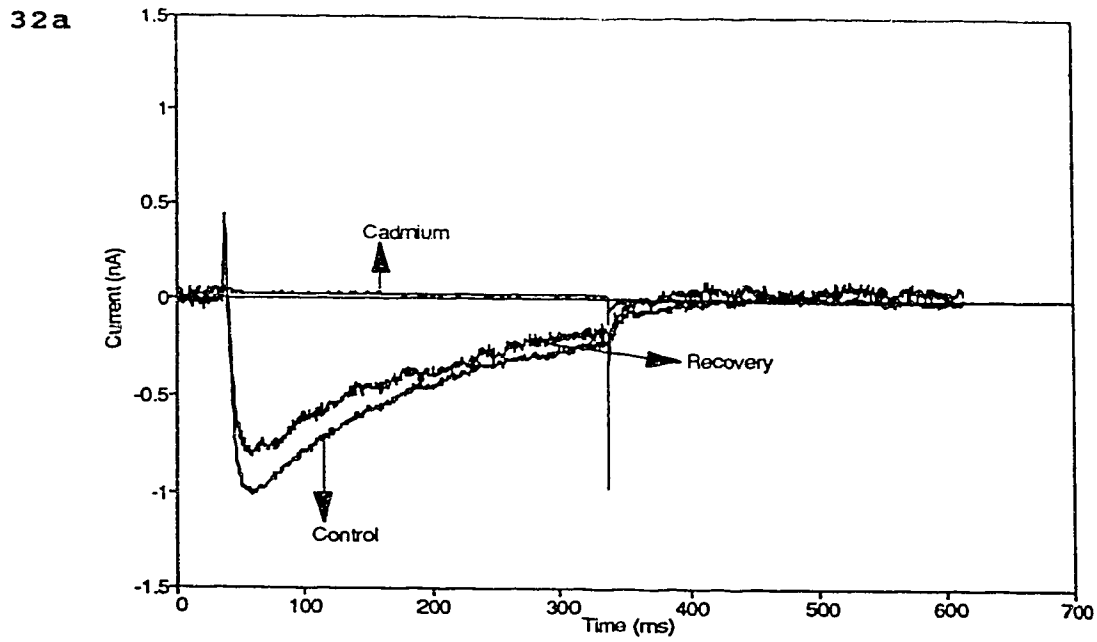


Figure 31a & b. Effect of Lanthanum.

a. Current traces obtained by a 320 ms depolarization from a holding potential of -60 mV to 0 mV, in the absence (control) and presence of 350 μM La^{3+} . Lanthanum blocked the inward current in a voltage independent manner and the IV plot (b.) of the current in 100 μM La^{3+} did not shift from the control. The blockade was incomplete with 350 μM La^{3+} because there remained a current component which showed slow inactivation. This slow component could be blocked with further increase in bath La^{3+} , however it was not possible to recover the blockade beyond 350 μM La^{3+} .



32b.

Effects of Cadmium, Cobalt & Nickel on Ca current. (Control = 3 cells; Cd, n = 3 cells; Co, n = 4 cells; Ni, n = 3 cells)

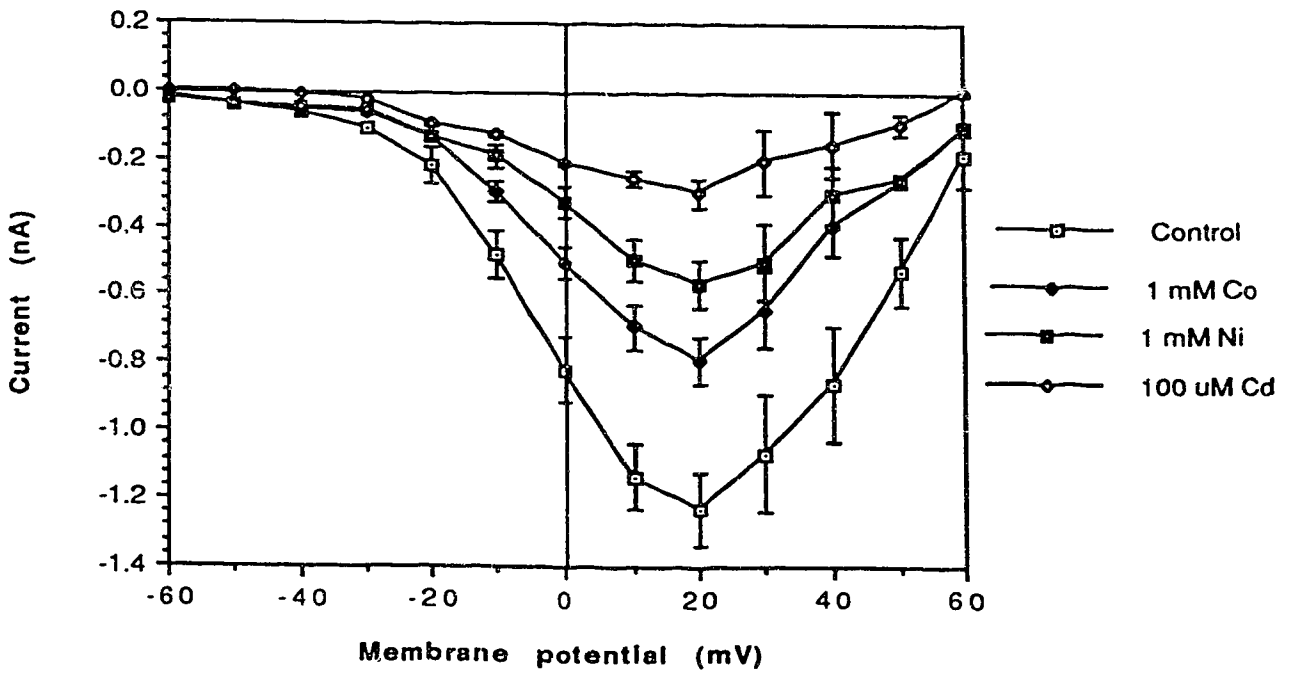


Figure 32a & b. Effect of Cd²⁺, Co²⁺ and Ni²⁺.

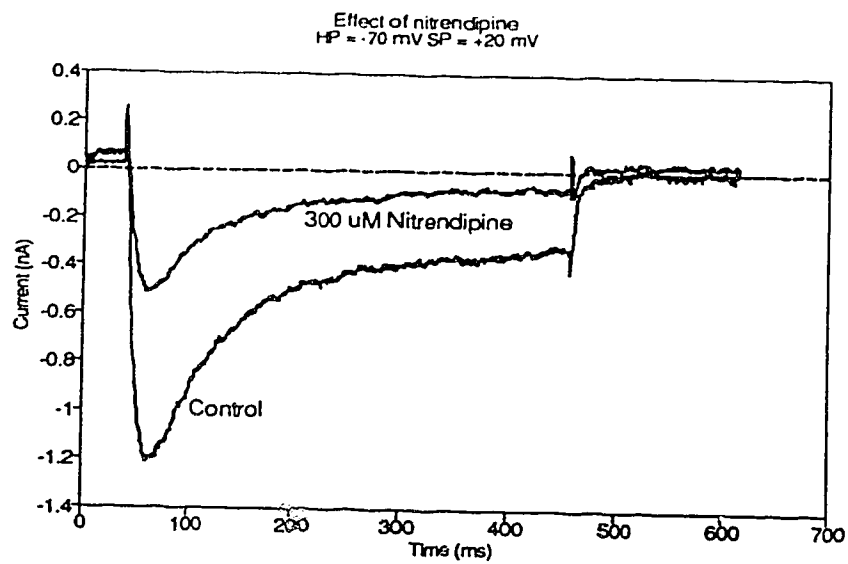
With 300 μM bath cadmium the calcium channel was completely blocked. Shown here are mean traces (n indicated) of current records generated from -60 to 0 mV. In general, the yield for recovery after washout was small. Blockade was not relieved with high depolarizing potentials. **b.** IVs plot, illustrating different potency of the divalent cations.

I tested the effect of nitrendipine and Bay K 8644 on the calcium channels. The channels were resistant to both the DHP agonist and antagonist at low doses (50 nM - 100 μ M). However, at concentrations above 200 μ M it was observed that the current magnitude decreased and increased in the presence of nitrendipine and Bay K 8644, respectively. The sensitivity of the channels to nitrendipine was not so much of blockade, even though if I waited long enough the current was obliterated, but on a change in the inactivation time course. Nitrendipine hastened the current turn-off (fig. 33a) and Bay K 8644 increased the current magnitude to about 20% (fig. 33b) and shifted the steady state activation to the left by 5-8 mV.

Omega Conotoxin

A peptide from the venom of the marine snail, Conus geographicus, ω -conotoxin, reversibly blocks the low-voltage-activated calcium channel (T - type) but irreversibly removes the two high-voltage-activated currents in sensory neurons (Tsien et al., 1987). In this system, ω -CgTx quickly blocked the calcium channels at 10 nM without recovery (fig. 34).

33a



33b

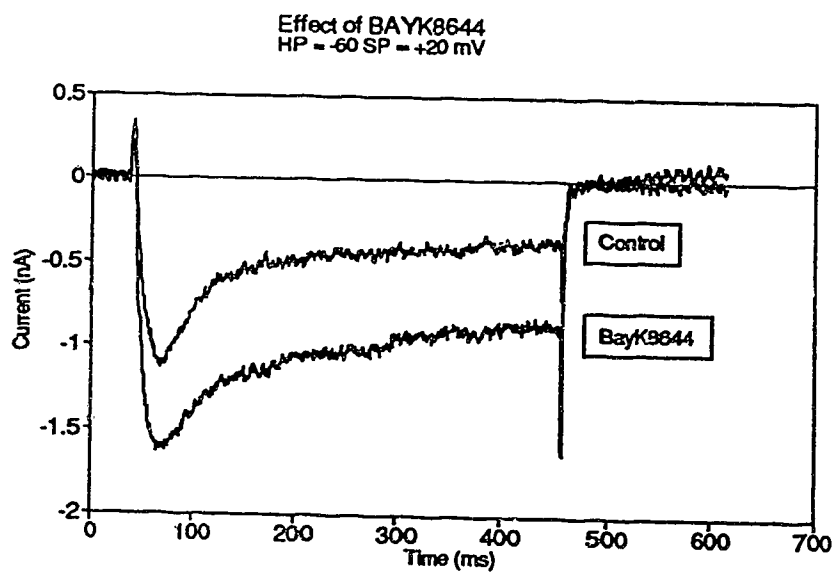


Figure 33a & b. The effect of the dihydropyridines.

The concentrations of the DHPs used to achieve any effect on the calcium channel were relatively high compared to that which has been reported in the literature. a. As much as 200 μM or more of nitrendipine was required to reduce the current. It was observed that the DHP calcium channel antagonist not only reduced the current magnitude but increased the decay of the current. b. The DHP calcium channel agonist BayK 8644 (300 μM) increased the current to about 20% with a slight left shift in the steady state activation curve (not shown).

Figure 34 Effect of Omega Conotoxin GVIA
HP = -60 SP = 20 mV

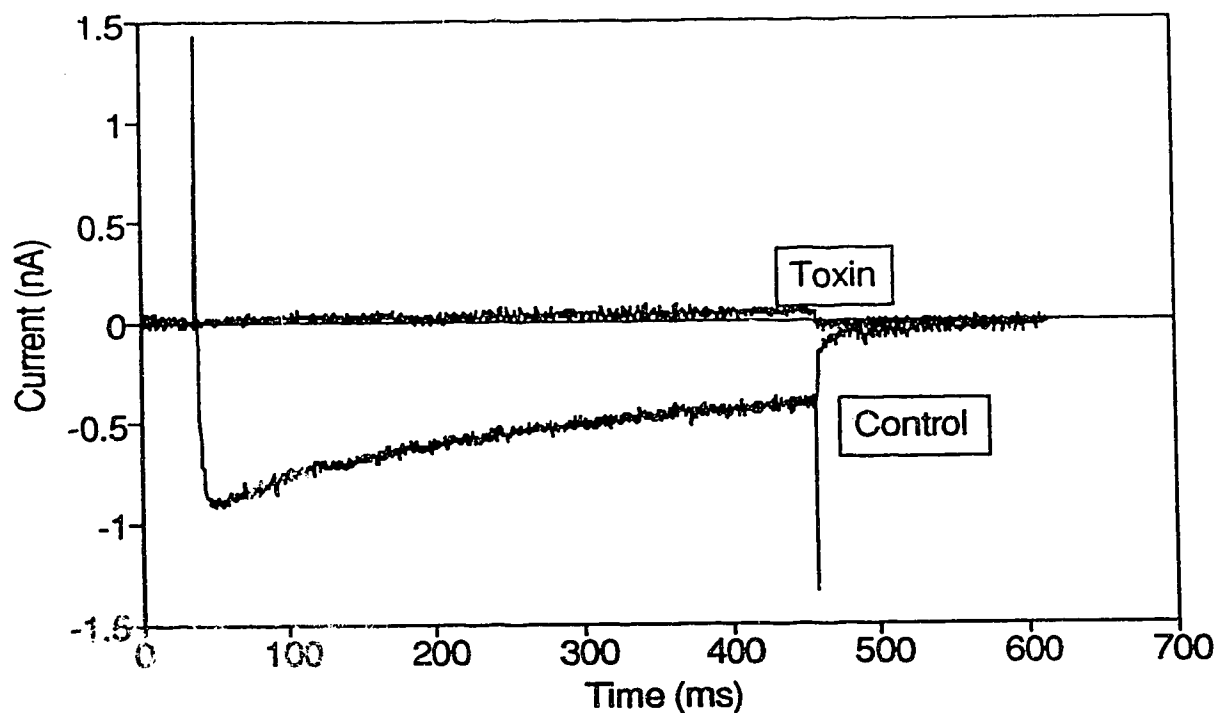


Figure 34. Effect of ω -conotoxin.

The channel is very sensitive to the organic blocker, ω -conotoxin. 10 nM irreversibly blocked the channel. Even transient application of the toxin persistently blocked the channel. The current demonstrated was elicited with a holding potential of -60 mV and stepped to +20 mV at 7°C. Leak current was subtracted on-line. After few seconds of application, the toxin removed the current completely and recovery was never achieved in these experiments.

Discussion on Calcium Current.

The concept of calcium permeation through excitable membranes was first indicated by Fatt and Ginsborg (1958) on their work on the crustacean muscle, but it was not until the mid-70s that techniques were developed that allowed recording of calcium currents (Keynes et al., 1973; Reuter, 1973; Hagiwara et al., 1975; Eckert & Lux, 1975; Connor, 1977). Subsequently, improved techniques (Kostyuk et al., 1977; Tillotson & Horn, 1978) and the use of pharmacological blockers of other ionic channels have permitted complete isolation of the calcium channel current. Apart from the recently discovered transient I_{Ca} (see Tsien et al., 1987), calcium channels usually require strong depolarization to activate compared to sodium channels (Hille, 1984). In addition, the time course of activation and inactivation is slow with activation often described by square law kinetics (Hille, 1984; Cena et al., 1989) in analogy to the third power used for sodium channels (Hodgkin & Huxley, 1952). The inactivation of calcium channels, has been reported to be dependent on current (Eckert and Chad, 1984), voltage (Adams & Gage 1979) or both (Brown et al. 1981). In addition, the presence of multiple calcium channels and other channels in cells compounds the problem associated with effective analysis of the inactivation kinetics of the channel. Because of the apparent complexity of I_{Ca} inactivation, no model, to date, has

been successful in predicting the behaviour of the channel(s) at all voltages (Eckert and Chad 1984). Where it has been possible to simulate the current, inactivation has been ignored or assumed to be absent, with short duration pulses (Llinas et al., 1981b; Cena et al., 1989). The exact mechanisms of the channel inactivation is needed to model the channel kinetics.

The majority of calcium channel populations studied in the identified cluster of neurons in Hermissenda crassicornis belong to one class. The current recorded from these neurons was homogeneous and the variations observed were not so much in the channel kinetics or pharmacology but of the current magnitude which might have resulted from the heterogeneity of channel densities in the neurons (Tillotson, & Gorman, 1980; Hagiwara & Byerly, 1981; Thompson & Coombs, 1989). The calcium channel current had a slow onset (compared to sodium current), had a sigmoidal time course of activation and slow inactivation kinetics, which was dependent on both voltage and calcium influx. Superficially, these findings are similar to reports from other systems, such as, the squid axon (Baker et al., 1973, Llinas et al., 1981a), amphibian and mammalian cardiac muscle (New & Trautwin, 1972; Campbell et al., 1988) cell bodies of Aplysia and Helix neurons (Eckert & Lux, 1976; Lux & Heyer 1979; Brown et al., 1981; Eckert & Chad 1984) and frog twitch muscle (Sanchez & Stafani, 1978). However, detailed mechanisms of activation and especially, inactivation

are different from system to system. Here I present properties of calcium channels (table 8) in Hermissenda neurons.

Table 8.

Summary of the characteristic properties of the calcium channel in identified FRMRamide sensitive neurons in Hermissenda crassicornis.

| Properties of voltage-dependent calcium channels in H. C. | |
|---|--|
| Activation range (10 mM Ca ²⁺) | Positive to -40 mV |
| Inactivation range | ≈ -100 to ≈ -20 mV |
| Relaxation rate at 0 mV (10 mM Ca ²⁺) | $\tau_{fast} \approx 20-29$ ms $\tau_{slow} \approx 410-536$ ms |
| Membrane conductance from slope of IV (10 mM Ca ²⁺) | ~29 nS |
| Cadmium & Lanthanum block | Sensitive |
| Cobalt & Nickel block | Less sensitive |
| Dihydropyridine sensitivity | -?- |
| ω -CGTX block | Persistent |

Identification of the Current

The conditions under which the experiments were conducted assumed suppression of all outward and sodium currents. Pharmacological blockade of the delayed rectifier and calcium activated potassium currents was achieved with 100 mM and 20 mM external and internal TEA respectively (Adams et al.,

1980). In addition, the transient outward current was suppressed with 5 mM 4-AP. The masking effect of outward current on the time course of the inward current was minimal, if not absent. Extracellular sodium was replaced with choline ions to remove sodium current. The possibility that a chloride conductance was present was ruled out based on the apparent reversal potential of the current and the fact that altered concentrations of either extra or intracellular chloride ions did not cause any detectable change in the recorded current.

The inward current recorded in H. C. neurons increased in magnitude with increased $[Ca^{2+}]_e$, and was blocked by cadmium, lanthanum or nickel. Also, the channel was sensitive to nanomolar concentrations of ω -conotoxin and was blocked by relatively high amounts of the dihydropyridine calcium channel antagonist, nitrendipine. Although the null potential of the current as extrapolated from the IV curve (85 ± 14 mV; mean \pm S.E of mean, from seven cells) did not coincide with the predicted Nernst equilibrium potential for calcium ions (+187 mV: equation 3-3, temperature = 9°C, $[Ca^{2+}]_i = 1.2$ nM, $[Ca^{2+}]_e = 10$ mM) the results were not surprising, considering the large asymmetry of calcium ion distribution in and outside the cell (Hagiwara & Byerly, 1981). In addition, calcium channels may be permeable to other ions (e. g. K^+ : Campbell et al., 1988) and in that case the null potential predicted by the Nernst equation will deviate from the actual reversal voltage.

Complementary to the present observation are reports from molluscan cells (Akaike et al., 1978) and squid pre-synaptic terminal (Llinas et al., 1981a) in which it was shown both experimentally and numerically that at high depolarized voltages I_{Ca} was immeasurable and that the reversal potential of calcium could be assessed properly only when $[Ca]_i$ was raised to 10^{-4} M or more. Raising intracellular calcium to such levels will, of course, induce an unstable experimental condition because of neuronal death following calcium overload. The evidence presented here, indicates that the inward current studied was calcium current. However it does not guarantee the purity of the current.

How pure was the calcium current? The blockade of potassium channels by cesium can be removed by strong depolarization (French & Wells 1977; Fukushima, 1982) and there is evidence to suggest that monovalent ions permeate calcium channels (Reuter & Scholz, 1977; Lee & Tsien, 1982). Either or both of these, if present in H. C. neurons would have been detected as an outward contamination of I_{Ca} being evident with increasing depolarization.

The occasional outward currents recorded at potentials greater than +80 mV, with I_{Ca} were not blocked with calcium channel blockers which suggested that the passage of cesium or other monovalent ions through the channel was probably not applicable in this situation. In general, increased depolarization did not enhance the decay of I_{Ca} . There were

some voltage ranges where reduced depolarizing steps elicited current traces with faster time course of inactivation than increased depolarization. This should not be taken as evidence for inadequate space clamping (see appendix) nor should it be interpreted as an indication of the presence of two calcium channel types, but as it will be discussed later, it result, predominantly, from a single class of channels with a calcium dependent inactivation component (Chad & Eckert, 1984; Plant, 1988).

Number of Channel/s.

Calcium channels appear in different subtypes, even in the same neuron (Tsien et al., 1987). Whereas the channels in vertebrates have been distinctly grouped into three types, it has been difficult to do likewise to invertebrate neuronal calcium channels (Tsien, et al., 1988). The limited classification can be attributed to inadequate information and of the variability of calcium channel properties in the phylogenetically diverse invertebrates. In this thesis, attempts have been made to draw parallels between I_{Ca} in H. C. neurons and that of vertebrates rather than categorizing it as a novel channel.

Alkon et al. (1984) were the first to record calcium currents in H. C. neurons followed by Collins et al., (1988), but outward current contamination of the early work did not

allow for detail biophysical analysis. Despite the unique nature of the cells (photoreceptors) Alkon and co-workers recorded from, there were some similarities between their findings and the present report. They observed that their I_{Ca} appeared at potentials around -40 and -30 mV and the channel was sensitive to cadmium blockade (Collins et al., 1988). Implicitly, their evidence suggested that there were only one type of calcium channel in photoreceptors.

The current-voltage curve of I_{Ca} from the cluster of neurons studied, like that in other molluscan neurons (Brown et al., 1981), was bell-shaped for both the peak and steady state current records and the activation time course was monophasic. On one hand these results could be interpreted as evidence for one distinct channel population and on the other hand, it could be inferred that there are two classes of channels with similar activation, (e. g. N and L channels) but perhaps different inactivation kinetics.

In normal extracellular calcium (10 mM, sea water), the decay of the current required two exponential fits but with reduced bath calcium (5 or 6 mM), a single time constant was appropriate to fit the inactivation profile. Thus the double exponential decay seen in normal calcium resulted not from two channel subtypes, exhibiting different inactivation properties, but from a calcium dependent component of the inactivation kinetics of one channel type. I conclude, based on the experimental conditions, that at least in this cluster

of neurons, only one predominant class of calcium channel population is present.

Are low-voltage-activated channels present?

Most of the recordings in this study were made at holding potentials of -60 mV; a potential at which a majority of low-voltage-activated channels, if present, would be in the inactivated state. Nevertheless, the data presented have traces of evidence which indicate that a small proportion of the current had characteristics of a low-voltage channel. (1) The current voltage relationship drawn from traces elicited at -80 mV (fig. 14b) had a small 'shoulder' (≤ 100 pA) at -50 to -30 mV. (2) Cobalt ions removed this 'shoulder' (see fig. 32b). Hyperpolarizing holding potentials (> -80 mV) were avoided because of potential membrane breakdown at those voltages. (3) On one instance when currents were examined at -90 mV; see fig. 25), the inactivation curve appeared biphasic. (4) The time constant of activation with voltage (fig 20) was reduced to a mono-phasic process to simplify the interpretation of the data. However, it is equally possible to describe the curve as bi-phasic. Taking together, it appears that there are low-voltage activated channels in the neurons studied. But the channel population must be small or the current magnitude was reduced under the conditions examined here.

Pharmacology of the Channel

The effects of inorganic and organic blockers of calcium channels are well-known and extensive reviews of their mechanisms of action have been made (Hille, 1984; Miller, 1987). In this system, cadmium blocked the channel in a voltage independent fashion. As suggested earlier by Jones and Marks (1989), this action reflects Cd^{2+} 's blockade of the channel even at closed state. There was no evidence, however, to suggest that the block was removed with large depolarization as seen in bullfrog sympathetic neurons (Jones and Marks, 1989). Certainly, I cannot rule-out the possibility that such mechanism could occur in this system, since the intensity of potentials used in these experiments (+60 mV; pre-pulse) were lower than that used in sympathetic neurons (+80 mV: pre-pulse).

La^{3+} decreased I_{Ca} without causing any shift in the steady state current-voltage relationship. As opposed to Cd^{2+} , the effect of La^{3+} was incomplete at the concentrations used, and it appears that La^{3+} could be pushed out of the channel with strong depolarization. Though lanthanum has been shown to be the most potent inorganic blocker of calcium channels in many systems (Hagiwara & Takahashi, 1967; Brown et al., 1981; Hille, 1984), I did not find it to be the case here. Presumably, the channels belong to a sub-class (N-type) which are more sensitive to Cd^{2+} than La^{3+} . Nickel and cobalt had a

less potent effect. While Cd^{2+} and La^{3+} substantially reduced I_{Ca} at micromolar range, Ni^{2+} and Co^{2+} were effective blockers only at millimolar concentrations.

In the past, it has been accepted that the sensitivity of a high threshold calcium channel to the dihydropyridines is a good indication that it is an L-type channel. Recently, it has been reported that at high concentrations (10 μM), nifedipine partially blocked the N-type channel (Jones & Jacobs, 1990). As mentioned by the authors, for one thing the lipophilic nature of the DHPs might have resulted in a non specific effect and for another, there have been similar reports that at high concentrations the drug blocked potassium (Nerbonne & Gurney, 1987) and sodium (Yatani & Brown, 1985) channels as well. In addition, the potency of the DHPs on calcium channels vary from system to system. For example, the EC_{50} for cardiac muscles is around 0.5 μM (Morad et al., 1983; Sanguinetti & Kass, 1984; Nerbonne et al., 1985) that of smooth muscles is about 0.25 μM (Bean et al., 1986; Hering et al., 1988; Nelson & Worley, 1989) and in Aplysia bag cells a value of 1.4 μM has been reported (Nerbonne & Gurney, 1987).

In consonance with the variability of the effectiveness of the DHPs as Ca-channel antagonist, is the fact that BayK 8644 is a calcium channel agonist at the single channel level but in some cases appears to have no effect on the whole cell currents (Nowycky et al., 1985). Also Bay K 8644 has mixed actions, agonist and antagonist, and nifedipine has been found

to be an ineffective antagonist on channels which are sensitive to BayK 8644 (Boll & Lux, 1985). Thus evaluation of the effectiveness of the DHPs as calcium channel agonist or antagonist has been a bit inconsistent. Nevertheless they continue to be the drugs of choice in I_{Ca} studies. Where the actions of the DHPs appear unequivocal, the mechanism of calcium channel block is partly understood. The DHP blockers act independently of channel activation process but reduce the mean open time of channels (Kawashima & Ochi, 1988); consequently the decay of the macroscopic current is increased (Lee & Tsien, 1983; Nerbonne & Gurney, 1987).

In the present study, I found the concentration of the DHPs required to effect any action (200 - 500 μ M) on the calcium channel to be too high to make conclusions on the specificity of the drug on the channel. It is likely that the action seen here resulted from a non-selective effect of the drug. On the other hand, it can be argued that the temperature of the experimental conditions (7 - 9°C) may have resulted in high concentrations of the DHPs required to cause an effect. Nerbonne & Gurney (1987) studied the effects of the DHPs on Aplysia neurons at 14 - 15°C. The effective concentration used in those experiments was 6 times less than that used here. It is also possible that the channel is similar to the N-type channel and consequently large amounts of the DHP is require for blockade. Even so, the

concentrations used were a bit too high for the drug's selectivity when compared to other documented results.

Activation of Ca current.

Activation of the calcium current is simple based on these observations: (1) In leak-corrected current records, both the activation and deactivation phases were fitted by mono-exponential functions. (2) The apparent conductance of the channel could be described with the Hodgkin-Huxley scheme of m to the second power as opposed to higher powers used in other systems (Llinas et al., 1981b). A square law kinetics gave an equally good fit but showed a short delay on the current onset. (3) A change in bath calcium from 6 mM to 10 mM did increase the amplitude of the current, in accordance with the independent law of ionic permeation, but did not alter the kinetics of the current appreciably. (4) The IV curve for both the peak and steady state currents were uniform with no apparent kinks or shoulders.

The conductivity of the calcium channel saturated at modest bath calcium concentration ($[Ca]_e \geq 20$ mM). This was true for barium and strontium currents as well. In addition, the kinetics of activation remained unchanged when either Ba^{2+} or Sr^{2+} were the charge carriers. However, the channel's availability for activation with voltage was enhanced in barium and to a lesser extent in strontium than in calcium

external solution. In support of these findings is the suggestion made by Hagiwara & Byerly (1981), that the calcium channel contains a site which binds with Ca^{2+} more tightly than other divalent cations.

Inactivation of calcium channel.

The results presented show that the inactivation of calcium channels in the identified neurons in H. C. is dependent on both current and voltage. Evidence for current induced inactivation are as follows:

(1) The extent of inactivation increased as the current magnitude was raised with a change of bath calcium from 5 mM to 10 mM and the decay shifted from mono to bi-phasic kinetics as well. For some range of voltages, -30 to 0 mV, the τ_{fast} became smaller as calcium influx increased, but at more positive potentials the relationship became complex and was not predictable by any simple means. Alteration of the inactivation curve by changes in extracellular calcium was indicated first in stick insect muscle (Ashcroft & Stanfield, 1981; 1982) and later confirmed in atrial myocytes (Campbell *et al.*, 1988). In both cases and in this system as well, the calcium dependent component of inactivation was saturable with the saturation limit in stick muscle being 50 mM, atrial myocytes 7.5 mM and in Hermisenda neurons 20 mM. Were the inactivation dependent solely on voltage, as in sodium channel

(Hodgkin & Huxley, 1952), the h_{∞} or percent inactivation curve should be monotonic and independent of $[Ca^{2+}]_e$.

(2) Double pulse experiment with a short inter-pulse gap (6 - 10 ms) to avoid substantial time-dependent recovery of inactivation, for calcium, strontium and barium currents all showed an inverted U-shaped percent inactivation curve (or a U-shaped relative inactivation curve). A U-shaped inactivation curve is indicative of a current dependent inactivation (Eckert & Chad, 1984; Plant, 1988) however, it does not exclude the possible effect of voltage, especially when the shape is incomplete (Bezanilla & Armstrong, 1977; Meves, 1978; Yeh & Oxford, 1985; Campbell *et al.*, 1988).

(3) If the process of inactivation operated without the involvement of calcium, then introduction of intracellular chelators, irrespective of their binding affinities, should leave the decay unaffected. Qualitatively, BAPTA a more efficient Ca-chelator, reduced the turn-off of I_{Ca} .

For the reasons stated above, I suggest that the current contributes to the inactivation of I_{Ca} in the identified FRMRamide sensitive neurons in Hermisenda. However, a pure current inactivation mechanism is incompatible with the data because: (a) High intracellular calcium ($\approx 10 \mu M$) did not reduce the available channels for activation substantially but instead, it resulted in a pseudo-monotonic function between inactivation and voltage. Thus, under conditions of high

$[Ca^{2+}]_i$, the channels behave as if they are readily available for inactivation with voltage but not current.

(b) Inactivation at a test pulse increased with calcium influx during conditioning pulses of ≈ 750 ms duration from -80 to $+10$ mV but beyond $+20$ mV some form of hysteresis developed in the relationship with inactivation increasing at voltages (≥ 50 mV) even though the calcium influx was relatively small at this potential range. Such findings which were first reported in Helix neurons (Brown et al., 1981) and recently confirmed by Gutnick et al., (1989), appear to implicate voltage as a participant in the mechanism of inactivation.

(c) An absolute current dependent inactivation implies that the U-shaped inactivation curve should be complete i. e. inactivation should increase as we approach the peak activation voltage (e. g. $+20$ mV in FSNs) and decline as the membrane potential moves towards the null potential. In contrast, the data obtained did not give a complete U-shaped inactivation curve, instead, at high depolarised potentials the inactivation was enhanced. Thus the contribution of voltage to I_{Ca} inactivation cannot be ignored.

Consistent with these findings are reports from Helix neurons (Brown et al., 1981; Gutnick et al., 1989), Bull-frog atrium myocytes (Mentrard et al., 1984; Campbell et al., 1988) and Stick insect muscles (Ashcroft & Stanfield, 1982) but in contrast are results from mouse pancreatic β -cells where the inactivation curve reaches 1.0 at potentials $\geq +60$ mV (Plant,

1988). In studies where the inter-pulse gaps were short (≤ 20 ms: Campbell et al., 1988; Gutnick et al., 1989; this report) the argument that the ascending limb of the U-shaped inactivation curve is controlled by the tail current does not hold (Chad & Eckert, 1984; Campbell et al., 1988). Therefore, it is apparent that current alone cannot be used to account for the decay of I_{Ca} .

(d) Intracellular EGTA and BAPTA were unable to obliterate I_{Ca} inactivation. BAPTA reduced the decay of the current but the effect is only quantitative during the first few hundred milliseconds of the current waveform. It is interesting to note that, theoretically, BAPTA should be capable of buffering Ca^{2+} at a distance closer to the channel than EGTA (Neher, 1986; Gutnick et al., 1989). Moreover the lack of BAPTA to cause a significant reduction in inactivation suggested that if the process of current turn-off were dependent on calcium then, the calcium binding site was restricted from the chelator by, for example, cytoplasmic diffusion at the vicinity of the channel (Neher, 1986). Furthermore, as suggested in Helix neurons, it is possible that the channel, once activated can move to the inactivated state via two pathways, a calcium and voltage dependent pathways (Gutnick et al., 1989).

An alternative mechanism which was mentioned, briefly, by Gutnick and others (1989) was the possibility that subsequent to activation of the channels a mode is reached where they

become unwilling to inactivate. A model of this kind can be used, at least superficially, to explain most of the present findings.

Models of inactivation mechanism.

The analysis of the inward calcium current records presented here strongly supports the idea that the underlying mechanism for inactivation rests on concerted action of both calcium and voltage. An absolute voltage-dependent mechanism of inactivation cannot account for the non-monotonic dependence of inactivation on voltage. Nor can a simple calcium-dependent inactivation explain the incomplete U-shaped inactivation curve and the inactivation observed in divalent cation substitution experiments. It can be argued quite reasonably, that Sr^{2+} and Ba^{2+} are perhaps capable of substituting for Ca^{2+} at the 'inactivation binding site' of the channel, to cause channel turn-off, at lower rates and affinities. But we cannot explain why intracellular BAPTA, a high affinity Ca^{2+} buffer, was unable to remove inactivation. It is conceivable that diffusional barriers at the sub-membrane space would prevent access to the vicinity of the channels. However, this is unlikely especially under whole cell patch conditions which can be maintained for at least an hour or more.

To account for some of the observations made, a model is developed where the calcium channels upon activation with depolarization, undergo a transition into two open state configuration in series before inactivation: First from a stable open state (difficult to inactivate) then to an unstable open state (inactivate readily with voltage). I predict that membrane hyperpolarization favours the transition to the stable-open configuration. However, the binding of calcium to the channel moves it to the unstable-open state. Under conditions where intracellular free calcium is relatively limited (in the presence of chelators e. g. 10 mM EGTA), the inactivation process depends on the transition to the stable-open state. However, it is predicted that when cytosolic free calcium rises, the equilibrium is shifted such that, the transition to the unstable state predominates and depolarization become the determining factor controlling inactivation.

Various models of the kinetics of calcium inactivation have been made in past to explain observations similar, but not identical, to the ones made in this project. Eckert & Ewald, (1984) and Standen & Stanfield (1982) ignored voltage and modelled inactivation on the basis of calcium-dependent process. Jones & Mark (1989) did the opposite. They were able to explain similar findings as sole voltage-dependent process. On the other hand Gutnick et al., (1989) considered an approach based on both voltage and calcium. In their model

they assumed that inactivation began from a lumped state of activation, independent of whether channels were closed or opened, and that channel transition to the inactivated state occurred via either a voltage dependent or a calcium dependent pathway. This model explains some of the present observations, for example, voltage-dependence of inactivation upon saturation of the calcium-dependent pathway. However, it falls short in accounting for the split in time constant of inactivation. Rather it predicts a biphasic time constant of inactivation for all step voltages and as such cannot be used to explain calcium channel inactivation in Hermisenda neurons. Moreover, it can be argued quite reasonably that under conditions when the two parallel processes of inactivation mechanism are at similar rates, they may be kinetically inseparable. This being the case, then the parallel model of Gutnick et al., (1989) can equally explain the observations made here.

The model predicted here can explain all the observed kinetic properties of the inactivation but only at the qualitative level. The present experiments, do not give all the necessary information for quantification. Single channel and biochemical data on the channel's properties will be required for such kinetic study. For example, single channel studies will make evident the possible number of open states of the calcium channels. Until the right conditions for attainment of a good seal resistance, measurement of single

channel calcium currents in H. C. will still be lacking. Dr. R. Etcheberrigaray has been successful in recording single channel potassium currents in H. C. (per. communication) and it is hoped that improvement on his techniques may perhaps be used for single calcium channel recordings in the future.

Physiological considerations.

The functional significance of I_{Ca} inactivation, as has been suggested in several reports, may perhaps be intended to prevent intracellular calcium overload. The negative feedback regulation of calcium influx by Ca^{2+} ions together with voltage dependence of calcium channel inactivation are finely tuned to regulate calcium. While the action of calcium may be transient, it is predicted that the effect of voltage may play a predominant role when the calcium mediated inactivation and perhaps intracellular calcium protein buffers have been exhausted. For example, during long lasting membrane depolarization, in the presence of a stimulator (FMFRamide) or light, voltage dependent inactivation may be important to shut-off excessive calcium influx.

Neurons may appear to operate to remove as much calcium from the cytosol as they possibly can but it should not be overlooked that most neuronal functions are partly or fully dependent on calcium. Thus it stands to reason that neurons adopt means to encourage calcium influx. The transition of

calcium channels from a state of open to stable-open state may be a plausible mechanism by which intracellular calcium can be increased to enhance intracellular biochemistry.

Concluding Remarks.

Hermissenda crassicornis has been a useful model system for studies related to the nature of memory trace (Alkon et al., 1987). In past two decades, Alkon and co-workers have observed several adaptive changes in the neurobiology of H.C. after the animal has been made to undergo Pavlovian conditioning. For example, it has been demonstrated that upon conditioning, there is persistent reduction of transient and delayed potassium currents (Alkon et al., 1982; Alkon & Sakakibara, 1985; Alkon, 1987; Collin, et al., 1988). Such biophysical adaptive changes, known as memory trace in some quarters, and the increase in the expression of novel proteins, subsequent to conditioning (Nelson et al., 1989), have been shown to be triggered by calcium. In fact, calcium, it seems, is the pivot on which long term changes in neurons rest (Alkon & Rasmussen, 1987).

We are far from understanding the underlying mechanisms for long term adaptive changes in neurons. However, it is clear at this point, that knowledge of calcium regulation in neurons is crucial for studies concerning 'memory'. Ideally, the target for studies in H. C. should be the photoreceptors

where most of the work has been done. At the moment, voltage-clamp studies of the photoreceptors have some basic problems that need to be solved before any meaningful biophysical analysis of calcium current and regulation can be made (see Collins et al., 1988).

The motive for the present project was therefore to develop a method of measuring, within limits of experimental error, calcium currents with the ultimate goal of understanding intracellular calcium homeostasis in Hermissenda neurons. It is recognized that in invertebrate neurons, the advantage of identifiability usually implies the sacrifice of heterogeneity in neuronal properties. However calcium channels are normally ubiquitous, and while it is expected that perhaps the minute details of the properties of calcium channels in H. C. photoreceptors may be different from the FSNs, it is predicted that the salient features of calcium channels in Hermissenda neurons will be the same. Interesting enough, the calcium currents recorded in the homogeneous cluster of FMRFamide neurons appear to have similar properties to those measured in the photoreceptors amid outward current contamination (Collins et al., 1989).

This project clearly indicates that regulation of intracellular calcium in neurons is not a one component event but is brought about as a result of a concerted effects of several mechanisms in which calcium current inactivation play a fundamental role. Ca^{2+} -mediated inactivation of I_{Ca} may be

one of the immediate mechanisms for prevention of unnecessary rise in $[Ca]_i$. Moreover, as shown in the body of this work, the effects of voltage dependent inactivation of I_{Ca} come into play when intracellular calcium is raised in conditions when, for example, the buffering capacity of intracellular proteins has been exhausted.

APPENDIX

Appendix A

VOLTAGE CLAMP

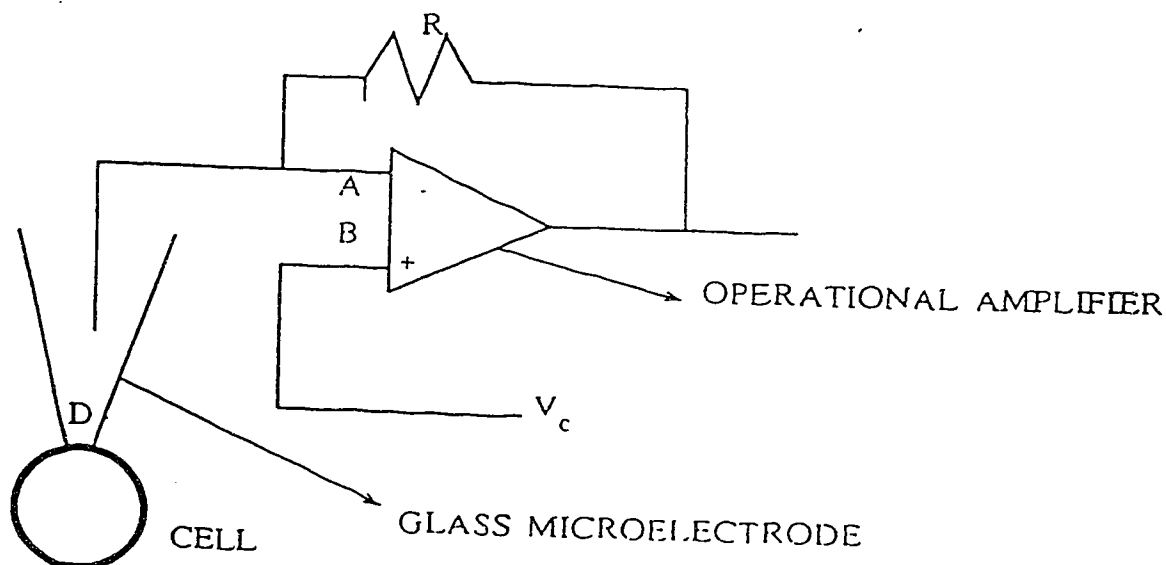
The voltage clamp technique was developed by K.S. Cole in 1949, for the study of currents underlying excitability. Since then, several modifications have been made to the technique depending on the preparation (Adrian et al., 1970) and the type of study (Brennecke and Lindermann, 1974; Hamill et al., 1981). Arbitrarily, I group the different forms of voltage clamp into two, namely; multiple electrode voltage clamp (MEVC) and single electrode voltage clamp (SEVC). The former is usually used for preparations which are accessible for penetration by two or more electrodes and in which mechanical injury caused by the electrodes is considered minimal (Hodgkin and Huxley, 1952; Finkel and Redman, 1984).

Single electrode voltage clamp on the other hand was developed initially to study visually inaccessible or small cells (Brennecke and Lindermann, 1974; Finkel and Redman, 1984). Moreover, other forms of this method have been used to study accessible single cells (Hamill et al., 1981; Jones, 1987). Discussions on the circuitry and limitations of MEVC and SEVC have been made (Cole, 1968; Moore, 1963; Adrian et al., 1970; Finkel & Redman, 1984). What I will do in this section is to mention the method used in this project and to

discuss its inherent limitations and how I have gone about reducing the ensuing errors.

The tight-seal whole-cell version (Hamill *et al.*, 1981) of SEVC was used. Approximately 30 μm diameter cells, without processes, were studied. With an operational amplifier (low input impedance: figure A-1) the voltage to ground of both terminals A and B should be similar. A is connected via a silver wire to an electrode, e.g. patch electrode, and the command voltage V_c elicited at a connection to B. V_c will be similar to the voltage at A and D. This is a very simplified explanation of how the patch clamp technique works.

Figure A-1. Simplified circuit of patch clamp.



(See text for description of circuit)

Microelectrodes have finite resistance. Debris at the pipette tip results in additional resistance between the headstage amplifier and the cell. The effective voltage at the tip of the electrode V_e , is therefore equal to the command voltage V_c minus the voltage drop across the electrode with series resistance (R_s).

$$V_e = V_c - (I * R) \dots\dots\dots (A-1)$$

From the above equation V_e moves far from V_c when the current I increases, assuming a large series resistance R_s . As a rule of thumb, the product of I and R_s should not be more than 3-5 mV (Marty & Neher, 1983). From this arbitrary voltage range, Marty and Neher (1983) defined a criterion which essentially stated that, the tight-seal whole cell recording (TSWCR) is more suitable for measurement of current less than 1.5 nA, or 15 nA if 90% of the series resistance is cancelled out, electronically. Based on the assumption that the outward current density of most cells is similar to that of the squid axon, 5 mA/cm² (Hodgkin and Huxley, 1952), the authors concluded; cells not larger than 3 μ m in diameter or 10 μ m for 90% R_s compensation meet the requirement for TSWCR.

The identified class of neurons studied had a range of diameters of 25-35 μ m (see chap. 2). The maximum calcium current recorded was 1.2-1.5 nA. If one assumes the series

resistance to be four times the electrode resistance (e.g. 0.8 M Ω ;Marty & Neher, 1983), then, the maximum voltage drop expected at the tip of the electrode is 3.84 - 4.8 mV (e.g. 3.2 M Ω \times 1.2 nA).

Series resistance can be measured (fig. A-2). In voltage clamp mode, the product of membrane capacitance (C_m) and the series resistance R_s equals the time constant (τ) of the capacitive transient ($\tau = C_m R_s$ i.e. $R_s = \tau / C_m$..A-2). τ is computed by fitting an exponential curve to the decay of the transient.

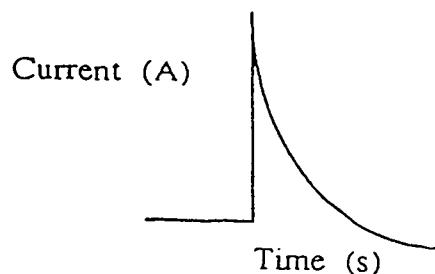


Fig. A-2 Capacitive transient

Integrating the area under the capacitive transient gives the charge (Q) in Coulombs:

$$Q = C_m V \quad \dots\dots\dots A-3$$

V is the step voltage. C_m can therefore be calculated and from the results R_s computed from equation A-2. The series resistances of most cells were measured and when R_s was high, the data were discarded. However, there were a few instances

when the R_s was not measured, commonly, when the pharmacology of the channels were studied.

A representative trace seen (after the capacitance of the electrode has been compensated) when a cell was held at -60 mV and stepped to -80 mV is shown in figure A3a. The time constant of relaxation of the transient, as calculated from the reciprocal of the slope of figure A3b. was 61 μ s (71 ± 19 μ s: mean + std. error, $n = 34$). The area above the transient curve, fig A3a., represents the charge in Coulomb C (5.30817×10^{-11} C). For a step potential of 20 mV, the capacitance of the cell (in picofarad) turned out to be 26.5 pF ($C_m = Q/V$). The series resistance as seen from a typical trace was therefore, 2.3 M Ω (patch pipette resistance was 0.5 M Ω). The average range of R_s varies between 1.71 and 3.52 M Ω ($n = 27$). Typically, patch electrode resistances used in all the experiments were 0.15 - 0.8 M Ω . These calculations were made assuming no R_s compensation. In general however, 20% R_s compensation was made to reduce the error further.

Series resistance varies, even, for a given cell. In the course of an experiment the tip of the pipette can either be cleared from debris to improve the voltage clamp or it can be plugged to increase the R_s . Normally, negative pressure was applied at the end of the pipette to prevent plugging of the tip.

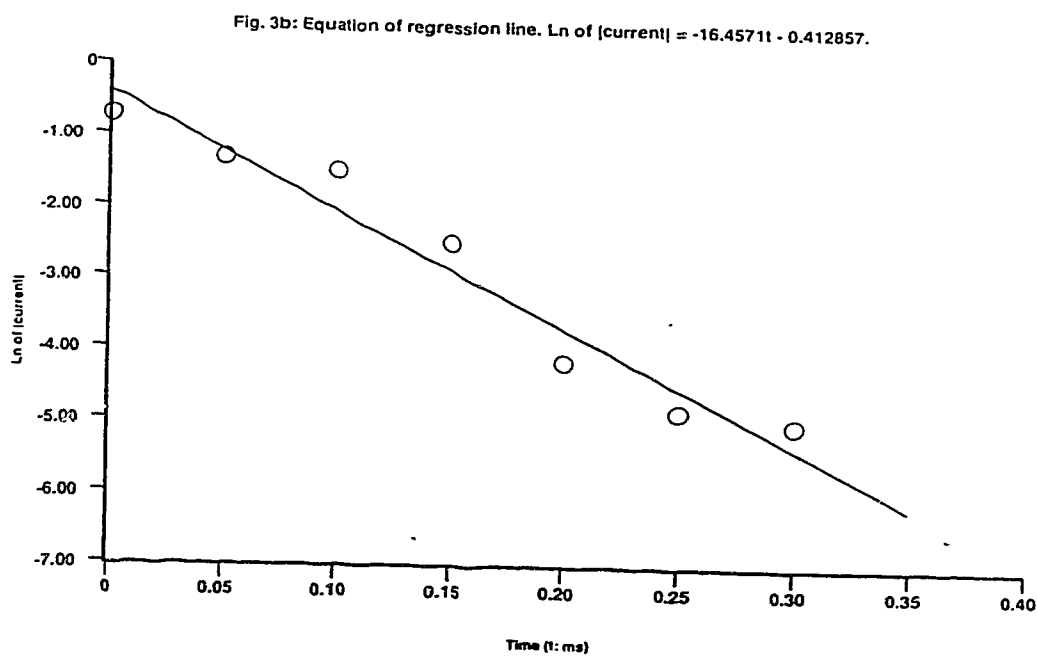
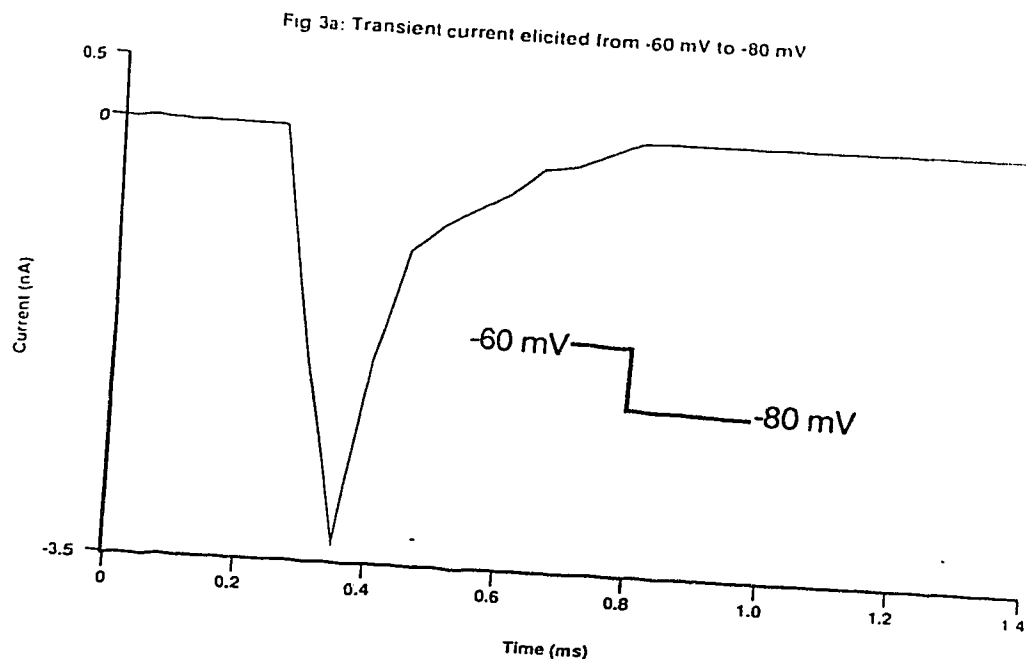


Figure A3a & b. Series resistance measurement.

After seal formation the capacitance of the patch-electrode was electronically cancelled. Neurons were then held at -60 mV and stepped to various potential without on-line leak correction. The transient illustrated here results mainly from the access resistance of the electrode. The time constant of the transient decay was calculated from b. From this, the series resistance was computed.

Moreover, small changes in R_s might have occurred undetected. It is important therefore, that the reported numbers are considered as estimates.

The assumption made in this discussion so far is that the voltage at the tip of the patch pipette is uniform over the area of the spherical cell. The tip of the patch pipette is in contact with the cell at a region which is a bit remote from the rest of the cell. Voltage applied at the pipette-tip has to spread to other regions of the cell through a resistive medium. As a result, a slight voltage drop will occur across the cell. Unfortunately, this question was not addressed when the TSWCR was developed (Hamill *et al.*, 1981). It is easy to presume that the best way to assess voltage gradient across a cell is to use two separate electrodes (one for applying and the other for measuring voltages), and so is it difficult to accept the validity of such an experiment using patch electrodes which do not form a relatively high resistance seal.

When two patch electrodes are used on a single cell, one has to assume that the seal resistances of both electrodes are extremely high. Figure 4Aa is a schematic diagram showing an electrical analogue of a cell with membrane resistance R_m (in ohms) and a capacitance C_m . If a second electrode is patched on the same cell at, for example, a point, 180° from the first electrode and it establishes a seal resistance R_{se} as shown in fig 4Ab., under conditions of relatively low seal resistance

(R_{se}), the total resistance R_t will be given by (a more detail circuit and equations are shown in appendix B):

Figure 4Aa.

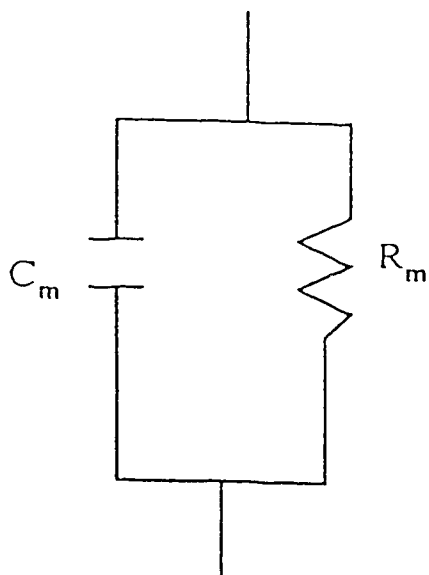
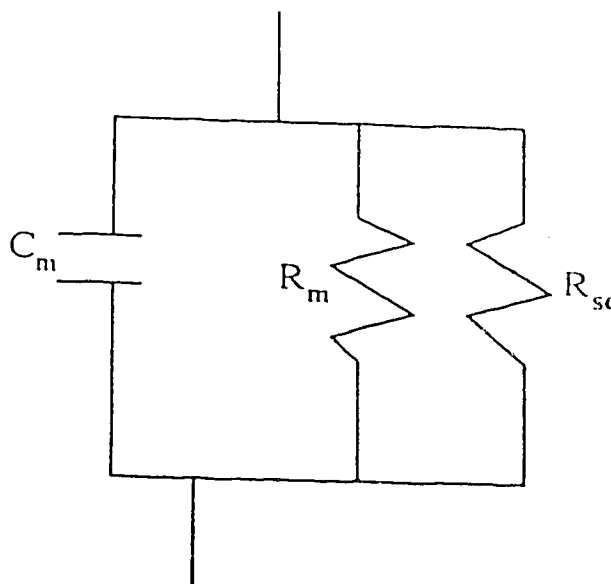


Figure 4Ab



$$R_t = \frac{(R_m * R_{se})}{(R_{se} + R_m)} = \frac{R_{se}}{1 + \frac{R_{se}}{R_m}} \dots\dots\dots (A-4)$$

As R_{se}/R_m , approaches zero R_t is approximately equal to R_{se} .

The above equation indicates that, under some limiting conditions, the voltage recorded at the second electrode can essentially be the voltage across the electrode itself and not the cell. It would, perhaps, be convenient to illustrate the above equation with relevant numbers:

For an ideal situation; if the resistance R_{se} is in the order of $G \Omega$ e.g. $20 G \Omega$ and the R_m of the cell equals $10 M \Omega$, R_t will be equal to $9.995 M \Omega$ a value which is close to R_m . The average seal resistance in the present studies was $0.9 G \Omega$, (R_{sc}) and the membrane resistance ranged from 80 to $120 M \Omega$. Arbitrarily, let us take $100 M \Omega$ as R_m . If these values were used in the above equation, R_t will be equal to $90 M \Omega$. This means a 10% drop in the effective R_m .

In cells in which it is difficult to obtain high seal resistance, the use of two patch electrodes to access voltage inhomogeneities will not be recommended.

One way of getting an idea about voltage inhomogeneities in a spherical cell is to adopt analytical expressions to suit the data. Unfortunately, such an expression, to the best of my knowledge, has not been given for TSWCR. For a spherical cell, the closest equations that are available are those of Eisenberg and Engel (1970). For isopotential conditions, the relationship between the membrane potential and current is ohmic. Equation A-5 describes this relationship. Note that R_m , here, is the specific membrane resistance measured in Ohm centimetre

squared; i_0 is current in ampere and a is radius of a spherical cell (cm).

$$V_m = \frac{i_0 R_m}{4\pi a^2} \dots\dots\dots (A-5)$$

Eisenberg and Engel (1970), derived equations which, essentially, described the error involved in the spread of voltage across a sphere. At steady state conditions, the equation turns out to be equal to the product of equation A-5 and a factor which, in this paper, I will call error factor (Errf:see equation A-6).

$$V_m = \frac{-\rho^2 R_m}{4\pi a^2} \text{Errf} \dots\dots\dots (A-6)$$

Errf. (equation A-7) should be less than one, as long as there is a voltage drop across the cell.

$$\text{Errf} = [(1 - 2a/\Lambda) (1 + (a/\Lambda) D - (a/\Lambda)^2 E_0) + (a/\Lambda) \csc\theta/2] \dots\dots (A-7)$$

The error factor involves the space constant of the cell, which is defined in equation A-8: R_i is the volume resistivity of the cell; units, $\Omega\text{-cm}$. D and E_o are defined in equations A-9 and A-10 respectively and the symbol, θ , refers to the angle between the electrode and a point on the sphere.

$$\Lambda = \frac{R_m}{R_i} \dots \dots \dots (A-8)$$

$$D = \ln \frac{\csc^2 \theta / 2}{1 + \csc \theta / 2} \dots \dots \dots (A-9)$$

$$E_o = \sum_{n=1}^{\infty} \frac{P_n(\cos \theta)}{n^2} \quad n=1, 2, 3, \dots \dots \dots (A-10)$$

A table for the respective values of θ , D and E_o has been given in Eisenberg and Engel (1970). When arbitrary values for R_m and R_i are plugged into equation 7, the profile of error seen, indicated that there was a huge error

at points close to the electrode. However, the error decreased till a point 60° from the electrode, where there was minimum error. Beyond 60° , the error increased again. This observation was consistent with that reported in Eisenberg and Engel (1970). The only difference between the calculations made in this paper and that of Eisenberg and Engel is that they considered the absolute error values (i.e. values which were sometimes greater than one) while the actual error involved were considered here.

The errors described by the original equations refer to the error at a point on the sphere and not the error involved in the region covered by the specified angle. To calculate the error at a region in the sphere, subtended at the angle (θ) the error at that point (from equation 7) should be multiplied by the region covered by this section of the sphere. Equation 11 described the region subtended by a sphere at an angle θ .

$$\frac{dS}{d\theta} = 2\pi a^2 \sin\theta \dots \dots \dots (A-11)$$

The derivation of equation 11 has been considered systematically in Appendix C: dS is the change in the

surface area, $d\theta$, is the change in θ and a , is the radius of the sphere.

During voltage clamp experiments, the worst case of voltage inhomogeneities happens when the recorded current is at its peak (i.e. when R_m is small). The worst case values of specific membrane resistance R_m ($5000 \Omega\text{-cm}^2$) and volume resistivity R_i ($100 \Omega\text{-cm}$: Gorman & Maurizio, 1972) were selected. R_m is an estimated value from experiments while R_i is an assumed value based on the literature of molluscan neurons. Low (Kuffler et al., 1984) and high (Hodgkin and Rushton, 1946; Hodgkin, 1947) values of R_i have been reported. However, the value chosen by Gorman and Mirolli, (1972) seemed to be a reasonable value to select. The diameter of cell selected for this calculation was $50 \mu\text{m}$, based on the theoretical assumption that the maximum size of cell suitable for TSWCR is about that size. Note that the error would be less if a $30 \mu\text{m}$ cell (average size of FSN) was considered. The total error over the entire region of the sphere as given by the area under figure A5 is 0.26%. What this means is that under steady state conditions if, for example, the voltage at the tip of a pipette was 10 mV, on the average, the voltage seen over the sphere would be 9.974 mV.

Figures A5 & A6.

Fig. 5 Error vrs Region of sphere

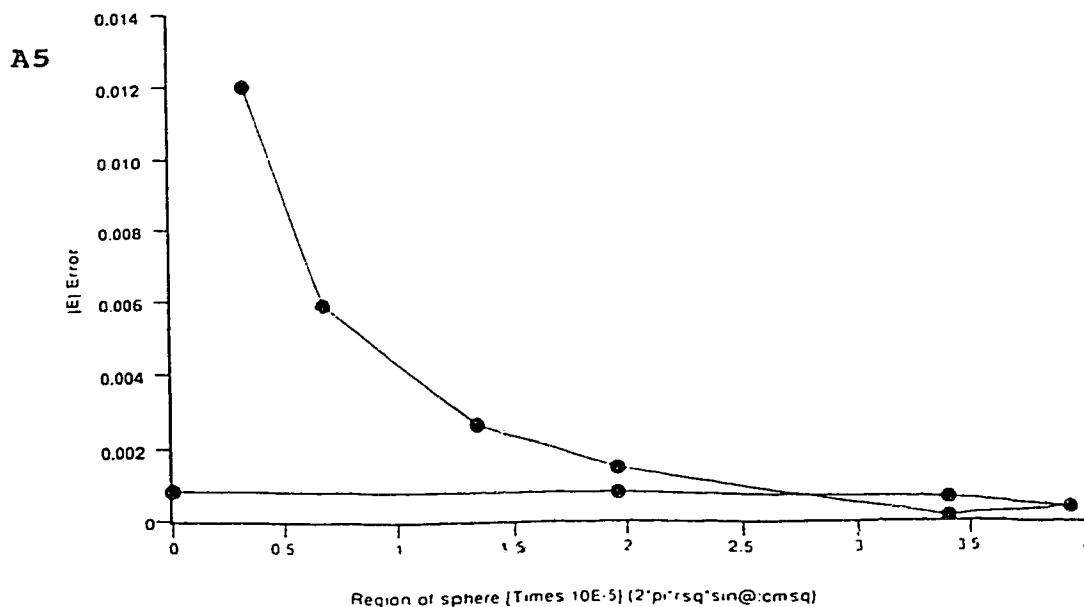
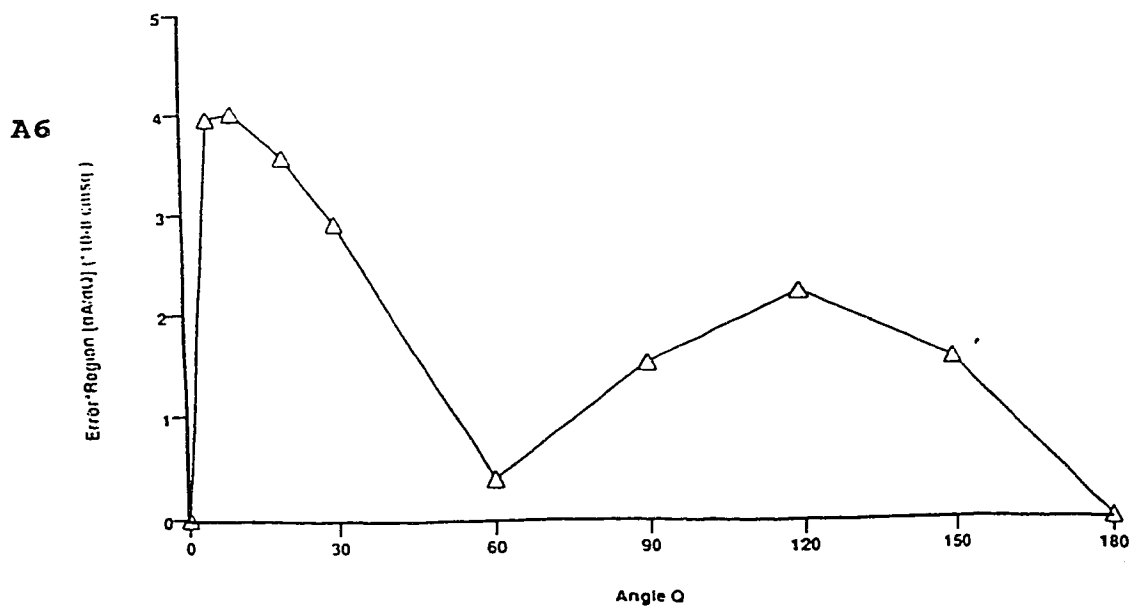


Fig. 6. Error profile over sphere.



5. The relation between the suspected error and the regions of a sphere ($50 \mu\text{m}$ in diameter) subtended at a reference point (the centre of the tip of the patched electrode; see appendix C) is illustrated. 6. Here the profile of the error as seen over the entire sphere indicates that the least error is expected at a point 60° from the patch electrode.

The worst case conditions, for calcium current (I_{Ca}), occur when the recorded current was at its peak e.g. 1.2 nA from holding potential of -60 mV to step potential of +20 mV (V_m). The input resistance R_i of the cell is given by; dV/dI ; where dV is the driving force (i.e. $V_m - V_r$; V_m and V_r are the membrane and reversal potential respectively). If we assume V_r for I_{Ca} to be +100 mV. R_i at peak current is 66.67 M Ω . Assuming a spherical cell of diameter 50 μ m, the specific membrane resistance becomes 5238.1 Ω -cm².

Moreover, the error profile as observed from the angle of region subtended at the pipette is non-uniform. Table 1Aa & b illustrates errors involved at different regions of a sphere subtended at the angle θ . When I also considered the time variable, with a τ of 1 μ s the error increases to 0.75% (see Appendix C for equations). As τ increases to 10 μ s the error is not appreciably different from the steady state conditions.

Figure A7 describes the relationship between voltage and conductance (reverse potential for I_{Ca} was assumed to be equal to +100 mV) of the calcium current being studied. The slope of the line in fig. A7 corresponds to a limiting voltage sensitivity of 10 mV for a e-fold change in

conductance. In table A1, the voltage error at different regions are given. These errors, even at the worst conditions (when θ is small), are small. The relation between calcium conductance and voltage is sigmoidal and the error in voltage should increase in a similar fashion. It is reasonable to assume that the calcium current begins to activate at -30 mV, from a holding potential of -60 mV (see figure A7). Given that, estimates of the potentials beyond which the error increases above 5% are given in table A1d. Note that the situation is worst at the region covered at 5° from the electrode.

Let us consider the relation between voltage and calcium conductance once again (figure A7). The steepest part of the curve occurs between 0 and 10 mV. At this voltage range, the conductance of the current increases by 0.4699 nS for 1 mV change in voltage. The error becomes 1.7 times worse compared to the mean. The last column of table A-1 lists the voltages beyond which the error increases above 5% at the steepest region of the conductance curve.

The region of the cell close to the electrode (between 0° and 10°) will experience an error greater than 5% when currents are elicited at voltages above -5 mV.

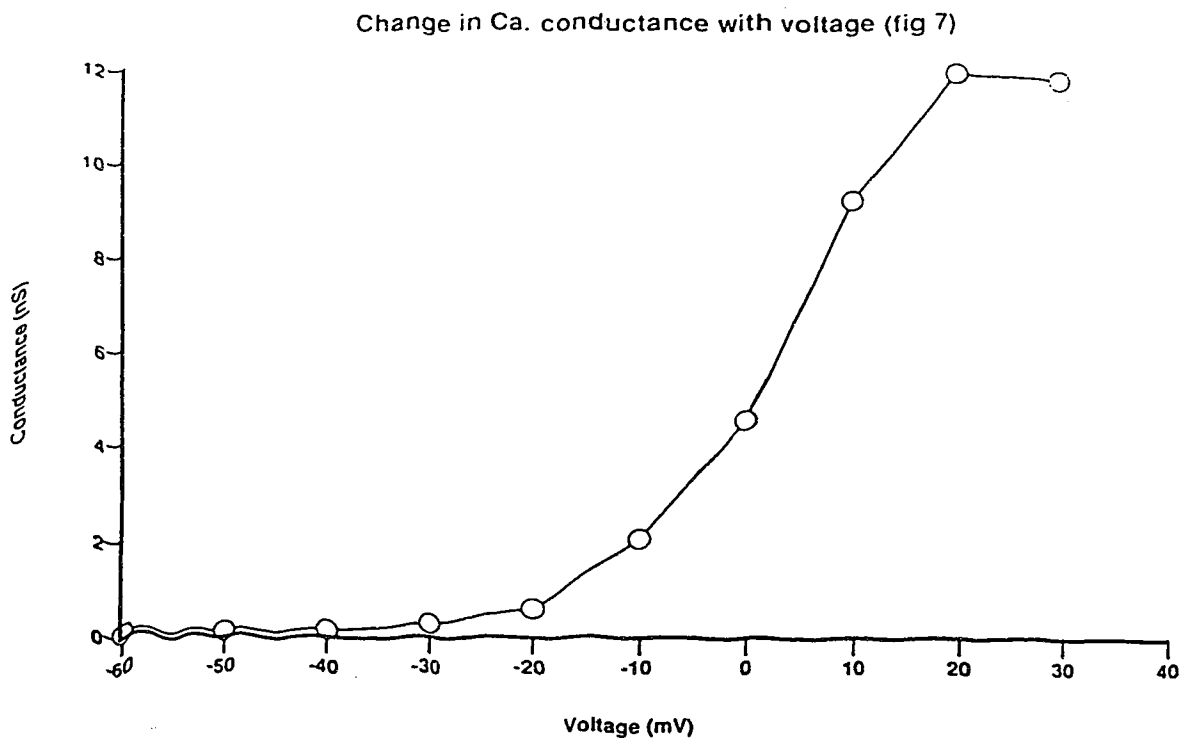


Figure A-7.

The activation of I_{Ca} increases in a sigmoidal fashion. The estimated conductance (g) of the current was calculated from the equation: $g = I_{Ca} / (V - V_{rev})$, where V is the step potential and V_r is the reversal potential of calcium (assumed to be +100 mV in this case). The steepest part of the curve occurs between at 0 and 10 mV and it is at this voltage range that the highest error of voltage inhomogeneity is expected.

Table A-1.

| Table A-1-1 | | | |
|-----------------------------|---|---|---|
| Angle θ (degrees) | Region of subtension (cm $\times 10^{-6}$) | Error at θ ($\times 10^{-4}$) | Total error at region ($\times 10^{-8}$) |
| 5 | 3.3 | 120.1 | 4.0 |
| 10 | 6.8 | 59.1 | 34.9 |
| 30 | 19.6 | 14.9 | 3.0 |
| 60 | 34.0 | 1.1 | 0.4 |
| 90 | 39.3 | 3.9 | 1.5 |
| 120 | 34.0 | 6.6 | 2.3 |
| 150 | 19.6 | 8.0 | 1.6 |
| 180 | 0 | 8.5 | 1.6 |

| Table A-1-2 | | |
|--------------------------|---|--|
| Angle θ (degrees) | % error at point θ from electrode | % error at region subtended by θ ($\times 10^{-8}$) |
| 5 | 1.20 | 1.98 |
| 10 | 0.60 | 3.14 |
| 30 | 0.20 | 6.60 |
| 60 | 0.01 | 8.84 |
| 90 | 0.04 | 8.92 |
| 120 | 0.07 | 9.29 |
| 150 | 0.08 | 9.54 |
| 180 | 0.09 | 10.44 |

| Angle θ (degrees) | Voltage (mV) at θ when command voltage = 10 mV. |
|--------------------------|--|
| 5 | 9.88 |
| 10 | 9.94 |
| 30 | 9.98 |
| 60 | 9.99 |
| 90 | 9.99 |
| 120 | 9.99 |
| 150 | 9.99 |
| 180 | 9.99 |

| Angle θ (degrees) | Voltage (mV) beyond which error exceeds 5%. | Voltage (mV) beyond which error exceed 5% at steepest region in figure 5. |
|--------------------------|---|---|
| 5 | +12 | -5 |
| 10 | +55 | +20 |
| 30 | +248 | +134 |
| 60 | +4970 | +2911 |
| 90 | +1220 | +705 |
| 120 | +684 | +390 |
| 150 | +595 | +338 |
| 180 | +338 | +338 |

A larger portion of the cell however, (between 10° and 180°) is not subject to any significant error within the voltage ranges at which calcium currents were recorded.

The analysis made, using experimental and theoretical parameters, indicates that, within limits, the potential of a spherical cell, $50 \mu\text{m}$ diameter, is close to isopotential

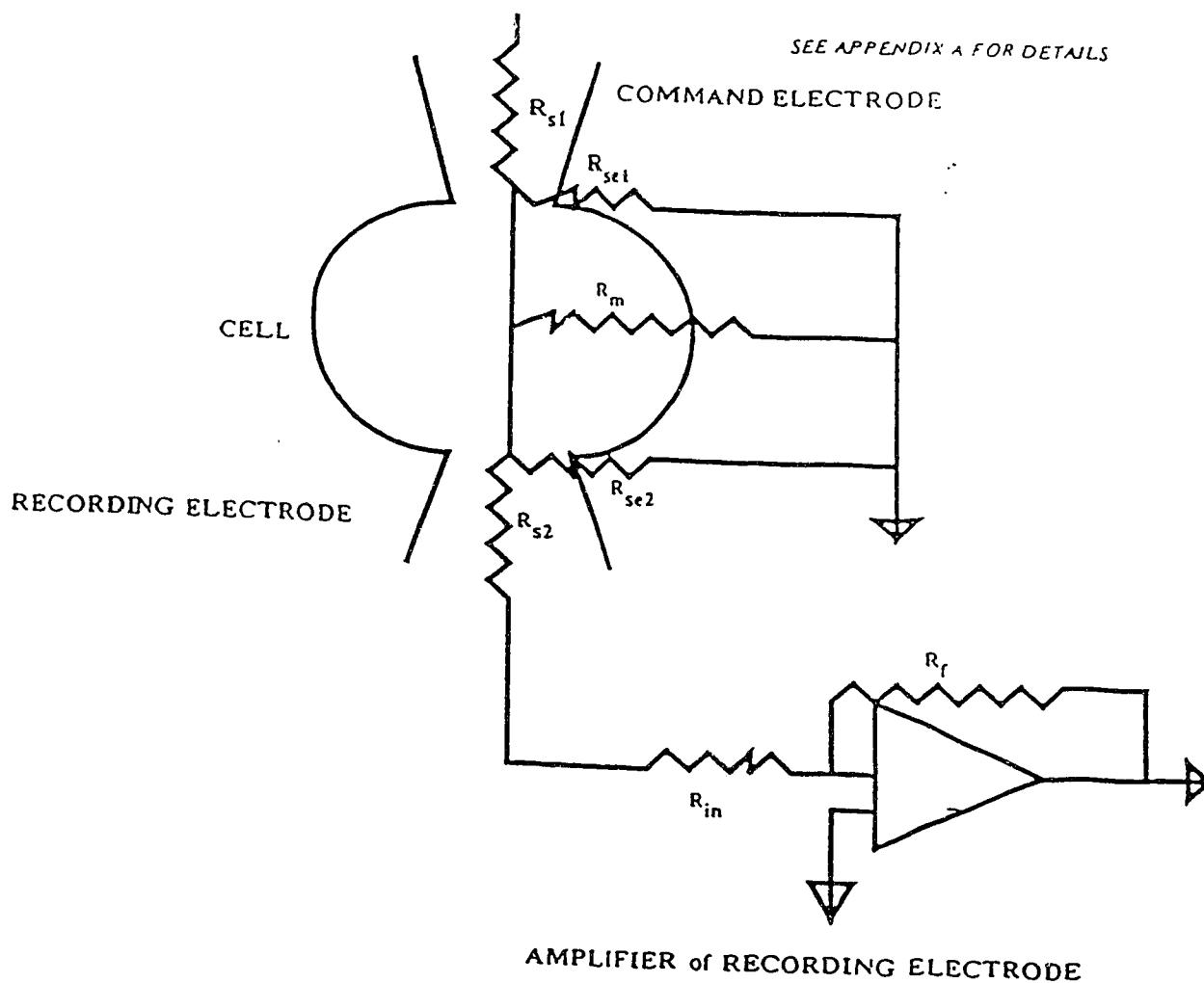
conditions. This is consistent with other reported cases (Jack, et al., 1975). It is perhaps important to reiterate the fact that the neurons which were studied had an average size of 30 μm . Theoretically, the error should be less in a 30 μm cell.

Evidence of serious space clamp problems can be detected from the recorded current traces and the current voltage (IV) relationship. Commonly, 'bumps', occur in the current traces and also, beyond the threshold voltage, action potentials can be elicited even when the cell is electronically clamped. The IV curve, for a badly clamped cell may look like an upside-down action potential (Jones, 1987). None of the signs of space clamp problems were observed in the experiments. The shape of the current-voltage relationship for sodium and calcium currents were close to bell-shape: an indication that the space clamp conditions were close to being ideal.

Appendix B (figure)

Below is a circuit which describes the resistances involved when two patch electrodes are used to record from one cell.

- R_{s1} = Series resistance of command electrode
- R_{se1} = seal resistance of command electrode with cell
- R_{se2} = seal resistance of recording electrode
- R_{s2} = series resistance of recording electrode
- R_{in} = input resistance of recording amplifier.



Appendix B
Assumption:

R_{s1} is a large number
The quality of a voltage clamp depends on the ratio:

$$\frac{V_e}{V_p}$$

V_e = effective command voltage and V_p is the potential applied at the end of the pipette.

$$\frac{V_e}{V_p} = \frac{R_{ns}}{R_{total}}$$

where R_{total} is the total resistance and R_{ns} is defined as:

$$R_{ns} = \frac{1}{\frac{1}{R_{in} + R_{se}} + \frac{1}{R_{se2}} + \frac{1}{R_m}}$$

$$\frac{1}{R_{in} + R_{se2}} \approx \frac{1}{R_{in}}$$

$$R_{ns} = \frac{1}{\frac{1}{R_{in}} + \frac{1}{R_{se2}} + \frac{1}{R_m}}$$

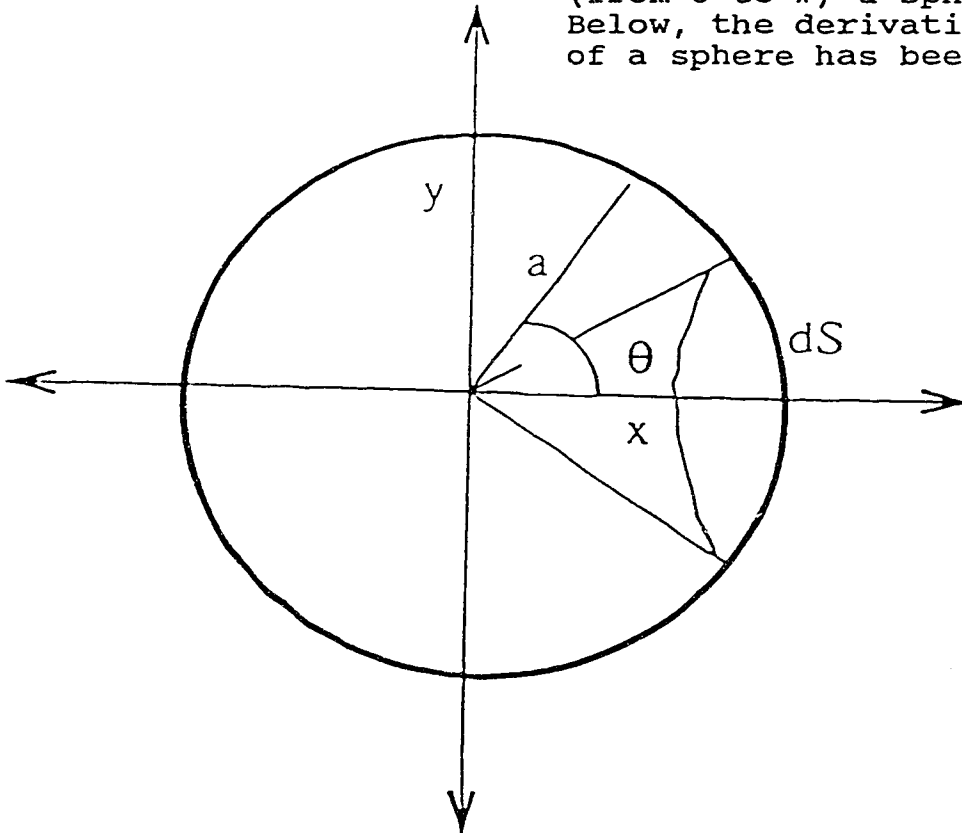
The value of R_{ns} is determined by R_{se2} and R_m (see equation A-4).

$$\frac{V_e}{V_p} = \frac{1}{1 + \frac{R_{s1}}{R_{ns}}}$$

As R_{s1} approaches zero the quality of the voltage clamp improves. Perfect voltage clamp is obtained by reducing R_{s1} or increasing R_{ns} .

Appendix C.

The figure below shows a circle with radius a , at the center of the Cartesian plane $(0,0)$. As the circle is revolved about the plane (from 0 to π) a sphere emerges. Below, the derivation of the area of a sphere has been made.



$$x^2 + y^2 = a^2 \quad (1)$$

(1: Equation of a circle with center at the origin of X and Y Cartesian plane).

$$\delta s = a \delta \theta \quad (2)$$

(2: The change in surface area s : θ is in radians).

$$y = a \sin \theta \quad \delta y = a \cos \theta \delta \theta \quad (3) \quad (\text{Sine rule})$$

$$x = a \cos \theta \quad \delta y = -a \sin \theta \delta \theta \quad (4) \quad (\text{Cosine rule})$$

$$\delta s = \sqrt{\delta x^2 + \delta y^2} \quad (5)$$

$$\delta s = \sqrt{a^2 \sin^2 \theta + a^2 \cos^2 \theta} \delta \theta \quad (6: \text{from 1--5})$$

$$S = \int_0^\pi 2 \pi y \delta s \quad (7)$$

$$S = \int_0^\pi 2 \pi a \sin \theta a \delta \theta \quad (8)$$

$$S = 2 \pi a^2 \int_0^\pi \sin \theta \delta \theta \quad (9)$$

$$S = 2 \pi a^2 [-\cos \theta]_0^\pi \quad (10)$$

$$S = 2 \pi a^2 [1 + 1] \quad (11)$$

$$S = 4 \pi a^2 \quad (12: \text{Area of a sphere})$$

Appendix D

$$V_m = \frac{i_o R_m}{4\pi a^2} [L(t) + \psi(a/\lambda, \theta)] \quad (1)$$

$$\psi = (1 - 2a/\lambda) (1 + (a/\lambda)D - (a/\lambda)^2 E_o) + [(a/\lambda) \csc \theta / 2] - 1 \quad (2)$$

$$L(t) = 1 - e^{-t/R_m C_m} \quad (3)$$

References

- Adams, D. J., Smith, S. J. and Thompson, S. H. 1980. Ionic currents in molluscan soma. Annu. Rev. Neurosci. 3:141-167.
- Adams, D. J., Dwyer, J., Hille, B. 1980. The permeability of endplate channels to monovalent and divalent metal cations. J. Gen. Physiol. 75:493-510.
- Adams, D. J. & Gage, P. W. 1979. Characteristics of sodium and calcium conductance changes produced by membrane depolarization in an Aplysia neuron. J. Physiol. 289:143-161.
- Adams, P. R. 1981. The calcium current of a vertebrate neuron. Adv. Physiol. Sci. 4:564-578.
- Adrian, R.H. Chandler, W.K., & Hodgkin. 1970. Voltage clamp experiments in striated muscle fibers. J. Physiol. 208:607-644.
- Akaike, N. Tsuda, Y. & Oyama, Y. 1988. Separation of current-and voltage-dependent inactivation of calcium current in frog sensory neuron. Neurosci. Lett. 84: 46-50.

Akaike, N. Lee, K. S. & Brown, A. M. 1978. The calcium current of Helix neuron. J. Gen Physiol. 71: 509-531.

Alkon, D. C. 1987. Memory Traces in the Brain. Cambridge Univ. Press, London.

Alkon, D. L. Collin, C. Lederhendler, I. Etcheberrigaray, R. Huddle, P. Sakakibara, M. Redlich, S. Yamoah, E. Papageorge, A. & Nelson, T. 1989. Functional and structural consequences of activation of protein kinase C (PKC) and injection of G-Protein substrates of PKC in Hermisenda neurons. Bio Bull., 177: 320-321

Alkon, D. L. Lederhendler, I. & Shoukimas, J. J. 1982. Primary changes of membrane currents during retention of associative learning. Science. 215:693-695.

Alkon, D. L. & Rasmussen, H. 1988. A spatial-temporal model of cell activation. Science 239: 998-1005.

Alkon, D. L. & Sakakibara, M. 1985. Calcium activates and inactivates a photoreceptor soma potassium current. Biophys. J. 48:983-985.

Aosaki, T & Kasai, H. 1989. Characterization of two kinds of high-voltage-activated Ca-channel currents in chick sensory neurons: Differential sensitivity to dihydropyridines and ω -conotoxin GVIA. Pfluger Arch. **414**:150-156.

Arstrong, C. M. & Matteson, D. R. 1985. Two distinct population of calcium channels in a clonal line of pituitary cells. Science **227**:65-67.

Ashcroft, F. M. & Stanfield, P. R. 1982. Calcium inactivation in skeletal muscle fibres of the stick insect Carausius morosus. J. Physiol. **323**: 93-115.

Ashcroft, F. M. & Stanfield, P. R. 1981. Calcium dependence of the inactivation of calcium currents in skeletal muscle fibers of an insect. Science **213**:224-226.

Auerbach, S. B., Grover, L. & Farley, J. 1989. Neurochemical and immunocytochemical studies of serotonin in the Hermissenda central nervous system. Brain Res. Bull. **22**:353-361.

Augustine, G. J. Charlton, M. P. & Smith, S. J. 1987. Calcium action in synaptic transmitter release. Annu. Rev. Neurosci. **10**: 633-693.

Augustine, G. J. Charlton, M. P. & Smith, S. J. 1985. Calcium entry into voltage-clamped presynaptic terminals of squid. J. Physiol. 367:143-162.

Augustine, G.J. Charlton, M.P. Smith, S.J. 1985. Calcium entry and transmitter release at voltage-clamped nerve terminals of squid. J. Physiol. 369: 163-181.

Baker, P. F. Meves, H. & Ridgway, E. B. 1973. Calcium entry in response to maintained depolarization of squid axons. J. Physiol. 231: 527-548.

Bean, B. P. 1985. Two kinds of calcium channels in canine atrial cells. Differences in kinetics, selectivity and pharmacology. J. of Gen. physiol. 86:1-30.

Bean, B. P. Sturek, M. Puga, A. Hermsmeyer, K. 1986. Calcium channels in muscle cells isolated from rat mesenteric arteries: modulation by dihydropyridine drugs. Circ. Res. 59: 229-235.

Benninger, C., Einwachter, H.M., Haas, H.G., Kern, R. 1976. Calcium-sodium antagonism on the frog's heart: A Voltage-Clamp Study. J. Physiol. 259:617-645.

Berridge, M. J. 1987. Inositol trisphosphate and diacylglycerol: two interacting second messengers. Ann. Rev. Biochem. 56:159-193.

Berridge, M. J. & Irvine, R. F. 1984. Inositol trisphosphate, a novel second messenger in cellular signal transduction. Nature 319:514-516.

Bezanilla, F. & Armstrong, C. M. 1977. Inactivation of the sodium channel. I. Sodium current experiments. J. Gen Physiol. 70: 549-566.

Boll, W. & Lux, H. D. 1985. Action of organic antagonists on neuronal calcium currents. Neurosci. Letts. 56: 335-339.

Bolton, T. B. 1979. Mechanisms of action of transmitters and other substances on smooth muscle. Physiol. Rev. 59:606-718.

Brehm, P. Eckert, R. 1978. Calcium entry leads to inactivation of calcium channel in paramecium. Science. 202:1203-1206.

Brehm, P., Eckert, R. & Tillotson, D. 1980. Calcium-mediated inactivation of calcium current in Paramecium. J. Physiol. 306:193-203.

Brennecke, R. & Lindermann, B. 1974. Design of a fast voltage clamp for biological membranes, using discontinuous feedback, Rev. Sci. Instr. 45:656-661

Brenner, B. & Eisenberg, E. 1986. Rate of force generation in muscle: correlation with actomyosin ATPase activity in solution. Proc. Natl. Acad. Sci. 83:3542-3546.

Brezina, V., Eckert, R. & Erxleben, C. 1987. Modulation of potassium conductances by an endogenous neuropeptide in neurons of Aplysia californica. J. Physiol. 382:267-290.

Brezina, V., THE LATE R. ECKERT & Erxleben, C. (1987). Suppression of calcium current by an endogenous neuropeptide in neurons of Aplysia californica. J. Physiol. 388:565-595.

Brinley, F. J. Jr. 1978. Calcium buffering in squid axons. Ann. Rev. Biophys. Bioeng. 7:363-392.

Brown, A. M. Lux, H.D. & Wilson, D.L. 1984. Activation and inactivation of single calcium channels in snail neurons. J. Gen. Physiol. 83: 751-769.

Brown, A. M., Morimoto, K., Tsuda, Y. & Wilson, D. L. 1981. Calcium current-dependent and voltage-dependent inactivation

of calcium channels in Helix aspersa. J. Physiol. 320:193-218.

Brown, A. M., Wilson, D. L. & Lux, H. D. 1984 Activation of calcium channels. Biophys. J. 45:125-127.

Buchanan, J. T., Brodin, L., Hokfelt, T., Van Dongen, P. A. M. & Grillner, S. 1987. Survey of neuropeptide-like immunoreactivity in the lamprey spinal cord. Brain Res. 408:299-302.

Burlhis, T. M. & Aghajanian, G. K. 1988. Pacemaker potentials of serotonergic dorsal raphe neurons: contribution of a low-threshold Ca^{2+} conductance. Synapse 1: 582-588.

Byne, N. G. & Large, W. A. 1987. Action of noradrenaline on single smooth muscle cells freshly dispersed from the rat anococcygeus muscle. J. Physiol. 328:143-170.

Byerly, L. & Hagiwara, S. 1982. Calcium currents in internally perfused nerve cell bodies of Lymnea stagnalis. J. Physiol. 288:263-284.

Callaway, J. C., Masinovsky, B. and Graubard, K. (1987). Co-localization of SCP_{β} -like and FMRFamide-like

immunoreactivities in crustacean nervous systems. Brain Res. 405:295-304.

Campbell, D.L., Giles, W.R., Hume, J. R., Noble, D., Shibata, E.F. 1988. Reversal potential of the calcium current in bull-frog atrial myocytes. J. Physiol. 403: 267-286.

Campbell, D.L., Giles, W.R., Hume, J.R., Shibata, E.F. 1988. Inactivation of calcium current in bull-frog atrial myocytes. J. Physiol. 403: 287-315.

Campbell, D.L. Giles, W.R. Shibata, E. F. 1988. Ion transfer characteristics of the calcium current in bull-frog atrial myocytes. J. Physiol. 403: 239-266.

Campbell, D. L., Giles, W. R., Robinson, K. & Shibata, E. F. 1988. Studies of the sodium-calcium exchanger in bull-frog atrial myocytes. J. Physiol. 403:317-340.

Campbell, D. L. & Giles, W. R. 1985. Possible roles of the $\text{Na}^+/\text{Ca}^{2+}$ exchanger and ATP-dependent Ca^{2+} pump in bullfrog atrial myocytes. J. of Mol. & Cellu. Cardio. 17:R 019.

Cena, V. Stutzin, A. & Rojas, E. 1989. Effects of calcium and Bay K-8644 on calcium currents in adrenal medullary chromaffin cells. J. Memb. Biol. 112:255-265.

Chad, J., Eckert, R. & Ewald, D. 1984. Kinetics of Ca-dependent inactivation of calcium current in neurons of Aplysia californica. J. Physiol. 347:279-300.

Charlton, M.P. Smith, S.J. Zucker, R.S. 1982. Role of presynaptic calcium ions and channels in synaptic facilitation and depression at the squid giant synapse. J. Physiol. 323: 173-193.

Cheung, W. Y. 1980. Calmodulin plays a pivotal role in cellular regulation. Science. 207:19-27.

Chronwall, B. M., Olschowka, J. A. and O'Donohue, T. L. (1984). Histochemical localization of FMRFamide-like immunoreactivity in the rat brain. Peptides 5:569-584.

Cohen, C. J., McCarthy, R. T., Barrett, P.O. & Rasmussen, H. 1988. Ca channel in adrenal glomerulosa cells: K⁺ and angiotensin II increase T-type Ca channel current. Proc. Natl. Acad. Sci. U.S.A 85:2412-2416.

- Cole, K.S. 1949. Dynamic electrical characteristics of the squid axon membrane, Arch. Sci. Physiol. 3:253-258.
- Cole, K.S. 1968. Membranes, ions and impulses. University of California Press, Berkeley.
- Collin, C. Ikeno, H. Harrigan, J. F. Lederhendler, I. & Alkon, D. L. 1988. Sequential modification of membrane currents with classical conditioning. Biophys. J. 54: 955-960.
- Connor, J. A. 1977. Time course separation of two inward currents in molluscan neurons. Brain Res. 199:487-492.
- Cottrell, G. A and Davies, N. W. (1987) Multiple receptor sites for a molluscan peptide (FMRFamide) and related peptides of Helix. J. Physiol. 382:51-68.
- Cottrell, G. A., Davies, N. W., and Green, K. A. (1984) Multiple actions of a molluscan cardio-excitatory neuropeptide and related peptides on identified Helix neurones. J. Physiol. 356:315-333.
- Croll, R.P. 1987. Distribution of Monoamines in the central nervous system of the nudibranch gastropod, Hermisenda Crassicornis. Brain Res. 405:337-347.

Crow, T. and Forrester, J. 1986. Light paired with serotonin mimics the effect of conditioning on phototactic behaviour of Hermissenda. Proc. Natl. Acad. Sci. 83:7975-7978.

Eckert, R. & Chad, J. E. 1984. Inactivation of Ca channels. Prog. Biophys. molec. Biol. 44: 215-267.

Eckert, R. & Ewald, D. 1983. Inactivation of calcium conductance characterized by tail current measurements in neurons of Aplysia californica. J. Physiol. 345: 549-565.

Eckert, R., Ewald, D. & Chad, J. 1982. Calcium-mediated inactivation of calcium current in neurons of Aplysia californica. In The Physiology of Excitable Cells (eds. A.D. Grinnell & Wm. Moody). Alan Liss. Inc., New York.

Eckert, R., Ewald, D. & Chad, J. 1982. A single Ca-mediated process can account for both rapid and slow phases of inactivation exhibited by a single calcium conductance. Biol. Bull. 398.

Eckert, R. & Lux, H. D. 1976. A voltage-sensitive persistent calcium conductance in neuronal somata of Helix. J. Physiol. 254:129-151.

Eckert, R. & Lux, H. D. 1975. A non-inactivating inward current recorded during small depolarizing voltage steps in snail pacemaker neurons. Brain Res. 83:486-489.

Eckert, R., Tillotson, D. & Brehm, P. 1981. Calcium mediated control of Ca and K currents. Fedn. Proc. 40:226-2232.

Eisenberg, R.S. & Engel, E. 1970. The spatial variation of membrane potential near a small source of current in a spherical cell. J. Gen. Physiol. 55:736-756.

Farley, J., and Wu, R. (1989). Serotonin-modulation of Hermisenda B photoreceptor ionic currents. Brain Res. Bull. 22:335-351.

Fatt, P. & Ginsborg, B. L. 1958. The ionic requirement for the production of action potentials in crustacean muscle fibers. J. Physiol. 142:516-543.

Fatt, P. & Katz, B. 1953. The electrical properties of crustacean muscle fibers. J. Physiol. 120:171-204.

Fenwick, E. M., Marty, A. & Neher, E. 1982a. A patch-clamp study of bovine chromaffin cells and their sensitivity to acetylcholine. J. Physiol. 331:577-597.

Fenwick, E. M., Marty, A. & Neher, E. 1982b. Sodium and calcium channels in bovine chromaffin cells. J. Physiol. 331:599-635.

Finkel, A.S. & Redman, S. 1984. Theory and operation of the single microelectrode voltage clamp. J. Neurosci. Met 11:101-127.

French, R.J. & Wells, J. B. 1977. Sodium ions as blocking agents and charge carriers in potassium channel of the squid giant axon. J. Gen. Physiol. 70:707-724.

Fox, A. P. 1981. Voltage-dependent inactivation of a calcium channel. Proc. Natn. Acad. Sci. U.S.A. 78:953-956.

Fox, A.P. Nowycky, M.C. & Tsien, R.W. 1987. Single-channel recordings of three types of calcium channels in chick sensory neurones. J. Physiol. 394: 173-200.

Fredman, S.M. 1987. Intracellular staining of neurons with nickel-lysine. J. Neurosci. Met. 20:181-194.

Fukushima, Y. & Hagiwara, S. 1985. Currents carried by monovalent cations through calcium channels in mouse neoplastic B lymphocytes. J. Physiol. 358:255-284.

Fukushima, Y. 1982. Blocking kinetics of the anomalous potassium rectifier of tunicate egg studied by single channel recording. J. Physiol. 331:311-331.

Giles, W., Hume, J. & Noble, S. 1980. The ionic mechanism underlying the interval-duration relationship in bullfrog atrium. J. Physiol. 211: 217-244.

Greenberg, M. J. and Price, D. A. (1983). Invertebrate neuropeptide: native and naturalized. Annual Review of Physiology 45, 271-288.

Gorman, A.L.F. & Maurizio, M. 1972. The passive electrical properties of the membrane of a molluscan neuron. J. Physiol. 227:35-49.

Gutnick, M.J., Lux, H.D., Swandulla, D., Zucker, H. 1989. Voltage-dependent and calcium-dependent inactivation of calcium channel current in identified snail neurones. J. Physiol. 412: 197-220.

Hagiwara, S. & Byerly, L. 1981. Calcium channel. Ann. Rev. of Neurosci. 4:69-125.

- Hagiwara, N., Irisawa, H. & Kameyama, M. 1988. Contribution of two types of calcium currents to the pacemaker potential of rabbit sino-atrial node cells. J. Physiol. 395:233-253.
- Hagiwara, S. & Ohimori, H. 1982. Studies of calcium channels in rat clonal pituitary cells with patch electrode voltage clamp. J. Physiol. 331: 231-252.
- Hagiwara, S., Ozawa, S. & Sand, O. 1975. Voltage clamp analysis of two inward current mechanisms in the egg cell membrane of a starfish. J. Gen. Physiol. 65:617-644.
- Hagiwara, S. & Takahashi, K. 1967. Surface density of calcium ions and calcium spikes in the barnacle muscle fibre membrane. J. Gen Physiol. 50: 583-601.
- Hamill, O.P., Marty, E. Neher, B Sakmann, and F.J. Sigworth 1981. Improved patch clamp techniques for high-resolution current recording from cells and cell-free membrane patches. Pfluegers Arch. 391:85-100.
- Hering, S. Beech, D. J. Bolton, T. B. & Lim, S. P. 1988. Action of nifedipine or Bay K8644 is dependent on calcium channel state in single smooth muscle cells from rabbit ear artery. Pfluegers Arch. 411: 590-592.

Hess, P. 1990. Calcium channels in vertebrate cells. A Rev. Neurosci. 13: 337-356.

Hille, B. 1984. Ionic channels of excitable membranes. Sinauer Associates Inc. Sunderland, Mass.

Hirning, L. D., Fox, A. P., McCleskey, E. W., Oliver-Boldomers, M., Thayer, S. A., Miller, R. J., & Tsien, R. W. 1988. Dominant role of N-type Ca^{2+} channels in evoked release of nor-epinephrine from sympathetic neurons. Science 239:57-61.

Hodgkin, A.L. 1947. The membrane resistance of a non-medullated nerve fibre. J. Physiol. 106:305-318.

Hodgkin, A.L. & Huxley, A.F. 1952. A quantitative description of membrane current and its application to excitation and conduction in nerve. J. Physiol. 117:500-544.

Hodgkin, A. L. & Katz, B. 1949. The effect of sodium ions on the electrical activity of the giant axon of the squid. J. Physiol. 108:31-77.

Hodgkin, A.L. & Rushton, W.A. 1946. Electrical constant and velocity of nerve fibers. Proc. R. Soc. B 133: 444-479.

- Hofmann, F., Nastainczyk, W., Rohrkasten, A., Schneider, T. & Sieber, M. 1987. Regulation of the L-type calcium channel. Trends in Pharmacol. Sci. **8**: 393-398.
- Horn, R. 1978. Propagating calcium spikes in an axon of Aplysia. J. Physiol. **301**:191-204.
- Hume, J. R. & Giles, W. 1983. Ionic currents in single isolated bullfrog atrial cells. J. Gen. Physiol. **81**:153-194.
- Jack, J.J. B., Noble, D. & Tsien, R.W., 1975. Electric current flow in excitable cells. Clarendon Press, Oxford p. 132-134.
- Jerussi, T. P. & Alkon, D. L. 1981. Ocular and extraocular responses of identifiable neurons in pedal ganglia of Hermisenda crassicornis. J. Neurophysiol. **46**:659-671.
- Jones, S.W. 1987. Sodium currents in dissociated bull-frog sympathetic neurons. J. Physiol. **389**:605-627.
- Jones, S. W. & Jacobs, S. L. 1990. Dihydropyridine actions on calcium currents of frog sympathetic neurons. J. of Neurosci. **10(7)**: 2261-2267.

Jones, S. W. & Marks, T. N. 1989. Calcium currents in bullfrog sympathetic neurones. I. Activation kinetics and pharmacology. J. Gen. Physiol. 94:154-167.

Kaczmarek, L. K. Finbow, M. Revel, J. P. & Strumwasser, F. 1979. The morphology of coupling of Aplysia bag cells within the abdominal ganglion and in cell culture. J. Neurobiol. 10: 535-550.

Kongsamut, S. & Miller, R. 1986. Nerve growth factor modulates the drug sensitivity of neurotransmitter release from PC-12 cells. Proc. Natn. Acad. Sci. USA. 83:2243-2247.

Katz, B. & Miledi, R. 1971. The effect of prolonged depolarization on synaptic transfer in stellate ganglion of the squid. J. Physiol. 216: 503-512.

Kavaliers, M., Hirst, M. & Mathers, A. 1985. Inhibitory influences of FMRF-amide on morphine- and deprivation-induced feeding. Neuroendocrinology 40: 533-535.

Kawashima, Y & Ochi, 1988. Voltage-dependent decrease in availability of single calcium channels by nitrendipine in guinea-pig ventricular cells. J. Physiol. 402: 219-235.

Kennedy, M. B. 1989. Regulation of neuronal function by calcium. TINS. 12:417-419.

Keynes, R. D. Rojas, E. Taylor, R. E. & Vergara, J. 1973. Calcium and potassium system of a giant barnacle muscle fibre under membrane potential control. J. Physiol. 229:409-455.

Kobayashi, M., and Muneoka, Y. 1989. Functions, Receptors, and mechanisms of the FMRFamide-related peptides. Bio. Bull. 177:206-209.

Kostyuk, P. G. & Krishtal, O. A. 1977. Effects of calcium-chelating agents on the inward and outward current in the membrane of mollusc neurones. J. Physiol. 270:569-580.

Kostyuk, P. G. Krishtal, O. A. & Shakhovalov, Y. A. 1977. Separation of sodium and calcium currents in the somatic membrane of mollusc neurons. J. Physiol. 270:545-568.

Kostyuk, P. G., Krishtal, O. A. & Pidoplichko, V. I. 1975. Effect of internal fluoride and phosphate on membrane currents during intracellular dialysis of nerve cells. Nature. 267:70 - 72.

Kuffler, S.W., Nicholls, J.G., & Martin, R. A. 1984. From neuron to brain. Sinauer Asso. Inc. Massachusetts. p. 171.

Land, P. W. & Crow, T. 1985. Serotonin immunoreactivity in the circumesophageal nervous system of Hermisenda crassicornis. Neurosci. Lett. 62:199-205.

Lee, K. S. & Tsien, R. W. 1983. Mechanism of calcium channel blockade by verapamil, D600, diltiazem and nitrendipine in single dialysed heart cells. Nature. 302: 790-794.

Lederhendler, I. I., Etcheberrigaray, R., Yamoah, E. N. Matzel, D. & Alkon, D. 1990. Outgrowths from Hermisenda photoreceptor somata are associated with activation of protein kinase C. Brain Res. 534:195-200.

Llinas, R. 1980. A model of presynaptic Ca⁺⁺ current and its role in transmitter release. CSH Reports in the Newsience 1: 55-64.

Llinas, R., Steinberg, I. Z. & Walton, K. 1981a. Presynaptic calcium currents in squid giant synapse. Biophys. J. 33: 289-322.

Llinas, R., Steinberg, I. Z., & Walton, K. 1981b. Relation between presynaptic and postsynaptic potential in squid giant synapse. Biophys. J. 33: 323-352.

Llinas, R. & Yarom, Y. 1981. Electrophysiology of mammalian inferior olive neurons in vitro. Different types of voltage dependent ionic conductances. J. Physiol., 315:549-567.

Llinas, R., Hess, R. 1976. Tetrodotoxin-resistant dendritic spikes in avian Purkinje cells. Proc. Natl. Acad. Sci. U.S.A. 73:2520-2523.

Llinas, R., Steinberg, I. Z., & Walton, K. 1976. Presynaptic calcium currents and their relation to synaptic transmission: Voltage clamp study in squid giant synapse and theoretical model for the calcium gate. Proc. Natl. Acad. Sci. U.S.A. 73:2918-2922.

Llinas, R., Sugimori, M. & Cherksey, B. (1989) Voltage-dependent calcium conductances in mammalian neurons Ann. N.Y. Acad. Sci. 560:103-111.

Lopresti, V. Macagno, E. R. & Levinthal, C. 1973. Structure and development of neuronal connection in isogenic organisms: cellular interactions in the development of the optic lamina of Daphnia. Proc. natl. Acad. Sci. 70: 433-437.

Lux, H. D. & Heyer, C. B. 1979. A new electrogenic calcium-potassium system. In The Neurosciences: Fourth study program. F. O. Schmitt & F. G. Worden. eds. M.I.T. press, Cambridge, Mass.

MacDermott, A. B., Mayer, M. C., Westbrook, G. L., Smith, S. J., Barker, J. L. 1986. NMDA-receptor activation increases cytoplasmic calcium concentration in cultured spinal cord neurons. Nature 321:519-522.

MacFarland, M. F. 1966. Studies of the Opisthobranchiata Mollusks of the pacific coast of north America. In memoirs of the california academy of sciences vol. VI San Francisco p.358-368.

Mackey, S. L., Glanzman, D. L., Small, S. A., Dyke, A. M., Kandel, E. R., and Hawkins, R. D. 1987. Tail shock produces inhibition as well as sensitization of the siphon-withdrawal reflex of Aplysia: Possible behavioral role for presynaptic inhibition mediated by the peptide Phe-Met-Arg-Phe-NH₂. Proc. Natl. Acad. Sci. 84:8730-8734.

Man-Son-Hing. H. Zoran, M. J. Lukowiak, K. & Haydon, P. G. (1989). A neuromodulator of synaptic transmission acts on

the secretory apparatus as well as on ion channels. Nature 341:237-239.

Marchetti, C., Carbone, E. & Lux, H. D. 1986. Effects of dopamine and noradrenaline on Ca channels of cultured sensory and sympathetic neurons of chick. Pflug. Arch. 406:104-111.

Marder, E. Calabrese. M.P. Nusbaum, & Trimmer, B.A. 1987. Distribution and partial characterization of FMRFamide-like peptides in the stomatogastric nervous system of the rock crab, Cancer borealis and the spiny lobster Panulirus interruptus. J. Comp. Neurol. 259:150-164.

Marty, A. & Neher, E. 1985. Potassium channels in cultured bovine adrenal chromaffin cells. J. Physiol. 367:117-141.

Marty, A & Neher, E. 1983. Tight-seal whole-cell recording. In Single Channel Recordings. ed. Sakmann and Neher. Plenum Press, New York p. 107-122.

Matteson, M.P. & Kater, S.B. 1987. Calcium regulation of neurite elongation and growth cone motility. J. of Neurosci. 7: 4034-4043.

Matzel, L. D., Lederhendler, I. and Alkon, D. L. 1990. Regulation of short-term associative memory by calcium dependent protein kinase. J. Neurosci. 10:2300-2307.

Mechmann, S. & Pott, L. 1986. Identification of Na-Ca exchange current in single cardiac myocytes. Nature 319:597-599.

Meech, R. W. 1974. The sensitivity of Helix aspersa neurons to injected calcium ions. J. Physiol. 237:259-277.

Meech, R. W. & Standen, N. B. 1975. Potassium activation in Helix aspersa neurons under voltage clamp: a component mediated by calcium influx. J. Physiol. 249: 211-239.

Mentrard, D. Vassort, G. & Fischmeister, R. 1984. Calcium-mediated inactivation of the calcium conductance in cesium-loaded frog heart cells. J. Gen Physiol. 83: 105-131.

Meves, H. 1978. Inactivation of the sodium permeability in squid axon giant fibers. Progress in Biophysics & Mol. Biol. 33: 207-230.

Mitchell, M. R., Powell, T., Terrar, D. A. & Twist, V. W. 1983. Characteristics of the second inward current in cells

isolated from rat ventricular muscle. Proc. R. Soc. Lond. B 219:447-469.

Miller, R. J. 1987. Calcium channels and neuronal function. Science 235:46-52.

Moore, J.W. 1963. Operational amplifiers. In Physical techniques in biological research. ed. W.L. Nastuk. Academic press. New York p. 77-97.

Morad, M. Goldman, Y. E. & Trentham, D. R. 1983. Rapid photochemical inactivation of Ca^{2+} antagonists shows that Ca^{2+} entry directly activates contraction of frog heart. Nature. 304: 635-638.

Neher, E. 1986. Concentration profiles of intracellular calcium in the presence of a diffusible chelator. Exp. Brain Res. 514: 80-96.

Nelson, T. J. Collin, C. & Alkon, D. L. 1990. Isolation of a G protein that is modified by learning and reduces potassium currents in *Hermissenda*. Science 247: 1479-1483.

Nelson, M. T. & Worley, J. F. 1989. Dihydropyridine inhibition of single calcium channels and contraction in

rabbit mesenteric artery depends on voltage. J. Physiol. 412: 65-91.

Nerbonne, J. M. Richard, S. & Nargeot, J. 1985. Ca²⁺ channels are unblocked within a few msec after photoconversion of nifedipine. J. Mol. Cell. Cardiol. 17: 511-515.

Nerbonne, J. M. & Gurney, M. A. 1987. Blockade of Ca²⁺ and K⁺ currents in bag cell neurons of Aplysia californica by dihydropyridine Ca²⁺ antagonists. J. of Neurosci. 7(3): 882-893.

New, W. & Trautwein, W. 1972. The ionic nature of slow inward current and its relation to concentration. Pflugers Arch. 334: 24-38.

Norris, B. J. & Calabrese, R. L. 1987. Identification of motor neurons that contain a FMRFamide-like peptide and the effects of FMRFamide on longitudinal muscle in the medicinal leech, Hirudo medicinalis. J. of Comp. Neurol. 266: 95-111.

Nowycky, M. C., Fox, A. P. & Tsien, R. W. 1985. Three types of neuronal calcium channel with different calcium agonist sensitivity. Nature 316:440-443.

- O'Donohue, T.L., Bishop, B.M. Chronwall, J.Groone, & Watson, W.H. 1984. Characterization of FMRFamide immunoreactivity in the rat central nervous system. Peptides 5:563-568.
- Okamoto, H., Takahashi, K. & Yoshi, M. 1976. Two components of calcium current in the egg cell membrane of the tunicate. J. Physiol. 255: 527-561.
- Parsons, T. D. & Chow, R. H. 1989. Neuritic outgrowth in primary cell culture of neurons from the squid, Loligo pealei. Neurosci. Lett. 97: 23-28.
- Perney, T. M., Hirning, L. D., Leeman, S. E. & Miller, R. J. Multiple calcium channels mediate neurotransmitter release from peripheral neurons. Proc. Natl. Acad. Sci. USA 83: 2243-2247.
- Piomelli, D. Voltera, A. Dale, N. Siegelbaum, S. A. Kandel, E. R. Schwartz, J. H. & Belardetti, F. 1987. Lipoxygenase metabolites of arachidonic acid as second messengers for presynaptic inhibition of Aplysia sensory cells. Nature 328:38-43.
- Plant, T.D. 1988. Properties and calcium-dependent inactivation of calcium currents in cultured mouse pancreatic β -cells. J. Physiol. 404: 731-747.

Plummer, M. R., Logothetis, D. E. & Hess, P. Elementary properties and pharmacological sensitivities of calcium channels in mammalian peripheral neurons. Neuron 2: 1453-1463.

Price, D. A. & Greenberg, M. J. 1977. Structure of a molluscan cardioexcitatory neuropeptide. Science 197: 670-671.

Przysieznik, J. & Spencer, A. 1991. Calcium currents in identified neurons from a hydrozoan jellyfish, Polyorchis penicillatus. (submitted to J. Neurosc.).

Ready, D. F. & Nicholls, J. G. 1979. Identified neurons isolated from leech CNS make selective connections in culture. Nature. 281: 67-69.

Reuter, H. 1973. Divalent cations as charge carriers in excitable membranes. Prog. Biophys. molec. Biol. 26: 1-43.

Reynolds, I.J. Wagner, J.A. Snyder, S.H. Thayer, S.A. Olivera, B.M. Miller, R.J. 1986. Brain voltage-sensitive calcium channel subtypes differentiated by ω -conotoxin fraction GVIA. Proc. Natl. Acad. Sci. USA. 83: 8804-8807.

Rosenberg, R. L., Hess, P. & Tsien, R. W. 1988. L-type channels and calcium-permeable channels open at negative membrane potentials. J. Gen. physiol. 92: 27-54.

Sakakibara, M. Collin, C. Kuzirial, A. Alkon, D. L. Heldman, E. Naito, S. & Lederhendler, I. 1987. Effect of α 2-adrenergic agonist and antagonists on photoreceptor membrane currents. J. Neurochem. 48:405-416.

Sakmann, B & Neher, E. 1983. Geometric parameters of pipettes and membrane patches. In Single Channel Recording. Plenum Press, New York.

Sanchez, J. A. & Stefani, E. 1978. Inward calcium current in twitch muscle fibers of the frog. J. Physiol. 283: 197-209.

Sanguinetti, M. C. & Kass, R. S. 1984. Voltage dependent block of calcium channel current in calf cardiac Purkinje fibre by dihydropyridine calcium channel antagonists. Circ. Res. 55: 336-348.

Scott, R. H., Pearson, H. A. & Dolphin, A. C. 1991. Aspects of vertebrate neuronal voltage-activated calcium currents and their regulation. Prog. in Neurobio. 36: 485-520.

- Scott, R. H., Dolphin, A. C., Bindokas, V. P. & Adams, M. E. (1990) Inhibition of neuronal Ca^{2+} channel currents by the funnel web spider toxin ω -Aga-IA. Molec Pharmac. **38**: 711-718.
- Sombati, S. Forman, R. Lee, R. & DeLorenzo. 1989. A simple method for growing and maintaining dissociated Hermisenda CNS neurons in culture. Soc. Neurosci. Abst. **13**:570.
- Spat, A., Bradford, P. G., Mckinney, J. S. Rubin, R. P. & Putney, W. J. Jr. 1986. A saturable receptor for ^{32}P -inositol-1,4,5-trisphosphate in hepatocytes and neutrophils. Nature **319**:514-516.
- Standen, N.B. Stanfield, P.R. 1982. A binding-site model for calcium channel inactivation that depends on calcium entry. Proc. R. Soc. Lond. B. **217**: 101-110
- Stanley, E. F. & Goping, G. 1991. Characterization of a calcium current in a vertebrate cholinergic presynaptic nerve terminal. J. Neurosc. **11**(4): 985-993.
- Strong, J. A., Fox, A. P., Tsien, R. W. & Kaczmarek, L. K. 1987. Stimulation of protein kinase C recruits covert calcium channels in Aplysia bag-cell neurons. Nature **325**:714-717.

Swandulla, D. & Lux, H. D. 1985. Activation of a nonspecific cation conductance by intracellular Ca^{2+} elevation in bursting pacemaker neurons of Helix pomatia. J. Neurophysiol. 54:1430-1443.

Tabata, M. & Alkon, D. L. 1982. Correlated receptor and motorneuron changes during retention of associative learning of Hermissenda crassicornis. J. Neurophysiol. 48:174-191.

Takahashi, K., Wakamori, M & Akaike, N. 1989. Hippocampal CA1 pyramidal cells of rat have four voltage-dependent calcium conductances. Neurosci. Lett. 104: 229-234.

Taussig, R. & Scheller, R.H. 1986. The Aplysia FMRFamide gene encode sequence related to mammalian brain peptides. DNA 5:453-461.

Thayer S. A. & Miller, R. J. 1990. Regulation of intracellular free calcium concentration in single rat dorsal root ganglion neurones in vitro. J. Physiol. 425:85-115.

Thompson, S.H. & Coombs, J. 1988. Spatial distribution of Ca current in molluscan neuron cell bodies and regional differences in the strength of inactivation. J. Neurosci. 8:1929-1939.

- Thomson, A. M., West, D. C. & Lodge, D. 1985. An N-methylaspartate receptor-mediated synapse in rat cerebral cortex: a site of action of ketamine. Nature 313:479-481.
- Thornton, V. F. 1982. Incomplete inactivation of the secretory response during maintained depolarization of pituitary melanotrophs. J. Physiol. 334:127P.
- Tillotson, D. 1980. Ca²⁺ dependent inactivation of Ca²⁺ channels. In Molluscan Nerve Cells (eds. J. Koester & J. H. Byrne), Cold Spring Harbor Laboratory, Cold Spring Harbor.
- Tillotson, D. 1979. Inactivation of Ca conductance dependent on entry of Ca ions in molluscan neurons. Proc. Natn. Acad. Sci. U.S.A 77:1497-1500.
- Tillotson, D. & Gorman, A. L. F. 1980. Non-uniform Ca²⁺ buffer distribution in a nerve cell body. Nature 286: 816-817.
- Tillotson, D. & Horn, R. 1978. Inactivation without facilitation of calcium conductance in caesium-loaded neurons in Aplysia. Nature 273:312-314.
- Tsien, R.W. 1983. Calcium channels in excitable cell membranes. Ann. Rev. Physiol. 45: 341-358.

Tsien, R. W., Hess, P., McCleskey, E. W. & Rosenberg, R. L. 1987. Calcium channels: Mechanisms of selectivity, permeation and block. Annu. Rev. Biophys. Chem. **16**:265-290.

Tsien, R.W. Lipscombe, D. Madison, D.V. Bley, K.R. & Fox, A.P. 1988. Multiple types of neuronal calcium channels and their selective modulation. TINS **10**:431-438.

Weiss, S. Goldberg, J. I. Chohan, K. S. Stell. W. K. Drummond, G. I. & Lukowiak, K. 1984. Evidence for FMRFamide as a neurotransmitter in the gill of Aplysia californica. J. of Neurosci **4**:1994-2000.

Wong, R. G. Hadley, R. D. Kater, S. B. & Hauser, G. C. 1981. Neurite outgrowth in molluscan organ and cell cultures: the role of conditioning factor(s). J. Neurosci. **1**: 1008-1021.

Yamoah, E. N. Kuzirian, A. L. & Tamase, C. 1991. Development of FMRFamide neurons in Hermisenda. Bio. Bull. (submitted).

Yamoah, E. N. 1989. The causes of supernormal period in neurons and cardiac membrane models. MSc Thesis Univ. of Alberta.

Yatani, A. & Brown, A. M. 1985. The calcium channel blocker nitrendipine blocks sodium channels in neonatal rat cardiac myocytes. Circ. Res. 56: 868-875.

Yeh, J. Z. & Oxford, G. S. 1985. Interactions of monovalent cations with sodium channels in squid axon. II. Modification of pharmacological inactivation gating. J. of Gen. Physiol. 85: 603-620.